INFORMATION TO USERS

This manuscript has been reproduced from the microfilm master. UMI films the text directly from the original or copy submitted. Thus, some thesis and dissertation copies are in typewriter face, while others may be from any type of computer printer.

The quality of this reproduction is dependent upon the quality of the copy submitted. Broken or indistinct print, colored or poor quality illustrations and photographs, print bleedthrough, substandard margins, and improper alignment can adversely affect reproduction.

In the unlikely event that the author did not send UMI a complete manuscript and there are missing pages, these will be noted. Also, if unauthorized copyright material had to be removed, a note will indicate the deletion.

Oversize materials (e.g., maps, drawings, charts) are reproduced by sectioning the original, beginning at the upper left-hand corner and continuing from left to right in equal sections with small overlaps. Each original is also photographed in one exposure and is included in reduced form at the back of the book.

Photographs included in the original manuscript have been reproduced xerographically in this copy. Higher quality 6" x 9" black and white photographic prints are available for any photographs or illustrations appearing in this copy for an additional charge. Contact UMI directly to order.

UMI

A Bell & Howell Information Company
300 North Zeeb Road, Ann Arbor MI 48106-1346 USA
313/761-4700 800/521-0600

TRANSPORT OF NON-AQUEOUS PHASE LIQUID IN AN UNSATURATED SOIL

RENÉ DESJARDINS

A thesis submitted to the Faculty of Graduate Studies And Research

in partial fulfillment of the requirements

for the degree of Master of Engineering

Department of Civil Engineering and Applied Mechanics

McGill University

Montréal, Québec

February 1997

Puisqu'on ne peut être universel et savoir tout ce qu'on peut savoir sur tout, il faut savoir un peu de tout. Car il est bien plus beau de savoir quelque chose de tout que de savoir tout d'une chose; cette universalité est la plus belle.

PASCAL, Pensées

ABSTRACT

The present study includes two broad sections: experimental work and modelling. The core of the experimental work is the oil imbibition experiment in two unsaturated mixtures of silica sand and kaolinite clay (80%/20% and 60%/40% by weight). To investigate the effect of capillary forces on multiphase flow, three series of oil imbibition tests were performed with each type of soil:

1. Maximum capillary forces system, in which the soil mixtures were moulded with distilled water.
2. Intermediate capillary forces system, in which the soil mixtures were moulded with a 3% aqueous surfactant solution.
3. Minimum capillary forces system, in which the soil mixtures were moulded with a 6% aqueous surfactant solution.

The durations of the oil imbibition experiments were 1, 2 and 3 days for the 80/20 mixture, and 3, 5 and 10 days for the 60/40 soil, for a total of 18 tests (9 per soil types). At the end of each experiment, the soil mixtures were sectioned to determine the water and oil contents of a predetermined number of samples. Additional laboratory work was carried out to characterize the soil mixtures, moulding liquids and motor oil used in this study.

The modelling of oil migration in an unsaturated soil was carried out with the one dimensional form of the classical diffusion equation. Using the oil concentration profile curves and the Boltzmann transform technique, the oil diffusivities, D, were computed. The

commercial program Tablecurve was then employed to determine the diffusivity function and parameters that best fit the computed D-θ relationship. The diffusivity function was then substituted in the finite difference form of the above-mentioned flow equation. By comparing the simulated results with the experimentally derived curves, the model was calibrated prior to predicting the time required to saturate the soil mixtures.

RÉSUMÉ

La présente étude se divise en deux grandes composantes: les expériences en laboratoire et la modélisation. L'élément central de la composante expérimentale est l'imbibition d'huile à moteur Ultramar 5W30 dans deux sols artificiels composés de sable siliceux et d'argile kaolinitique (80%/20% et 60%/40% au poids). Afin d'étudier l'influence des forces capillaires sur l'écoulement multiphase, trois séries d'essais ont été effectués sur chaque sol:

1. essais avec forces capillaires maximales, où les sols ont été mouillés avec de l'eau distillée;
2. essais avec forces capillaires intermédiaires, où les sols ont été mouillés avec une solution aqueuse de surfactif (3% v/v);
3. essais avec forces capillaires minimales, où les sols ont été mouillés avec une solution aqueuse plus concentrée de surfactif (6% v/v).

La durée de ces essais étaient de 1, 3 et 5 jours pour le sol 80/20, et de 3, 5 et 10 jours pour le sol 60/40, pour un total de 18 tests (9 par sol). À la fin de chaque expérience, les sols étaient sectionnés afin de mesurer la teneur en eau et en huile d'un nombre prédéterminé d'échantillons. Des test additionnels ont été effectués pour la caractérisation des sols, de l'eau distillée, des solutions de surfactif et de l'huile à moteur.

L'équation de diffusion unidimensionnelle a été utilisée pour modéliser l'écoulement de l'huile dans un sol non-saturé. La diffusion, D, de l'huile a été calculée en employant les profils de concentration d'huile et la technique de transformation de Boltzmann. À

l'aide du logiciel Tablecurve, une fonction de diffusion, et ses paramètres, représentant le mieux la relation entre la diffusion et la teneur volumétrique en huile ont été définis. Cette fonction a ensuite été incorporée dans l'équation de diffusion transformée en équation algébrique par la méthode des différences finies. Le model ainsi calibré, i.e., en comparant les simulations aux résultats expérimentaux, a été utilisé pour déterminer le temps requis pour saturer les sols en huile.

ACKNOWLEDGEMENTS

The author would like to express his sincere appreciation and gratitude to Dr. A.M.O. Mohamed, Associate Director, Geotechnical Research Centre, Faculty Lecturer, Department of Civil Engineering and Applied Mechanics, McGill University and Dr. R.N. Yong, Distinguished Research Professor, Division of Civil Engineering, Cardiff School of Engineering, University of Wales, Cardiff and Adjunct Professor, Department of Civil Engineering and Applied Mechanics, McGill University, for directing this research program and for their scientific and technical advice.

Much appreciation is expressed for the support and assistance given by the staff members of the Geotechnical Research Centre during the course of the laboratory work. Special thanks is given to Mr. F. Caporuscio for his technical assistance.

Finally, the author gratefully acknowledges the financial support provided by the Natural Sciences and Engineering Research Council of Canada (NSERC).

TABLE OF CONTENTS

ABSTRACT i

RÉSUMÉ iii

ACKNOWLEDGEMENTS v

LIST OF TABLES ix

LIST OF FIGURES x

CHAPTER 1 INTRODUCTION 1

1.1 STATEMENT OF THE PROBLEM 1

1.1.1 Oil Recovery from Oil Reservoirs 1

1.1.2 Non-Aqueous Phase Liquid Recovery from Contaminated Soils 3

1.2 OBJECTIVES 7

1.3 APPROACH 7

1.4 THESIS ORGANIZATION 8

CHAPTER 2 LITERATURE REVIEW 11

2.1 MECHANISMS OF MULTIPHASE FLOW 11

2.2 WETTABILITY 19

2.3 EFFECT OF WETTABILITY ON CAPILLARY PRESSURE 21

2.4 EFFECT OF WETTABILITY ON RELATIVE PERMEABILITY 27

2.5 REDUCTION OF CAPILLARY FORCES BY SURFACTANTS 29

2.6 GOVERNING EQUATIONS FOR MULTIPHASE FLOW 31

CHAPTER 3 EXPERIMENTATION 36

3.1 MATERIAL 37

3.2 APPARATUS 40
3.2.1 Oil Imbibition 40
3.2.2 Hydraulic Conductivity 41
3.2.3 Surface and Interfacial Tensions 41
3.2.4 Capillary-Moisture Content Relationship 41
3.3 SOIL SAMPLE PREPARATION 43
3.3.1 Oil Imbibition and Hydraulic Conductivity 43
3.3.2 Capillary-Moisture Content Relationship 44
3.4 EXPERIMENTAL PROCEDURE 44
3.4.1 Oil Imbibition 44
3.4.2 Geotechnical Characterization 47
3.4.3 Geochemical Characterization 47
3.4.4 Capillary-Moisture Content Relationship 50
CHAPTER 4 RESULTS AND DISCUSSION 51
4.1 EFFECT OF SURFACTANT ON PHASES INTERACTION 51
4.2 EFFECT OF SURFACTANT ON HYDRAULIC CONDUCTIVITY 59
4.3 OIL IMBIBITION 63
4.3.1 Oil Content Variations 63
4.3.2 Water Content Variations 68
4.3.3 Wetting Front Advance 69
CHAPTER 5 MODELLING 73
5.1 INTRODUCTION 73
5.2 GOVERNING EQUATIONS 75
5.3 CALCULATION OF OIL DIFFUSIVITY 76

5.4 DETERMINATION OF DIFFUSIVITY FUNCTION 80

5.5 MODEL CALIBRATION/SIMULATION 89

5.6 PREDICTION 92

CHAPTER 6 SUMMARY AND CONCLUSIONS 99

6.1 SUMMARY 99

6.2 CONCLUSIONS 100

6.3 SUGGESTIONS FOR FURTHER STUDIES 102

CHAPTER 7 REFERENCES 104

APPENDIX I TECHNICAL DRAWINGS OF THE LUCITE CELL AND MARIOTTE FLASK 116

APPENDIX II PHYSICAL TESTING ON THE SOIL MIXTURES 120

APPENDIX III CALCULATIONS 125

APPENDIX IV TURBO PASCAL COMPUTER PROGRAMS 139

LIST OF TABLES

Table 3.1 Soil material properties 38

Table 3.2 Properties of moulding liquids 39

Table 3.3 Ultramar 5W30 motor oil properties and composition 39

Table 4.1 Summary of calculated hydraulic conductivities 62

Table 5.1 Calculated parameters of the diffusivity function for 80/20 mixtures 83

Table 5.2 Calculated parameters of the diffusivity function for 60/40 mixtures 84

LIST OF FIGURES

Figure 1.1 Factors upon which the main types of enhanced oil recovery methods act . 3

Figure 1.2 Research program flow chart 9

Figure 2.1 Relative permeabilities as a function of saturation for: (a) two-phase flow, and (b) three-phase flow 14

Figure 2.2 Molecular attraction forces between two phases 16

Figure 2.3 Capillary forces in a system with two liquid phases in contact with a solid phase 17

Figure 2.4 Typical capillary pressure curves for: (a) strongly water-wet porous medium, and (b) strongly oil-wet porous medium 22

Figure 2.5 Oil displacing water from a pore for: (a) strongly oil-wet medium, and (b) strongly water-wet medium 28

Figure 2.6 Schematic of surface tension versus surface concentration 31

Figure 3.1 Molecular structure of surfactant compounds 40

Figure 3.2 Layout of oil imbibition apparatus 42

Figure 3.3 Schematic diagram of test procedure for oil imbibition and determination of oil and moisture content 46

Figure 3.4 Schematic diagram of procedure to measure surface and interfacial tensions 49

Figure 4.1 Capillary pressure curves for soil samples moulded with: (a) distilled water, and (b) 6% surfactant solution 52

Figure 4.2 Surface and interfacial tensions versus surfactant concentration 57

Figure 4.3 Oil concentration profile for 80/20 mixture after: (a) 1 day, (b) 2 days, and (c) 3 days 64-65

Figure 4.4 Oil concentration profile for 60/40 mixture after: (a) 3 days, (b) 5 days, and (c) 10 days 66-67

Figure 4.5 Oil concentration and moisture content profile for: (a) 80/20 moulded with distilled water after 1 day, and (b) 60/40 moulded with distilled water after 3 days 71

Figure 4.6 Oil front advance versus square root of time for (a) 80/20 mixture, and (b) 60/40 mixture 72

Figure 5.1 Calculation of diffusivity from volumetric oil content profile 79

Figure 5.2 Calculation of diffusivity program flow chart 81

Figure 5.3 Diffusivity versus volumetric oil content for 80/20 mixture moulded with: (a) distilled water, (b) 3% surfactant solution, and (c) 6% surfactant solution 85-86

Figure 5.4 Diffusivity versus volumetric oil content for 60/40 mixture moulded with: (a) distilled water, (b) 3% surfactant solution, and (c) 6% surfactant solution 87-88

Figure 5.5 Volumetric oil content prediction program flow chart 90

Figure 5.6 Grid used for oil migration simulation 91

Figure 5.7 Comparison of simulated and experimental oil concentration profiles for 80/20 mixture moulded with: (a) distilled water, (b) 3% surfactant solution, and (c) 6% surfactant solution 93-94

Figure 5.8 Comparison of simulated and experimental oil concentration profiles for 60/40 mixture moulded with: (a) distilled water, (b) 3% surfactant solution, and (c) 6% surfactant solution 95-96

Figure 5.9 Predicted oil concentration profile curves 98

Tech dwg End caps, top view 117

Tech dwg Plexiglass cell, cross-section 118

Tech dwg Mariotte flask, side view 119

Figure II.1 Particle size distribution for 80% sand and 20% kaolinite 121

Figure II.2 Particle size distribution for 60% sand and 40% kaolinite 122

Figure II.3 Dry density-water content relationship for 80% sand and 20% kaolinite 123

Figure II.4 Dry density-water content relationship for 60% sand and 40% kaolinite 124

CHAPTER 1

INTRODUCTION

1.1 STATEMENT OF THE PROBLEM

1.1.1 Oil Recovery from Oil Reservoirs

In the 1990s, the demand for petroleum products remains very high as it is used for various fuels, lubricants, synthetic rubber, synthetic fibres, plastics, drugs and a myriad of other products. It is anticipated that industrialized countries will continue to be highly dependent on crude oil as a source of energy for transportation and raw material for petrochemicals. The World Energy Conference held in Montréal in September 1989 concluded that "oil will remain the leading energy source during the first half of the 21st century".

While the demand for petroleum products continues to be high, domestic petroleum production in North America is in steady decline since most existing oil reservoirs are in the final stages of production, i.e., production declines from peak years (Carcoana, 1992). Alternative transportation energy sources, such as nuclear, hydroelectric, solar and wind are still under development but are not expected to be available in the near future. Consequently, the balance of the oil demand is satisfied by imports from OPEC countries. As a means to reduce this reliance on foreign supply, which is considered detrimental to the economy and national security, new techniques are being developed to improve the efficiency of domestic production.

Conventional practice in the oil industry involved the recovery of oil in two successive periods of production, i.e., primary and secondary recovery. However, at the end of these stages, only a fraction of the original oil in place (OOIP) was usually recovered since parts of the reservoir were not swept due to high oil viscosity and reservoir heterogeneity, and/or pore spaces still contained a large proportion of oil as a result of poor microscopic displacement efficiency due to capillary forces.

It is now common practice to use enhanced oil recovery (EOR) techniques at the very beginning of the reservoir exploitation to improve the efficiency of oil production. Experts evaluate that about 100 billion tonnes could be recovered by EOR. According to Bavière (1991), the goal is to raise the oil recovery factor from about 30% to 45% of OOIP. Considering that 1% of the total amount of the oil discovered roughly represents world consumption over two years, the implications are great.

Some EOR processes are designed to ameliorate either sweep or displacement efficiency, whereas other methods aim at increasing both aspects. Figure 1.1 summarizes the main type of EOR techniques and the factors upon which they act. The use of surfactants and alkaline agents is very promising but still requires great research efforts to reduce the cost-efficiency ratio. It is very complex, expensive and requires extensive laboratory testing before field implementation. A successful surfactant flood must (1) mobilize the oil and reduce the residual saturation to near zero by lowering the interfacial tension by several orders of magnitude; (2) minimize the retention of the surfactant, via capillary phenomena, precipitation, and adsorption, so that it can be propagated across the entire reservoir using only a small amount of injected surfactant; (3) maintain good

mobility control by ensuring that each bank is less mobile than the one it is displacing, therefore promoting high sweep efficiency; and (4) the reservoir characterization and reservoir engineering must consider the characteristics of the reservoir (Pope and Bavière, 1991).

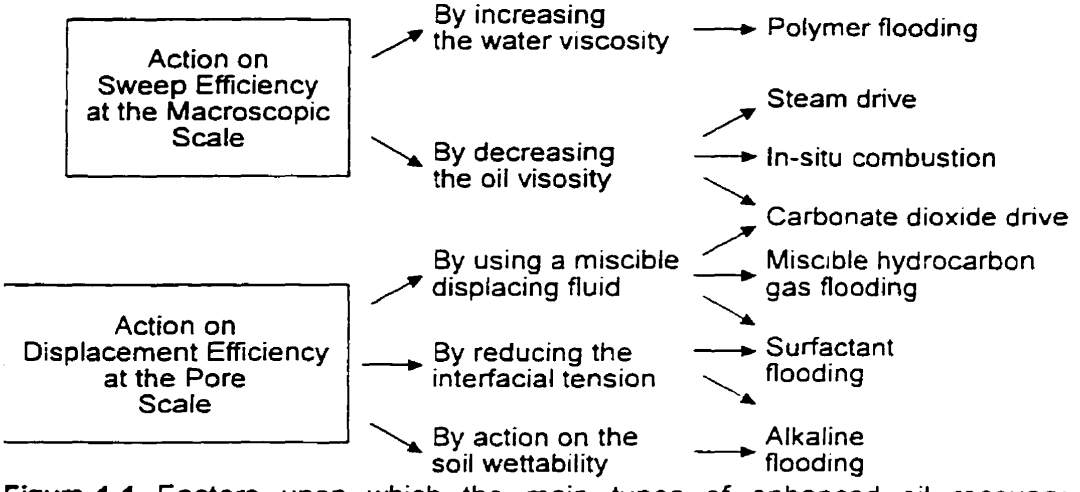

Figure 1.1. Factors upon which the main types of enhanced oil recovery methods act (from Marle, 1991).

Although most principles applied in EOR methods have been known for a long time, a number of research problems related to surfactant flooding still needs to be addressed. Among them, the role of low interfacial tension, hydrodynamic pressure difference, pore geometry, and interfacial viscosity of the oil-water interface needs to be clearly established.

1.1.2 Non-Aqueous Phase Liquid Recovery from Contaminated Soils

More recently, frequent discoveries of groundwater contamination by industrial products from atmospheric deposition, spills, leakage from underground storage tanks (USTs) and waste disposal sites have raised environmental concerns. Since the second world war, the variety and quantity of organic chemicals being produced has significantly

increased. Many of these chemicals, known as immiscible or non-aqueous phase liquids (NAPLs), slightly dissolve in water. However, because of their high toxicity, they have solubilities orders of magnitude greater than the drinking water standards. Further, investigation of contamination incidences indicate that some NAPLs, such as petroleum hydrocarbons (PHCs), are persistent. Because of these physicochemical and biological properties, PHCs can contaminate large volumes of groundwater. i.e., as much as 10,000 times their own volume (Mackay et al., 1985).

About 95% of fresh water, which represents 3% of the total water, is groundwater. Furthermore, less than half of one percent of fresh water is easily available to users. Groundwater is a major natural resource that serves many anthropogenic functions. It is an important source of drinking water, and is used for irrigation and industrial purposes. This resource also serves many vital ecological functions by providing fresh water for many lakes, rivers, inland wetlands, bays and estuaries. Although current estimates suggest that only a small percentage of groundwater is contaminated, incidences are often found in areas that heavily depend on this resource, since until recently the location of industries and waste disposal sites was not subjected to any environmental regulation.

The unsaturated zone is a key factor in the improvement and protection of groundwater supplies. The significance of this zone arises from its possible function as a protective buffer over the aquifer (Nielsen et al., 1986; Hillel, 1989). Unfortunately, until recently, research efforts mainly focused on groundwater pollution since the importance of contaminant behaviour in the unsaturated zone was not fully appreciated. Consequently, there is a lack of experimental and theoretical understanding of the

behaviour of organic contaminants in the unsaturated zone, which precludes accurate prediction and management of contaminant transport through it.

Pump and treat has been the remediation method used on a number of sites where groundwater is contaminated. It is generally considered that for NAPLs, this method can be effective at preventing the compounds from spreading, but is not very efficient at cleaning aquifers to drinking water standards (Hasbach, 1993; Brown et al., 1995). Often, there is a dramatic initial reduction in contamination, but when pumping stops the residual phase continues to dissolve, recontaminating the groundwater. According to Sabatini et al. (1995), this is in part due to the fact that a conventional pump and treat method only manages to remove the dilute portion of the groundwater plume, which, for NAPLs, is an important limiting factor due to mass transfer constraints (desorption of strongly hydrophobic contaminants or dissolution of residual saturation). Further, the trapped phase in the unsaturated zone may serve as a long term source of contamination to infiltrating rain water or a rising water table (Abriola, 1984). Consequently, to effectively address NAPL subsurface contamination, it is essential to deal with all four phases, i.e., the immiscible phase in the pores, the adsorbed phase, the soluble phase and the vapour phase. This requires that both the soil and groundwater be cleaned up using appropriate technologies.

Surfactant-based remediation technologies were identified as a promising avenue to remediate NAPL contaminated sites. Surfactants are generally used to enhance mobilization by reducing surficial forces responsible for droplet retention and/or to increase the aqueous solubility by micellar solubilization. For light non-aqueous phase liquids

(LNAPLs) mobilization is likely to be the primary recovery mechanism, whereas for dense compounds (DNAPLs) solubilization is preferred unless it can be confined and prevented from migrating vertically (Pope and Wade, 1995). In situ soil flushing, which is the logical extension of oil recovery techniques applied in the petroleum industry, can be used to address the source of contamination in the unsaturated zone by accelerating the mobilization of LNAPLs for recovery and treatment. It basically consists of applying or injecting a surfactant solution into the undisturbed soil and recovering the mobilized contaminant and injected fluid(s).

Although surfactant-based technologies are generally considered among the most promising emerging techniques, they are still at the developmental stage. Bench scale tests of soil flushing have been very successful, but field applications have not demonstrated the same success. Mann (1993) considered that a better understanding of the unsaturated zone is required to successfully implement this technique.

Finally, as pointed out by Abriola (1984), because it is difficult to remediate a contaminated site, it becomes important to study the processes involved in an effort to predict the migration of NAPLs and its potential impact on the groundwater or the performance of a remediation technique at the field scale. This is a formidable challenge when considering that subsurface contamination is a complex environmental problem because the transport of chemicals can involve multiple phases with a large number of potential reactions in nonhomogeneous, anisotropic media.

1.2 OBJECTIVES

The objectives of the present research can be summarized as follows:

1. To develop a simple experimental program, including the design of oil imbibition apparatus and procedure, that will allow the study of phenomena associated with multiphase flow in unsaturated porous media.
2. To evaluate the effect of capillary forces on the migration of non-aqueous phase liquid in unsaturated clay soil.
3. To quantify the movement of NAPL via a diffusivity function.
4. To develop a mathematical model for the simulation of oil migration, and compare with experimental data.

Besides the above mentioned objectives, the following questions will be posed:

1. What are the effects of the surfactant on the soil properties?
2. How effective is this surfactant at cleaning a contaminated soil?

These questions will be answered through a detailed research program that involved both oil imbibition experiments and characterization testing.

1.3 APPROACH

To achieve the above objectives, several oil imbibition experiments were performed on the following systems:

1. Maximum capillary forces system, in which the soil was moulded with distilled water.
2. Intermediate capillary forces system, in which the soil was moulded with 3%

aqueous surfactant solution.

3. Minimum capillary forces system, in which the soil was moulded with 6% aqueous surfactant solution.

At the end of the experiments, oil and moisture profile curves were determined by measuring moisture and oil content at several locations of the soil column.

The diffusivity, D, was computed using the method described by Wong (1973), which is a simplified version of that proposed by Bruce and Klute (1956). The method basically uses the profile curve to compute the value of the diffusivity as a function of volumetric oil content. Based on this information, an equation for D was proposed and the optimum parameters characterizing the function were obtained using a commercially available computer program (Tablecurve by Jandel Scientific, 1991).

Finally, by using a computer program with an explicit finite difference scheme, a simulation of oil migration was performed. For further details of the approach taken in this study see Figure 1.2.

1.4 THESIS ORGANIZATION

The thesis includes seven chapters and three appendices as follows:

Chapter 1 is an introductory chapter;

Chapter 2 presents a literature review of studies on the mechanisms of multiphase flow in the unsaturated (vadose) zone, their effects, and modelling equations;

Chapter 3 presents the experiments;

Chapter 4 presents the experimental results;

Chapter 5 presents the determination of the diffusivity function and parameters, and modelling;

Chapter 6 presents summary and conclusions with suggestions for further studies;

Chapter 7 presents references;

Appendix I presents technical drawings of the lucite cell and Mariotte flask;

Appendix II presents results of some physical testing on the soil mixtures;

Appendix III presents calculations of the thickness of the diffuse ion layer around kaolinite particles and the energies of interaction between two kaolinite particles;

Appendix IV presents the computer programs to determine the diffusivity parameter and to predict the migration of oil.

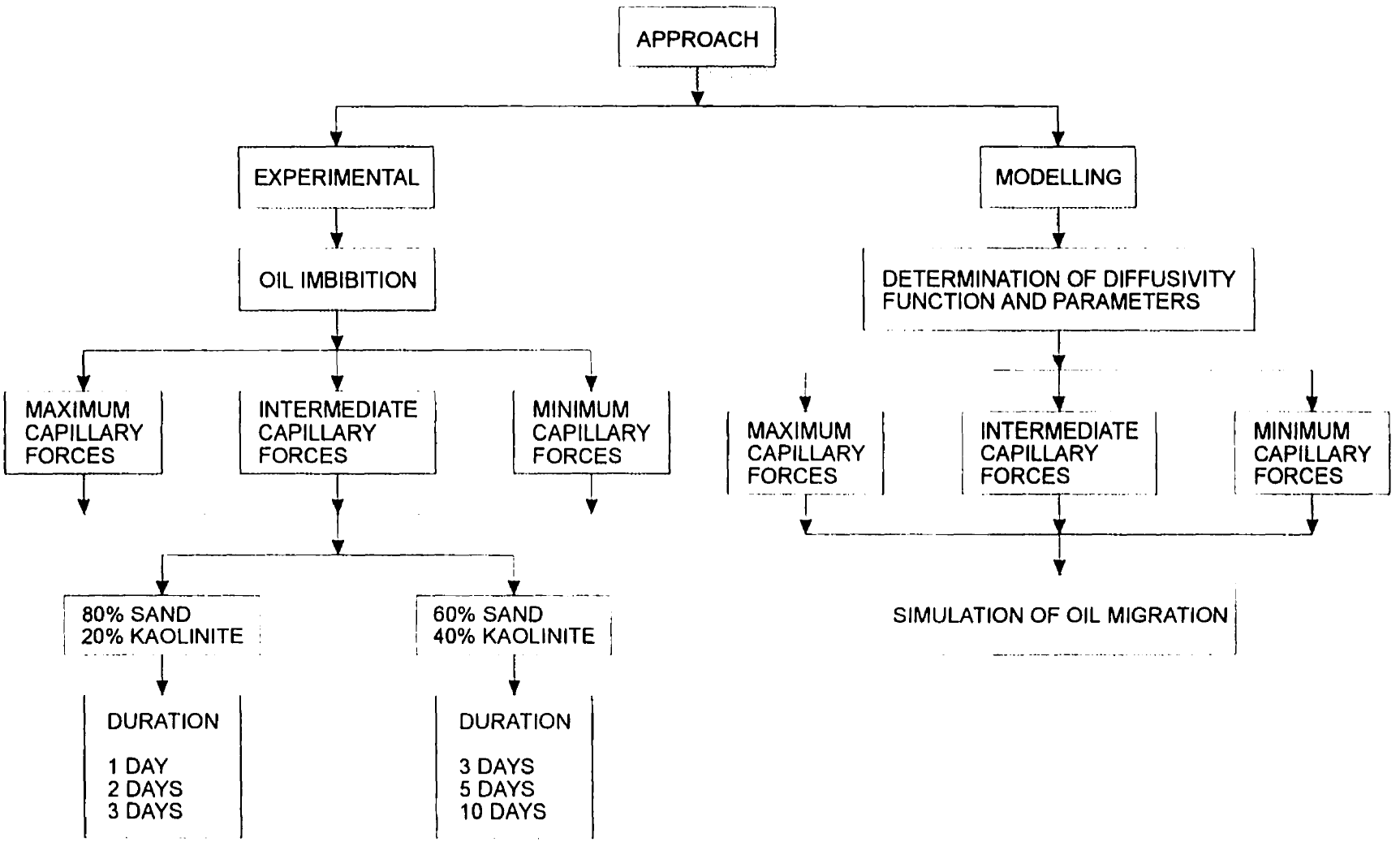

Figure 1.2. Research program flow chart.

CHAPTER 2

LITERATURE REVIEW

2.1 MECHANISMS OF MULTIPHASE FLOW

An organic contaminant released to the subsurface may be transported as a solute, a vapour, or a liquid immiscible phase, depending on the local conditions and the physicochemical properties of the compound. In all cases, the soil's ability to convey a fluid, represented by the hydraulic conductivity, is of prime importance. The movement of liquid organic chemicals that do not readily dissolve in water is governed by a set of factors different from those for dissolved organic chemicals. The migration of immiscible liquids in a soil is controlled by complex interactions of physical, chemical and biological processes. This section reviews the main physical and chemical mechanisms that are thought to affect PHC migration in the unsaturated zone.

According to Yong and Warkentin (1975), the behaviour of clay soils in relation to fluid movement is largely determined by the flow in the macropores. The size and arrangement of fabric units determine the distribution of void sizes and shapes. Permeability changes during permeation with chemicals can be largely explained on the basis of soil fabric alterations due to clay-chemical interactions (Mitchell and Madsen, 1987). Studies on the subject (Michaels and Lin, 1954; Acar et al., 1985; Fernandez and Quigley, 1988) showed that the low dielectric constant of nonpolar organics can cause the diffuse layer to depress, consequently changing the soil fabric. Mesri and Olson (1971) explained that clay particles tend to form stable aggregates more-or-less spherical in

shape with nonpolar fluids, whereas with water the formation of aggregates of parallel particles, termed domains, is more likely. Thus, for a constant void ratio, the channels between spherical aggregates would be considerably larger in size than those between domains, resulting in a smaller rate of flow in the latter case.

Mitchell and Madsen (1987) concluded that dilute solutions, i.e., at or below the solubility limit of the hydrocarbon in water have no effect on the permeability, whereas permeation with pure hydrocarbons invariably does. They also determined, based on a number of studies (Brown et al, 1984; Anderson et al., 1985; Brown et al., 1986), that permeation with pure hydrocarbons of a water saturated clay soil in a rigid cell permeater causes the hydraulic conductivity to increase. The literature on the subject does not fully support this conclusion. Results of investigations by Green et al. (1981) and Fernandez and Quigley (1985) suggest that under certain conditions the permeability increase does not occur.

Some insight is provided by research in the petroleum industry on multiphase flow. Anderson (1987b) explained that a soil's ability to convey a fluid when one or more fluids are present depends on the composite effect of wettability, pore geometry, fluid distribution, and saturation history. The fluid distribution (i.e., the range of pore size that each fluid occupies) depends on the wettability, the interfacial tension of the fluids and capillary pressure. Thus, for a hydrophillic porous medium, if the interfacial tension is sufficiently low and/or the pressure head sufficiently high, the nonpolar permeant will be able to penetrate in the micropores and alter the soil fabric, with a subsequent increase in permeability. Work by Fernandez and Quigley (1985) accredits this theory since they

found no significant increase in permeability when the hydrocarbon remained in the macropores, whereas it dramatically increased during three-stage permeation with an intermediate phase soluble in both water and the hydrocarbon. This caused a reduction in interfacial tension, thus permitting the hydrocarbon to enter the micropores.

The ability of a fluid to permeate a porous medium is reduced when there are several immiscible fluids present in the interstices. This phenomenon is described in terms of relative permeability and is defined in geoenvironmetal engineering as the ratio of the effective permeability of a fluid at a given saturation to the permeability at 100 per cent saturation:

$$k_{rp} = \frac{k_{ep}(S_p)}{k_p} \qquad (2.1)$$

where k_{rp} is the relative permeability, $k_{ep}(S_p)$ is the effective permeability at saturation S_p, and k_p is the permeability at complete saturation with phase p. Figure 2.1 shows typical relative permeability curves and isoperms for two-phase and three-phase flows respectively. From these diagrams, Schwille (1967) and van Dam (1967) pointed out a number of important characteristics for an air-oil-water system:

1. Below a certain degree of saturation, the fluids are immobile. This minimum value is coined irreducible water content for water, and residual oil saturation for oil.
2. The 1% water isoperm is almost parallel to the oil axis, indicating that the irreducible water content does not depend on oil and air saturations.
3. The convex shape of the 1% air isoperm with a maximum value near the

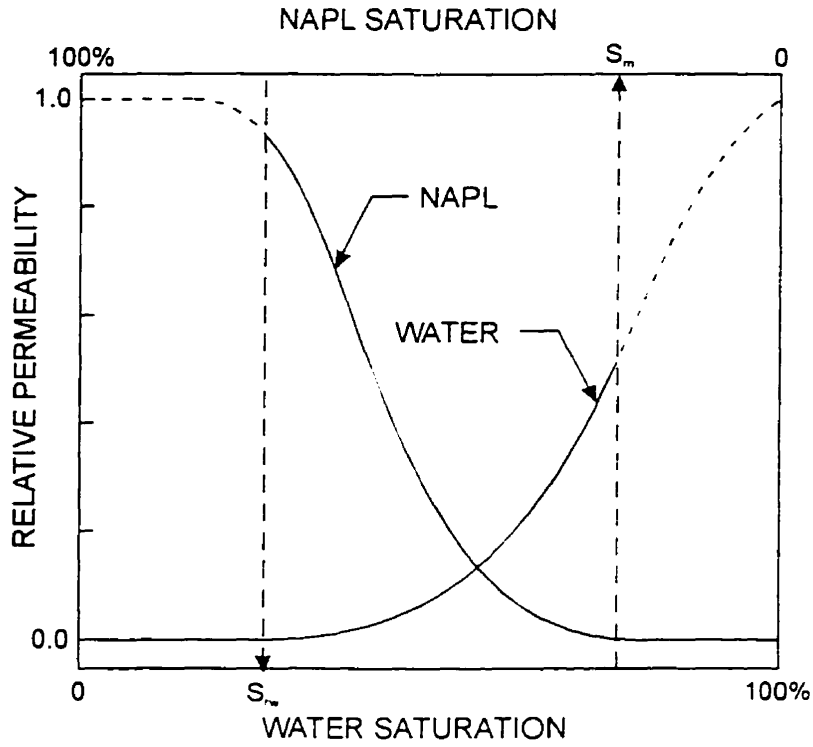

(a)

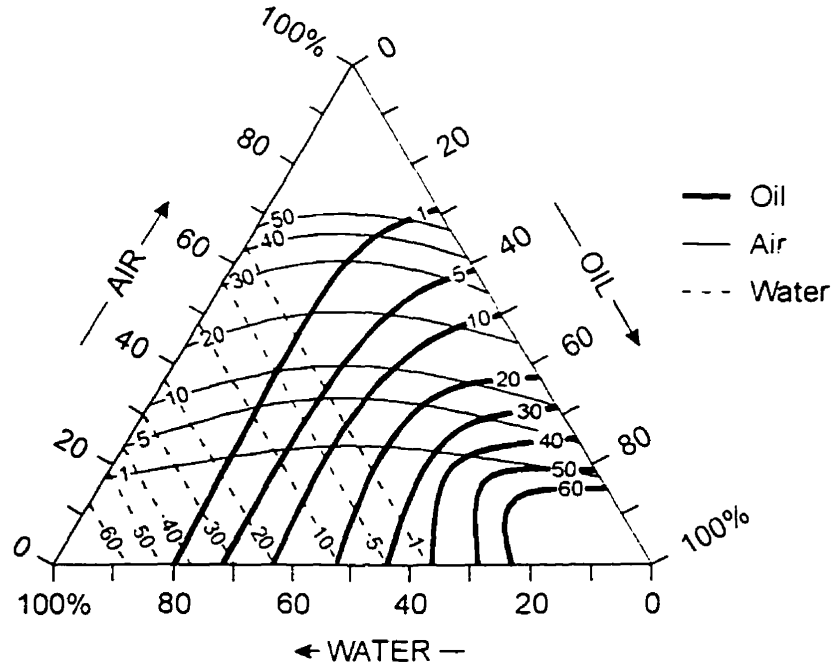

(b)

Figure 2.1. Relative permeabilities as a function of saturation for: (a) two-phase flow (adapted from Palmer and Johnson, 1989), and (b) three-phase flow (adapted from van Dam, 1967).

central region of the diagram suggests that the residual air saturation is largest where oil and water saturations are similar.

4. The residual oil saturation is largest below the irreducible water saturation and becomes nearly constant with increasing water content.
5. Simultaneous flow of all three phases occurs in a very limited region. It is more likely to have at least one of the three fluids immobile.
6. The distance between any two oil isoperms remains relatively constant, e.g., the distance between the 20% and 30% isoperms is the same from the oil axis to the water axis. This suggests that permeability change is by and large independent of the fluids restricting the pore space.
7. At low saturation, permeability changes more slowly.

For a given porous medium and group of fluids, it is generally assumed that the relative permeabilities depend only on the fluids saturation. However, this relationship is not unique as it shows hysteresis effects

Schwille (1967) described the migration process of oil in the unsaturated zone. Initially, the movement of the core of the infiltration body is primarily downward under the influence of gravitational forces. Around this oil percolation zone, a belt comparable in origin to the capillary fringe of an aquifer develops. In this oil wetting zone, the movement occurs in all directions due to capillary forces, with the oil saturation decreasing in an outward direction. If only a small volume of oil is involved, the migration zone may attain residual saturation before reaching the water table. On the other hand, when the volume is large, downward seepage ceases when the front reaches the water table or an

impermeable boundary. As the oil accumulates on the barrier, it spreads laterally, predominantly in the direction of groundwater flow. This movement initially occurs in response to gravity forces and later to capillary forces.

Calhoun (1953) defined capillary forces as the forces which express the molecular action between the various solid, liquid, and gas phases. Interfacial tension, which arises due to an unbalance of molecular forces, characterizes the contact between two phases. Figure 2.2 illustrates an interface between a liquid and a gas. A molecule inside the liquid phase is attracted in all directions by equal attraction forces, whereas a molecule at the surface is subjected to smaller forces from the molecules in the adjacent phase. By looking at it from the energy standpoint, Rosen (1989) explained that surface molecules have potential energies greater than those in the interior of the liquid. Interfacial tension is therefore a measure of the work required to bring sufficient molecules to the surface from the interior to expand it by unit area. When the interaction between molecules of adjacent phases is large, the interfacial tension is small since less work is required to expand the interface. The value of the interfacial tension is therefore an indication of the similarity (or dissimilarity) of the two phases.

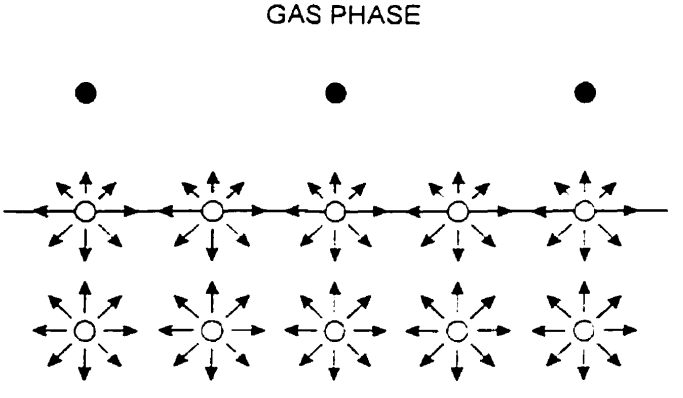

Figure 2.2. Molecular attraction forces between two phases.

According to Stumm and Morgan (1981), the intermolecular interactions producing surface tension in water are essentially composed of London - van der Waals dispersion attractions and hydrogen bonds, whereby about one-third is due to the former attraction, and two-thirds to the latter interaction mechanism. For liquid hydrocarbons the intermolecular attraction is almost exclusively attributed to London dispersion forces. For other liquids, the surface tension is due to dispersion forces and to more specific chemical forces such as hydrogen bonding, pi electron interactions in aromatic solvents, and metallic bonds in metals.

Figure 2.3 shows the capillary forces present when two liquid phases are in contact with a solid phase. The capillary forces are tangential to the interfaces, and directed towards these interfaces. The fluid that has the lowest interfacial tension with the solid preferentially wets the substrate by displacing the other fluid. At equilibrium, a characteristic contact angle (θ_{ABS}) is formed at the point where all three phases meet.

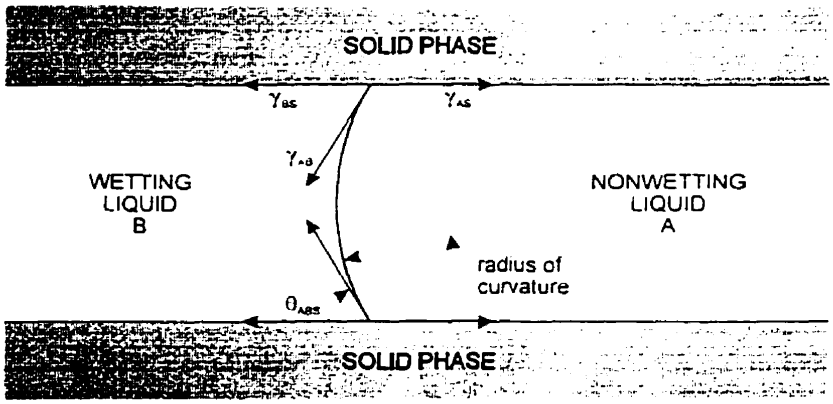

Figure 2.3. Capillary forces in a system with two liquid phases in contact with a solid phase.

The interactions between soil substrate and organic compounds can play an important role in the retardation of petroleum hydrocarbons (Yong and Rao, 1991). The

surface reactivity of the solid phase depends largely on the chemical behaviour of the surface functional groups. According to Yong (1987), both the inorganic hydroxyl and organic functional groups define the ability of a soil to attenuate a contaminant via adsorption reactions. Sposito (1989) also considered the ditrigonal cavity on the tetrahedral layer as a surface functional group capable of adsorption.

The inorganic hydroxyl surface functional group (OH^-) can be found in clay minerals, amorphous silicate materials, metal oxides, oxyhydroxides, and hydroxides. In general, the reactivity of this group depends on its coordination to the structure of the solid and can vary within the same soil particle. It develops a positive charge by protonation or a negative charge by deprotonation depending on the pH of the wetting liquid (Yong et al., 1992). The reactivity of the ditrigonal cavity depends on the nature of the layer charge.

Organic surface functional groups include carbonyl (–CO), amino ($–NH_2$), sulfhydryl (–SH), carboxyl (–COOH), and hydroxyl (phenolic and alcoholic) groups. Similarly to the inorganic hydroxyl, these functional groups have the ability to protonate or deprotonate depending on the pH of the surrounding liquid and their respective pK_a or pK_b (Yong et al., 1992).

The mechanisms of clay-organic interactions is a very wide and complex topic, which goes beyond the scope of this discussion. Readers can find a large body of literature reviewing these interactions (Mortland, 1970, Theng, 1974; Theng, 1982, Mortland, 1986). The discussion will therefore be limited to PHCs.

In general, PHC molecules are nonpolar with dipole moments less than 1, dielectric constants less than 3 (Yong et al., 1992), and have no electron-withdrawing units such as C = O and C = N resulting in a low CH activity of the molecule (Yong and Rao, 1991). According to Hoffman and Brindley (1960), the adsorption of nonionic organic compounds by clays is controlled by the CH activity, suggesting that PHCs are weakly adsorbed by the soil functional groups. By measuring low heats of adsorption for eicosane (an alkane) and anthracene (a polycyclic aromatic hydrocarbon), Meyers and Quinn (1973) concluded that the interaction is mainly by van der Waals attraction. According to van Olphen (1963), this force is small and decays rapidly with distance (inversely proportional to the 7^{th} power of distance) for a pair of short length molecules. However, van der Waals attraction is additive, resulting in a less rapid decay for molecules with a long structure (inversely proportional to the 3^{rd} power of distance).

Yong and Rao (1991) indicated that adsorption of hydrocarbons on clay surfaces occurs only when the solubility of the hydrocarbon is exceeded and the molecules aggregate in micelles. This phenomenon enhances van der Waals attraction due to the additive effect of combined molecules in a micelle.

2.2 WETTABILITY

Wettability is defined as "the tendency of one fluid to spread on or adhere to a solid surface in the presence of other immiscible fluids" (Craig, 1971). It is a major factor controlling the location, flow and distribution of fluids in a soil. In a porous medium that has definite preference for either of the fluid phases, the wetting phase has a tendency to occupy the smallest pores and to contact the substrate while the nonwetting phase is

consigned to the centre of the larger pores.

The wettability of a solid phase is determined by the polarity of the surface. Minerals with polar surfaces, such as quartz, clays, carbonates and sulphates are strongly water-wet, whereas a few minerals with nonpolar surfaces, such as sulphur, graphite, talc, coal, and many sulphides are mildly water-wet (hydrophillic) to oil-wet (organophillic) (Gaudin, 1957). The wettability of strongly water-wet minerals can be modified by the adsorption of organic polar compounds. The polar end adsorbs on the mineral surface, exposing the hydrocarbon end and making the surface organophillic. Boyd et al. (1988) found that hexadecyltrimethylammonium (HDTMA) enhances the organic sorptive capabilities of smectite. Research in the petroleum industry showed that the adsorption of asphaltenes and resins onto clays can make the mineral more oil-wet (Clementz, 1976; Somerton and Clayton, 1980; Collins and Melrose, 1983).

The contact angle (Figure 2.3), measured through the water phase, is used to specify the wettability of a porous medium. When the angle is between 0 and 60 to 75°, the solid phase is usually considered water-wet, whereas an angle between 180 and 105 to 120° defines an oil-wet surface. An angle of 90° indicates that neither fluid preferentially wets the solid (Anderson, 1986b, 1987a). On most surfaces a range of angles will be measured, the exception being a smooth and very homogeneous substrate. The maximum angle is obtained when the liquid is advancing, and the smallest when the liquid is receding. According to Anderson (1986b), there appears to be three causes for this display of hysteresis: (1) surface roughness, (2) surface heterogeneity, and (3) surface immobility on a macromolecular scale.

Changes in wettability have been shown to affect capillary pressure, relative permeability, irreducible water saturation, and residual oil saturation (Anderson, 1986a). The next two sections review in greater details these effects.

2.3 EFFECT OF WETTABILITY ON CAPILLARY PRESSURE

The following discussion is based on the article by Anderson (1987a). Whenever a curved interface exists, the pressure abruptly changes across the interface. This pressure jump, which is termed the capillary pressure, is given by the Laplace equation:

$$P_c = P_A - P_B = \gamma_{AB}\left(\frac{1}{r_1} + \frac{1}{r_2}\right) \qquad (2.2)$$

where P_c is the capillary pressure, P_A the pressure in the nonwetting phase, P_B the pressure in the wetting phase, γ_{AB} the interfacial tension between the two phases, and r_1 and r_2 the radii of curvature of the interface. In an oil-water system, Anderson (1987a) defined the capillary pressure as $p_{oil} - p_{water}$, since oil is usually the nonwetting phase and water the wetting liquid. Equation 2.2 was derived assuming that fluid phase pressures are governed strictly by capillary forces. However, as the wetting fluid thickness on the solid phase approach molecular dimensions, forces other than capillary forces may significantly affect the fluid pressure (Parker, 1989). Under those conditions the equation is no longer accurate.

Typical capillary pressure curves are shown in Figure 2.4 for water- and oil-wet media. Curve 1, the drainage capillary pressure curve is obtained by increasing the capillary pressure, causing the nonwetting phase to displace the wetting fluid. This

process continues until the wetting phase saturation is reduced to its irreducible saturation (point A). At that point the wetting phase remaining in the core is disconnected and hydraulic continuity is lost. The reverse process is then initiated by gradually reducing the capillary pressure to zero, allowing the wetting phase to imbibe. In general, the nonwetting phase saturation at zero pressure (point B) is still connected and is not considered to be residual. The curve between points A and B is referred to as the spontaneous imbibition curve as no external work is required for this process to occur. The displacement of the nonwetting phase by the wetting fluid can be further pursued by decreasing the capillary pressure to large negative values. The nonwetting phase saturation continues to decrease up to a point where it becomes disconnected (point C). This saturation where hydraulic continuity of the nonwetting phase is lost is called the residual saturation. Curve 3 is known as the forced imbibition curve since external work is needed to displace additional oil from its saturation at point B.

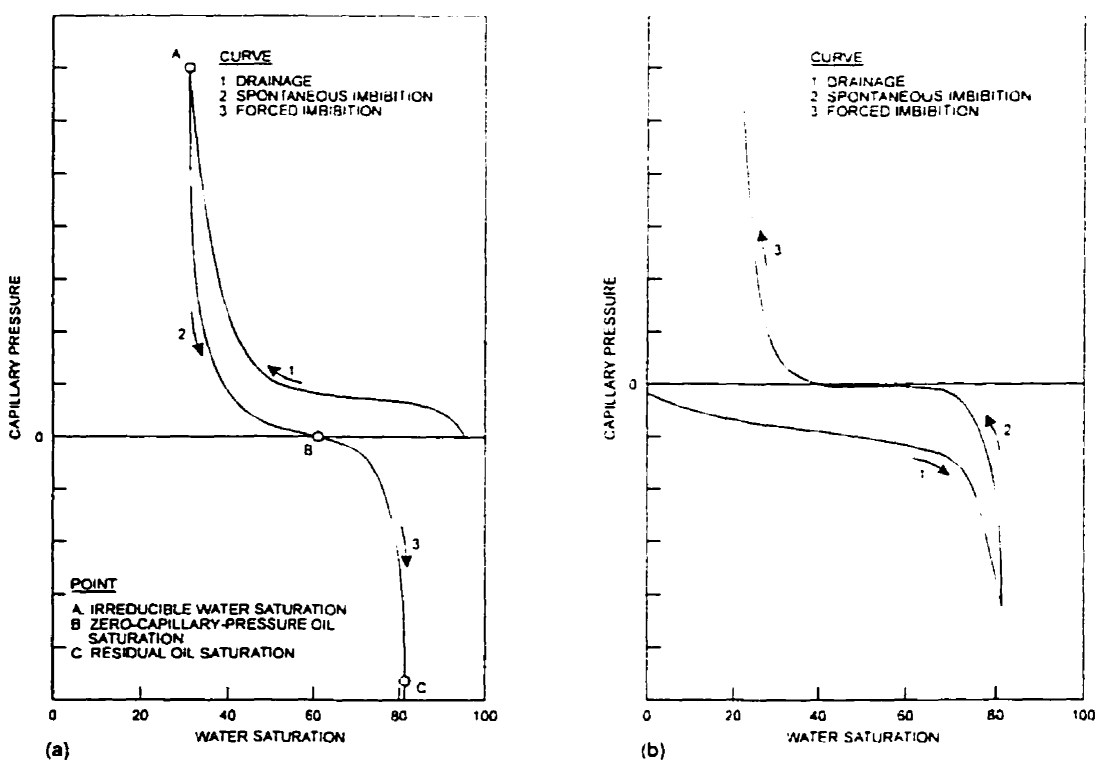

Figure 2.4. Typical capillary pressure curves for: (a) strongly water-wet porous medium, and (b) strongly oil-wet porous medium (adapted from Anderson, 1987a).

Generally, the drainage and imbibition curves are different. Hysteresis in the capillary pressure-saturation relation is partially caused by the contact angle hysteresis. In the drainage process, the wetting fluid is being displaced by the nonwetting phase, and the contact angle is the receding angle. During imbibition, the contact angle is the advancing one. Another cause of hysteresis is the ink bottle effect (Yong and Warkentin, 1975).

When the wetting fluid displaces the nonwetting fluid, little or no work must be expended on the system because of the favourable free energy change. Conversely, the displacement of the wetting phase by the nonwetting phase requires work to be done on the system. Morrow (1970a) demonstrated that the area under the capillary pressure curve represents the work required for the displacement of one fluid by another:

$$\Delta W_{ext} = -\Phi V_b \int_{S_{w_i}}^{S_{w_f}} P_c \, dS_w \qquad (2.3)$$

$$\Delta W_{ext} = \Phi V_b \int_{S_{o_i}}^{S_{o_f}} P_c \, dS_o \qquad (2.4)$$

where V_b and Φ are the bulk volume and the porosity of the soil sample respectively, S_w the water saturation, and S_o the oil saturation. Equation 2.3 represents the area under the drainage curve of a water-wet medium, and quantifies the external work required for oil to displace water. Equation 2.4, is the work required for water to displace oil and represents the area under the forced imbibition curve. The ratio of these curves shows the degree of water wetness and is the basis of the quantitative United States Bureau of Mines (USBM) method to determine wettability preference.

As the soil solid phase changes from strong wetting preferences to neutrally wet, the area under the drainage curve and the amount of spontaneous imbibition decreases. This occurs because less work is required for drainage and the driving force for imbibition is reduced. It implies that the nonwetting fluid is able to enter pores of smaller size as the medium becomes more neutrally wet.

Fatt and Klikoff (1959) examined the effect of wettability on the capillary pressure-saturation relationship of a fractional wettability system by mixing in different proportions water-wet and oil-wet sand grains. Their results generally show that as the fraction of oil-wet sand increases, the water saturation decreases at a given pressure. This implies that it is easier for the oil to displace water. They also observed that a porous medium with only the fines being oil-wet has a markedly different behaviour from a similar medium with oil-wet particles distributed over the entire size-range. This indicates that the location of the oil-wet vs. water-wet surfaces is important.

Work by Morrow and Mungan (1971) and Morrow (1976) with teflon cores and an assortment of pure organic fluids, including saturated hydrocarbons, showed that for uniformly wetted medium, the air-fluid drainage curve is insensitive to wettability when the contact angle, measured through the fluid, is less than 50°. This insensitivity is due to pore geometry effects and surface roughness (Anderson, 1987a). As the contact angle is increased beyond this threshold value, the fluid saturation decreases more rapidly with increasing capillary pressure, and the curve starts to develop a sharp knee. Similarly, the air-fluid spontaneous imbibition curve is not influenced by wettability when the contact angle is less than approximately 20°. Above this value, as the solid's affinity for the

organic fluid diminishes, the saturation increase is less pronounced with decreasing capillary pressure. The difference in threshold values for drainage and spontaneous imbibition is due to the different behaviour of the advancing and receding angles (Anderson, 1987a).

Experimental work by a number of investigators (Morrow and Mungan, 1971; Lorenz et al., 1974; McGhee et al., 1979) on uniformly wetted samples showed that the minimum irreducible and residual saturations are reached at around neutral wettability. As pointed out by Anderson (1987a), the irreducible wetting and residual nonwetting phase saturations depend not only on wettability, but also on pore structure and saturation history. In systems with simple geometry, such as beads and sandpacks, it was observed that wettability effects on these minimum saturations become unimportant.

There is some disagreement on the effects of wettability on the irreducible wetting phase saturation of fractionally wetted samples. Morrow (1970b), working with teflon and glass beads, and Fatt and Klikoff (1959), working with sandpacks, found only a small effect of wettability when all of the particle sizes had equivalent amounts of water-wet and oil-wet surfaces. Talash and Crawford (1961a, b) observed a significant decrease in irreducible water saturation as the proportion of oil-wet sand grains increased.

Additional effects occur in mixed wettability systems where water- and oil-wet surfaces are organized in some fashion (Anderson, 1987a). A number of investigators (Richardson et al., 1955; Schmid, C., 1964) concluded that mixed-wettability cores have a much higher irreducible wetting saturation than the same cores after they are cleaned

and made uniformly water-wet. According to Anderson (1987a), this is a result of faster trapping and loss of hydraulic continuity.

Morrow and Mungan (1971) and Morrow (1976) observed that the nonwetting phase (air) zero-capillary-pressure saturation increased as the affinity of the teflon core for the wetting phase (organic fluid) decreased. This is the exact opposite of the residual nonwetting phase saturation, which reaches a minimum around neutral wettability.

Imbibition is driven by the favourable free surface energy change and the rate and amount depend on the wettability, viscosity, interfacial tension, pore structure, saturation history, and initial saturation of the medium (Anderson, 1987a). In a strongly wetted soil, a large amount of wetting fluid imbibes rapidly due to the great decrease in free surface energy, whereas a smaller volume of the same fluid imbibes at a slower rate into a less strongly wetted medium. On the other hand, the pressure required to force the nonwetting fluid into the porous medium decreases as the medium becomes more neutrally wet.

Although spontaneous imbibition is expected to occur in uniformly wetted systems with contact angles less than 90°, McCaffrey (1973) and Calhoun (1951) showed that the threshold angle is much less due to the effects of pore structure. In free imbibition experiments, as opposed to imbibition experiments where capillary pressure is reduced in steps, work by Morrow and McCaffrey (1978) and McCaffrey (1973, 1974) confirms that in initially dry teflon cores the rate and amount of wetting phase imbibition becomes smaller as the contact angle is increased. They further found that the imbibition rates were much faster when the cores had an initial wetting phase saturation of 30%.

Work by Schmid (1964) with fractionally wetted sandpacks indicates that as the percentage of sand grains of opposite wettability increases, i.e., oil-wet for water and water-wet for oil, free imbibition rate decreases rapidly and no longer occurs above a proportion of 50%. Experiments by Mohanty and Salter (1983) with mixed-wettability cores showed that at irreducible saturation it is possible for both water and oil to imbibe freely.

2.4 EFFECT OF WETTABILITY ON RELATIVE PERMEABILITY

Investigators found that the relative permeability of the nonwetting fluid is generally higher than for the wetting fluid at equal saturation (Jennings, 1957; Chilingar and Yen, 1983). Further, the relative permeability of the nonwetting fluid at the irreducible wetting phase saturation is higher than the relative permeability of the wetting fluid at residual nonwetting phase saturation.

Anderson (1987b) hypothesized that in a multiphase flow system, the wetting fluid tends to travel along the walls of the larger pores and through the less permeable, smaller pores. The movement of the wetting phase along the solid boundary eventually causes the neck of the nonwetting fluid to become unstable and snap off (Figure 2.5). The disconnected phase exists as either small globules in the centre of pores or as larger patches extending over several interstices. In either case, it restricts the passage of the wetting fluid in the larger pores. On the other hand, the nonwetting fluid tends to travel in the centre of the larger, more permeable pores. Jennings (1957) demonstrated that when the wettability is reversed, the fluids exchange behaviour, yielding two identical sets of curves when plotted in function of the wetting phase saturation, i.e., water saturation in a water-wet system and oil saturation in an oil-wet system.

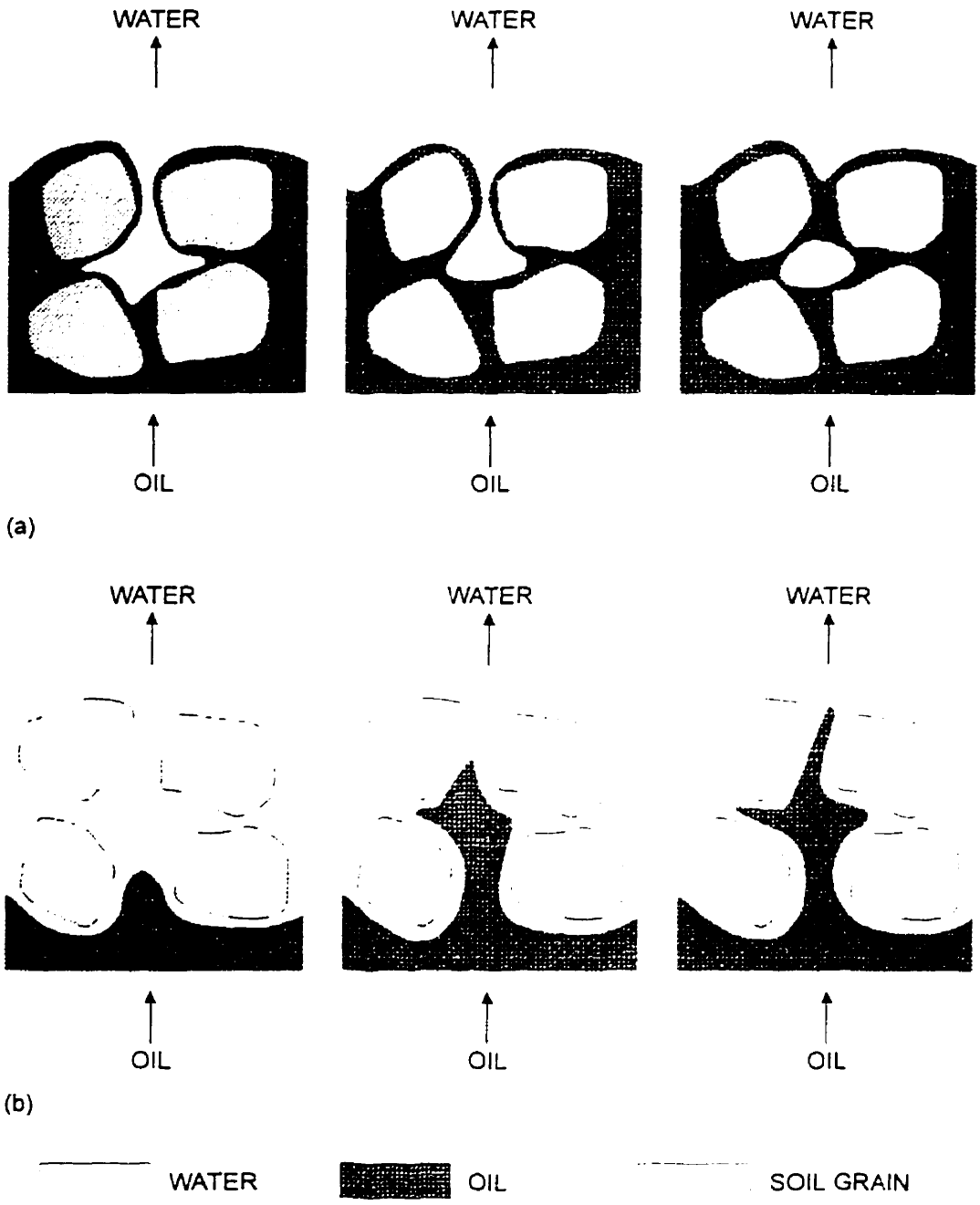

Figure 2.5. Oil displacing water from a pore for: (a) strongly oil-wet medium, and (b) strongly water-wet medium (adapted from Anderson, 1987b).

Experiments with natural uniformly wetted systems by Owens and Archer (1971), and Donaldson and Thomas (1971) proved that the oil relative permeability decreases as the medium changes from water- to oil-wet. whereas the opposite effect is observed with

water. Similar conclusions were arrived at with fractional wetting systems (Fatt and Klikoff, 1959; Singhal et al., 1976).

Work by Caudle et al. (1951) and Morgan and Gordon (1970) showed that although wettability is a major factor, the initial wetting phase saturation and pore geometry can also strongly influence the relative permeabilities.

2.5 REDUCTION OF CAPILLARY FORCES BY SURFACTANTS

The main parameters that influence the migration of oil at the pore scale are the wettability and fluids interfacial tension. According to equation 2.2, for the nonwetting fluid to enter narrow channels of a porous medium with a given wettability, the capillary pressure must be increased and/or the interfacial tension between the fluids must be reduced. This has long been recognized by the petroleum industry in an effort to recover additional oil. Considering that injection rates cannot be increased indefinitely, the interfacial tension must be reduced with the use of surfactants.

Melrose and Brandner (1974) investigated the correlation between the displacement efficiency and the ratio of viscous to capillary forces. They represented this ratio with a dimensionless number, N_c, the capillary number, and defined it as:

$$N_c = \frac{\mu_w V_w}{\Phi \gamma_{ow}} \qquad (2.5)$$

where μ_w and V_w are the water phase viscosity and interstitial velocity, and γ_{ow} the oil/water interfacial tension. They found that when the capillary number is increased

around 10^{-3} to 10^{-2} the displacement efficiency approaches 100 per cent. To increase the capillary number to such a value, ultralow interfacial tension, i.e., less than 10^{-3} to 10^{-4} dynes/cm, is required.

Surface-active agents are usually used to reduce interfacial tension, although there are occasions when they are used to increase it. According to Pope and Bavière (1991), when a surfactant is added to an aqueous solution, the molecules accumulate at the aqueous solution/immiscible fluid interface with the hydrophillic group oriented toward the solution and the hydrophobic group toward the nonpolar fluid (air or hydrocarbon).

The interaction across the interface is now between the hydrophillic moiety of the molecule and the water molecules on one side of the interface and between the hydrophobic part and the nonpolar fluid. Rosen (1989) explained that these interactions are much stronger than the original one, thus reducing the energy required to bring a water molecule to the surface. Without the adsorption of the surfactant molecules at the interface, there is no reduction of surface or interfacial tension. A necessary, but not sufficient condition for this to occur is the presence of the polar and nonpolar moieties.

As shown in Figure 2.6, at a temperature above the Krafft point, the minimum interfacial tension occurs at a compound-specific threshold concentration, corresponding to the maximum concentration of surfactant molecules in a monomeric form. Shah (1981) explained that at very low surfactant concentrations, the molecules remain as monomers in the solution in equilibrium with adsorbed molecules at the interface. As the concentration increases, the interface becomes saturated and the molecules begin to form

micelles in a very narrow range of concentration called the critical micelle formation (CMC). Beyond this point, the concentration of monomeric molecules remains constant due to the formation of additional micelles as the concentration is further increased. According to Rosen (1989), micelle formation is an important occurrence because a number of important phenomena, such as detergency and solubilization, depend on the existence of these colloidal-sized clusters.

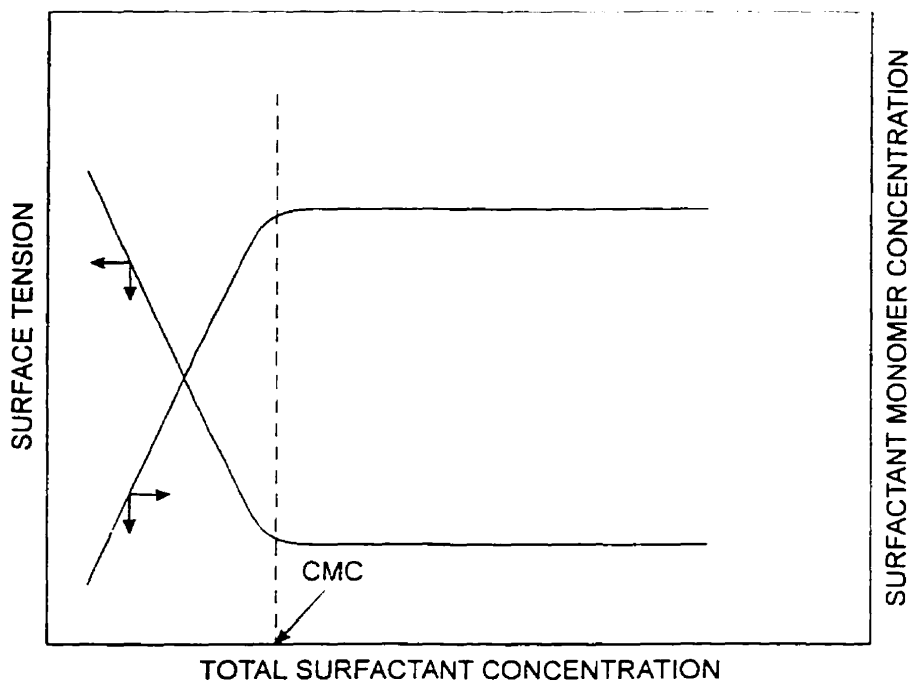

Figure 2.6. Schematic of surface tension versus surface concentration (from Pope and Bavière, 1991)

2.6 GOVERNING EQUATIONS FOR MULTIPHASE FLOW

On a microscopic scale the motion of fluids in a porous medium is governed by the Stokes-Navier equation. Due to mathematical difficulties involved in solving this equation and in defining the nature of flow channels and interactions between the fluid and porous media, the equation of motion is formulated on a macroscopic scale. The flow of fluid

through the pores of a soil mass is in most cases laminar, i.e., inertia forces are negligible. Under such conditions it is described by Darcy's law. In its generalized form for a single phase system it is represented as:

$$q_i = - \frac{k}{\mu} \frac{\partial \Psi}{\partial x_i} \qquad (2.6)$$

where x_i is the i^{th} Cartesian coordinate, q_i is the volume flux density or so-called Darcy velocity of fluid in the i direction, k is the intrinsic permeability of the soil, μ is the viscosity of the fluid, and Ψ is the fluid potential given by $\Psi_{pres} + \Psi_{grav}$, the former being the pressure potential and the latter the gravitational potential.

Equation 2.6 is empirical in nature and involves several assumptions. A fundamental assumption is that Darcy's law is valid in the porous medium. The equation was developed from experiments with water flowing through horizontal sand-filter beds (D'Arcy, 1856). Under those conditions, it was observed that the flow rate is directly proportional to the hydraulic gradient and that the relationship between flow rate and hydraulic gradient is linear through the origin.

These conditions are met for a wide range of soil types. However, experimental work by Hansbo (1960) showed that the condition of linearity through the origin is not valid for all clays. The saturated flow tests demonstrated that the relationship deviates from linearity for gradients less than 10. On the other hand, a number of studies indicate that the law is valid in clay soils. Olsen (1962) compared measured flow rates to those predicted from the Kozeny-Carman equation. He concluded that discrepancies could not

be adequately explained on the basis of violation of Darcy's law, but rather by unequal pore sizes in clays.

According to Yong and Warkentin (1975), clay-water forces may in certain cases affect the moisture migration and become increasingly important below the critical gradient. They suggested that these forces create an immobilized hydrodynamic layer of water surrounding each particle. The thickness of these layers depends on the interaction characteristics of the soil-water system and driving force. Flow will occur when the driving force exceeds the forces that immobilize the water. The flow channel between the clay particles increases in width as the driving force increases up to its maximum size. One can speculate that the gradient-velocity relationship becomes linear at or near the pressure where the channel reaches its maximum width.

In an effort to resolve the question of the validity of Darcy's equation, Olsen (1966) affirmed that the evidence as a whole indicates that the linear relationship condition is obeyed in many saturated natural clays, except in very fine-grained clays, such as montmorillonite, and in shallow, unconfined clays or granular soils with small amounts of clay.

Klute (1952) discussed the applicability of the equation for the flow of water in unsaturated soils. He considered that the presence of air in the pores has the effect of reducing the volume available for flow and does not in itself invalidate Darcy's law. Childs and George (1950a, 1950b) working with unsaturated sands arrived at the same conclusion. Laboratory studies conducted in the oil industry (Wyckoff and Botset, 1936;

Leverett, 1938) demonstrated that Darcy's equation can be extended to multiphase flow systems by the introduction of the saturation-dependent relative permeability, k_{rp} (Parker, 1989):

$$q_{pi} = - \frac{k_p k_{rp}}{\mu_p} \left[\frac{\partial \Psi_{pres}}{\partial x_i} + \frac{\partial \Psi_{grav}}{\partial x_i} \right] \qquad (2.7)$$

where the subscript p refers to a phase.

Another critical assumption is that the intrinsic permeability is a unique characteristic of the porous medium. This assumption is reasonably justifiable for rigid granular soils that do not undergo changes in fabric when permeated by a fluid. As can be inferred from the discussion in Section 2.1, this assumption breaks down for fine-grained soils.

In addition to the macroscopic law of motion, i.e., Darcy's law, the flow of fluid must obey the principle of continuity. For a system with n fluid phases, n continuity equations are required:

$$\Phi \frac{\partial \rho_p S_p}{\partial t} = - \frac{\partial \rho_p q_{pi}}{\partial x_i} + \Gamma_p \qquad (2.8)$$

where ρ_p is the phase density, Γ_p is a source-sink term to account for mass transfer between phases. Substituting equation (2.2) into (2.3), assuming both the fluids and the soil to be incompressible, and ignoring the source-sink term, yields a phase conservation equation for horizontal flow:

$$\Phi \frac{\partial S_p}{\partial t} = \frac{\partial}{\partial x}\left[\frac{k_p k_{rp}}{\mu_p}\frac{\partial \Psi_{pres}}{\partial x}\right] \qquad (2.9)$$

By defining a new parameter, the phase diffusivity, D, as:

$$D(\theta_p) = \frac{k_p\ k_{rp}}{\mu_p}\ \frac{\partial \Psi_{pres}}{\partial \theta_p} \qquad (2.10)$$

the above differential equation can be written in a form similar to the non-linear diffusion equation:

$$\frac{\partial \theta_p}{\partial t} = \frac{\partial}{\partial x}\left(D(\theta_p)\frac{\partial \theta_p}{\partial x}\right) \qquad (2.11)$$

where $D(\theta_p)$ and θ_p are the phase diffusivity and volumetric phase content respectively. This equation describes the flow of any phase in a multiphase system.

CHAPTER 3

EXPERIMENTATION

To study the effect of capillary forces on multiphase flow, three series of oil imbibition tests were performed:

1. maximum capillary forces system, in which the soil was moulded with distilled water;
2. intermediate capillary forces system, in which the soil was moulded with 3% aqueous surfactant solution;
3. minimum capillary forces system, in which the soil was moulded with 6% aqueous surfactant solution.

For each series of test, two artificial soils were used, i.e., prepared in the laboratory with commercial materials. Further, three durations were selected for the oil imbibition tests. These time spans, although the same for all three series of tests, were specific to each soil.

Additional experimental work was carried out to characterize the conditioned soils and motor oil. This involved grain size analysis, determination of the moisture-density and capillary-moisture (soil suction) relationships of the soils; measurement of the hydraulic conductivities; pH of distilled water, aqueous surfactant solutions, and motor oil; conductivity of distilled water and surfactant solutions; measurement of surface and interfacial tensions; and determination of the dielectric constant of the motor oil. Where

feasible, the testing procedures for the characterization work were adapted to duplicate as much as possible the conditions encountered during the oil imbibition experiments.

3.1 MATERIAL

The dry materials for both artificial soils were #40 silica sand and kaolinite hydrite PX. Commercial sand and kaolinite powder were used because it allowed better control on the uniformity of replicate samples. The proportions in one mixture were 80% sand and 20% kaolinite (hereinafter referred to as 80/20), on a weight basis, while for the other soil they were 60%-40% (60/40) respectively. The chemical and physical properties of the soils used in this study are summarized in Table 3.1.

Aqueous surfactant solutions were prepared with a commercial multipurpose liquid alkaline cleaner available under the trade name PowerCleaner 155 by West Penetone. This product, selected for its biological properties, is composed of water, sodium xylene sulphonate, tripotassium phosphate, tetrapotassium pyrophosphate, and trisodium N-hydroxyethyl ethylenediamine triacetate (Figure 3.1). Additionally, anionic surfactants experience minimal adsorption and precipitation. Concentrations of 3% and 6% (%v/v) of surfactant in distilled water were used based on their surface tension and interfacial tension with oil. Table 3.2 shows relevant properties of the aqueous surfactant solutions and distilled water.

The oil used in this study was Ultramar 5W30 motor oil. Table 3.3 shows the properties and composition of the fluid.

Table 3.1. Soil material properties

Geotechnical properties	Soil mixture	
	80/20	60/40
Grain-size analysis		
D_{50} (μm)	200	150
D_{10} (μm)	1	1.1
C_u	250	182
C_c	90	0.01
Compaction		
90% maximum dry density (Mg/m^3)	1.76	1.70
moisture content, dry side (%)	6.7	10.5
Hydraulic conductivity (m/s)[1]		
moulded with distilled water	1.3×10^{-8}	1.0×10^{-8}
moulded with 3% surfactant solution	2.0×10^{-7}	5.0×10^{-9}
moulded with 6% surfactant solution	4.0×10^{-8}	2.5×10^{-9}
Chemical properties of kaolinite[2]		
Soil pH (1:10 soil:water)	4.3-4.7	
Cation-exchange capacity (meq/100g)		
Na^+	0.31	
K^+	0.48	
Ca^{2+}	0.16	
Mg^{2+}	0.02	
exchangeable H^+	2.86	
exchangeable Al^{3+}	3.23	
Surface area (m^2/g)	24.0	
Total organic content (% w/w)	0	
Amorphous content (%)		
Al_2O_3	0.48	
Fe_2O_3	0.00	
SiO_2	0.70	
Total	1.18	

[1] Permeant: distilled water
[2] From Cabral (1992) and Galvez (1989)

Table 3.2. Properties of moulding liquids

Moulding liquid	Conductivity (25°C)	pH
Dist. water	47.5 µS	5.80
3% surf. sol.	4.77 mS	11.45
6% surf. sol.	8.65 mS	11.51

Table 3.3. Ultramar 5W30 motor oil properties and composition

Properties		
Viscosity (cSt)	@ 40°C	61.2
	@100°C	10.3
Specific gravity		0.872
pH		(5.65)[1]
Flash point (°C)		206
Water solubility (mg/l)		0
Surface tension (dynes/cm)		(28.3)
Dielectric constant		(2.5)
Components		**Approximate percentage**
Mineral oil		85%
Proprietary additive mix		15%
methacrylate polymer		
succinimides		
zinc dialkyldithiophosphates		

[1] Values in parentheses measured in laboratory.

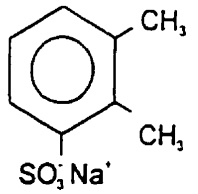

sodium xylene sulphonate
($C_8H_9SO_3Na$)

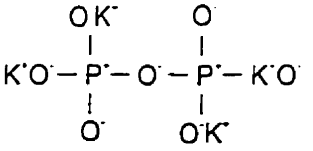

tetrapotassium pyrophosphate
($K_4P_2O_7$)

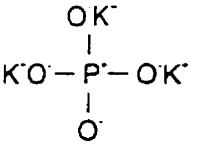

tripotassium phosphate
(K_4PO_4)

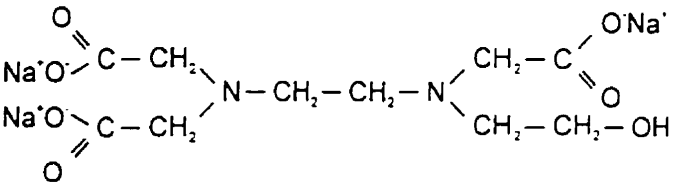

trisodium n-hydroxyethyl ethylenediamine triacetate

Figure 3.1. Molecular structure of surfactant compounds.

3.2 APPARATUS

3.2.1 Oil Imbibition

Each cell consisted of a lucite cylinder measuring 100 mm in length and 50 mm in internal diameter and two lucite end caps. The inlet end cap was provided with two openings, one for fluid supply and the other for air flushing. The outlet end cap was provided with one opening for fluid exhaust. A porous stone made of coarse silica sand and epoxy glue was built in both end caps to ensure proper distribution of permeant across the entire section of the soil sample at the inlet and adequate exhaust of the fluid(s) at the outlet. To prevent leaks, a rubber O-ring was placed between the cylinder and the end caps. To preclude the migration of fines out of the cell, saturated filter papers were placed at both ends of the soil samples. The cell components were fixed by four stainless steel rods and nuts.

Each individual cell was connected to a constant head fluid supply (mariotte flask),

filled with motor oil. The nylon tubing used to convey the oil from the mariotte flask to the cell was provided with a valve. To ensure that the movement of oil in the soil occurred only as a result of capillary forces, the total head throughout the longitudinal axis of the sample was kept at zero. This was achieved by placing the cell horizontally and maintaining atmospheric pressure at both ends. To minimize evaporation at the outlet, the flexible tube was partially immersed in the moulding liquid contained in a beaker. Technical drawings of the cells and mariotte flasks are provided in appendix I, and a layout of the oil imbibition apparatus used in this study is shown in Figure 3.2.

3.2.2 Hydraulic Conductivity

The lucite cells described above were used for hydraulic conductivity measurements. These were placed vertically and connected to a burette filled with distilled water.

3.2.3 Surface and Interfacial Tensions

The measurements were performed with a Fisher Model 215 Autotensiomat® surface tension analyzer. The instrument operates on the principles of the du Nouy and Wilhelmy plate methods, as described in the instruction manual. Results were registered on a recorder to obtain a graphic display of changes in surface/interfacial tension.

3.2.4 Capillary-Moisture Content Relationship

The determination of capillary-moisture relationship was accomplished with two apparatuses. At pF 0.0 and 1.0 a sand box was used, while at higher suction values a 15 bar pressure-membrane chamber by Soil Moisture Equipment was used. Soil samples of

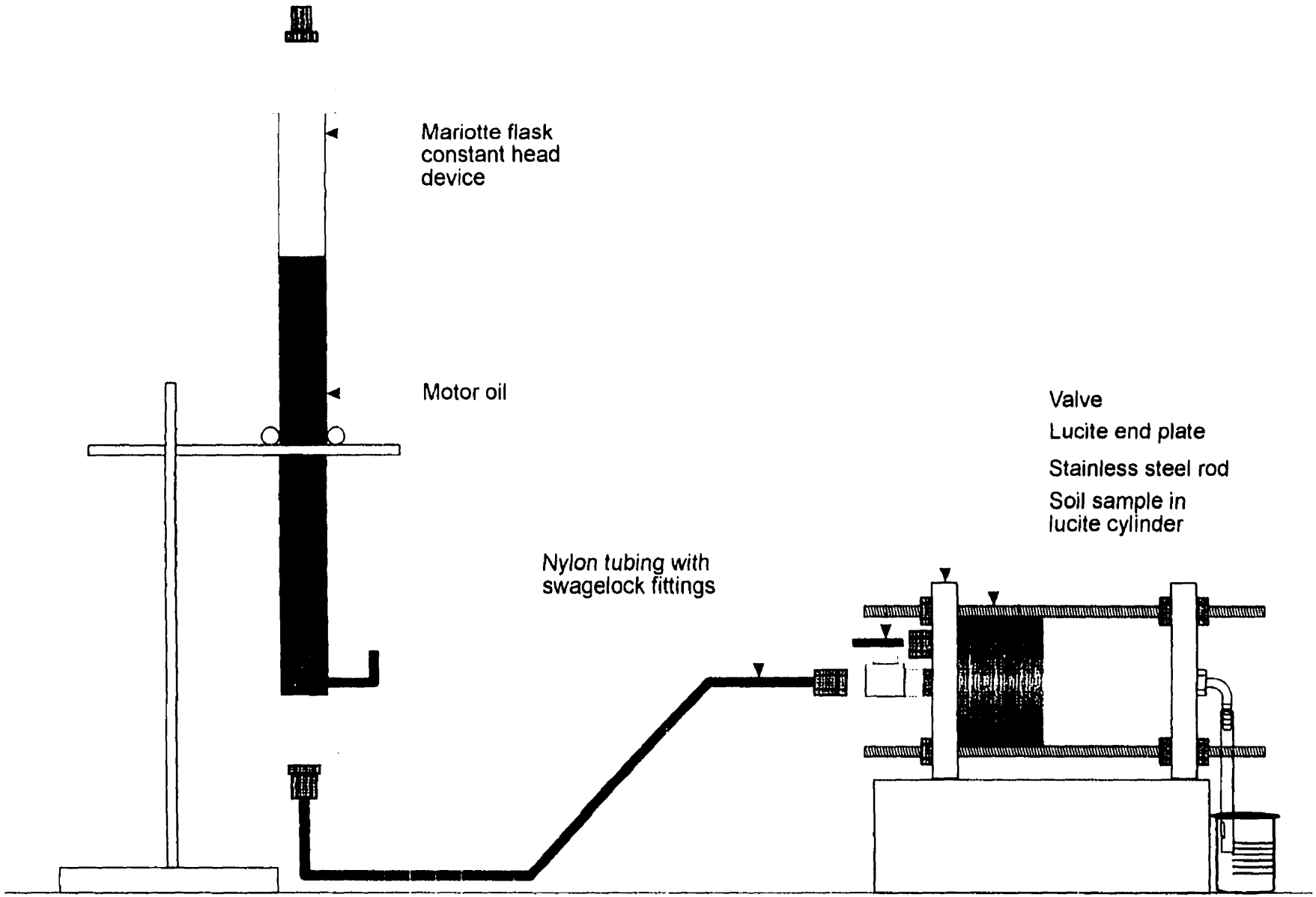

Figure 3.2. Layout of oil imbibition apparatus.

about 36 mm diameter and 15 mm high were placed in lucite retainer rings with a membrane at the bottom. These dimensions were based on ASTM 3152-72 standard, and considering the need to have representative samples and time required to reach equilibrium.

The sand box included a plastic container and cover partly filled with fine sand that was covered with a cellulose membrane. To reach pF 1.0, the sand material needs to be sufficiently small that the liquid will rise to the soil surface by capillarity when its free surface is lowered by 100 mm. A hole near the bottom of the container with appropriate fittings permitted the connection of a burette to monitor the liquid level.

The chamber used is similar in general arrangement and construction to that described by Richards (1947). A 15 bar (air entry value) porous ceramic plate was placed on three rubber supports inside the apparatus. The function of this plate is to provide support to the samples and still allow the passage of liquid through it. A small outlet tube in the plate was connected by a tight-fitting rubber sleeve to a flexible tube that connected to a burette. Compressed air was used as a pressure source. The pressure manifold comprised an air regulator and a pressure gauge.

3.3 SOIL SAMPLE PREPARATION

3.3.1 Oil Imbibition and Hydraulic Conductivity

The soil sample preparation was exactly the same for both experiments. The dry soil mixtures were wetted with distilled water or an aqueous surfactant solution to obtain the moisture content at 90% maximum dry density (dry side). To obtain the best uniformity

possible, the sand was first mixed with the kaolinite, then the moulding liquid was added and thoroughly mixed with the dry material. The soil was then transferred in a double plastic bag system that was placed in the humid room overnight for equilibration. The next day, the soil was ground with a porcelain pestle and mortar to break the large clods of material that formed during mixing, and statically compacted in six equal layers. The weight of wet soil needed for the individual compacted layers was calculated from its dry density and the corresponding moisture content. The compacted sample was returned to the humid room to equilibrate overnight.

3.3.2 Capillary-Moisture Content Relationship

It was considered desirable to prepare samples with a structure and fabric similar to the ones used in the imbibition tests. Thus, the soil mixtures were compacted in the lucite cells, as explained above, and immediately extruded and stored in the humid room overnight. The sample was then cut transversely in half and trimmed with a knife approximately to the diameter of the retainer rings using a metal cylindrical ring as a guide. The sharp cutting edge of the metal ring was placed downward on the top face of the specimen and forced down lightly and gradually, trimming the remaining excess material. With the use of a piston, the specimen was pushed in the retainer rings and cut with a wire saw.

3.4 EXPERIMENTAL PROCEDURE

3.4.1 Oil Imbibition

The durations of the oil imbibition tests were 1, 2 and 3 days for the 80/20 mixtures, and 3, 5 and 10 days for the 60/40 mixtures, for a total of 18 tests (9 per soil

types). At the end of each experiment, the sample was extracted from the cell, and sectioned for the determination of moisture and oil content. To minimize the amount of time required to analyze a sample, only a limited number of sections were used for measurements. To obtain representative profiles, it was found that generally six sections, each being 10 mm thick, were required for oil content and seven for moisture content. The remainder of the sample was discarded. Figure 3.3 schematically illustrates the oil imbibition and sectioning procedure.

The procedure to determine moisture content on a weight basis was adapted from ASTM D2216 standard. To allow the evaporation of the water or surfactant solution without loosing significant amount of oil, the oil-soil mixture was oven dried at low temperature (< 60°C). This step yielded the mass of moisture in the section, being the difference of weight before and after the drying process. The dry weight of solids could only be obtained after the oil content was determined since the mass at the end of the oven drying step was that of the dry oil-soil mixture.

The amount of oil in the sections was found by the Soxhlet extraction method (Greenberg et al., 1992; Yong et al., 1994; Mohammed, L.F., 1995). The oven dried sections were crushed and roughly 10 g was placed in a pre-weighed cellulose thimble. The thimble was placed in a Soxhlet extraction tube and washed with trichlorotrifluoroethane (freon) for at least two hours at a rate of 20 cycles/hour approximately. The oil content was determined as the ratio of the difference between the weight of the thimble before and after washing to the weight of the clean dry soil.

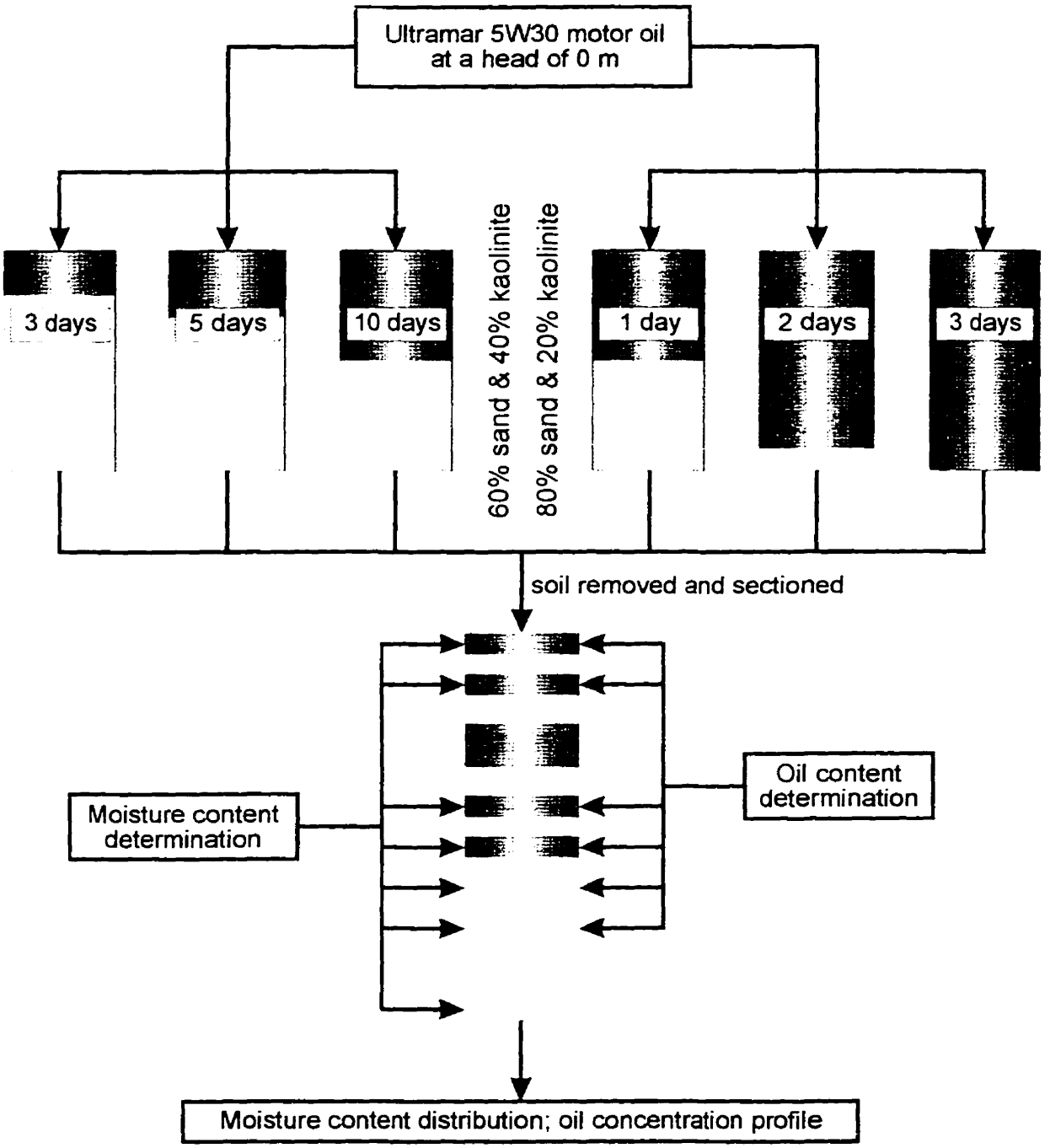

Figure 3.3. Schematic diagram of test procedure for oil imbibition and determination of oil and moisture content.

3.4.2 Geotechnical Characterization

The distribution of particle size, and moisture-density relation of both mixtures were obtained experimentally in accordance with ASTM standards D422-63 and D698-78 respectively. The moisture-density relationship was only established for the soils moulded with distilled water. The procedure to obtain the hydraulic conductivity was adapted from ASTM standard D5084-90. The falling head system included a graduated pipette connected to a permeameter cell and involved passing distilled water in the soil sample until equilibrium conditions prevailed. The maximum gradient (i_{max}) used for these measurements was between 2 and 5.5. The hydraulic conductivity was computed for both mixtures conditioned with the various liquids, for a total of six tests.

Distilled water was used instead of oil for the measurement of permeability because it is more convenient. As explained in more detail in Chapter 4, it is expected that the hydraulic conductivity would be higher with oil as the permeant.

3.4.3 Geochemical Characterization

Measurements of surface tension were made on distilled water, aqueous surfactant solutions with concentrations ranging from 0.5% to 6.0%, and motor oil. Interfacial tensions were determined between distilled water/surfactant solutions and motor oil. The procedure followed was as detailed in the apparatus instruction manual. For the surface tension measurements, the instrument was calibrated with a 1.0 g weight, allowing measurements up to approximately 100 dynes/cm. The measured surface tension for distilled water was compared to reported values as a check. The instrument was calibrated with a 200 mg weight for interfacial tension, allowing measurements up to

approximately 20 dynes/cm. To ensure proper calibration, the measured surface tension of acetone was compared to reported values. Following calibration, a pre-cleaned platinum-iridium ring is immersed in the sample liquid. Surface tension measurements are obtained by measuring the force required to withdraw the ring from the liquid phase. Interfacial tension measurements are made in a similar manner. The procedure differs only in that the less dense liquid is carefully poured on the surface of the denser liquid following immersion of the ring in the latter.

To examine the effect of soil, via adsorption of surfactant molecules and/or dissolved salts, soil suspensions were prepared with distilled water or surfactant solutions. The slurry was agitated for about 24 hours and centrifuged. The supernatant was recovered and used for the measurements. Generally, two readings were taken at each surfactant concentration. Figure 3.4 schematically represents the overall procedure to obtain surface and interfacial tensions.

The pH of the liquids was determined with a microcomputer pH meter by Hanna instruments (HI 9025). The instrument was calibrated with solutions with a pH of 7.01 and 10.01, and was used according to the manual instructions. The conductivity of the moulding liquids was measured with a multirange water-resistant conductivity meter by Hanna instruments (HI 9033).

The dielectric constant of oil was calculated from the capacitance measured with a simple capacitor connected to a bridge (Phillips PM630A programmable automatic RCL meter). The capacitor consisted of two thin copper plates (308 mm long x 175.5 mm wide)

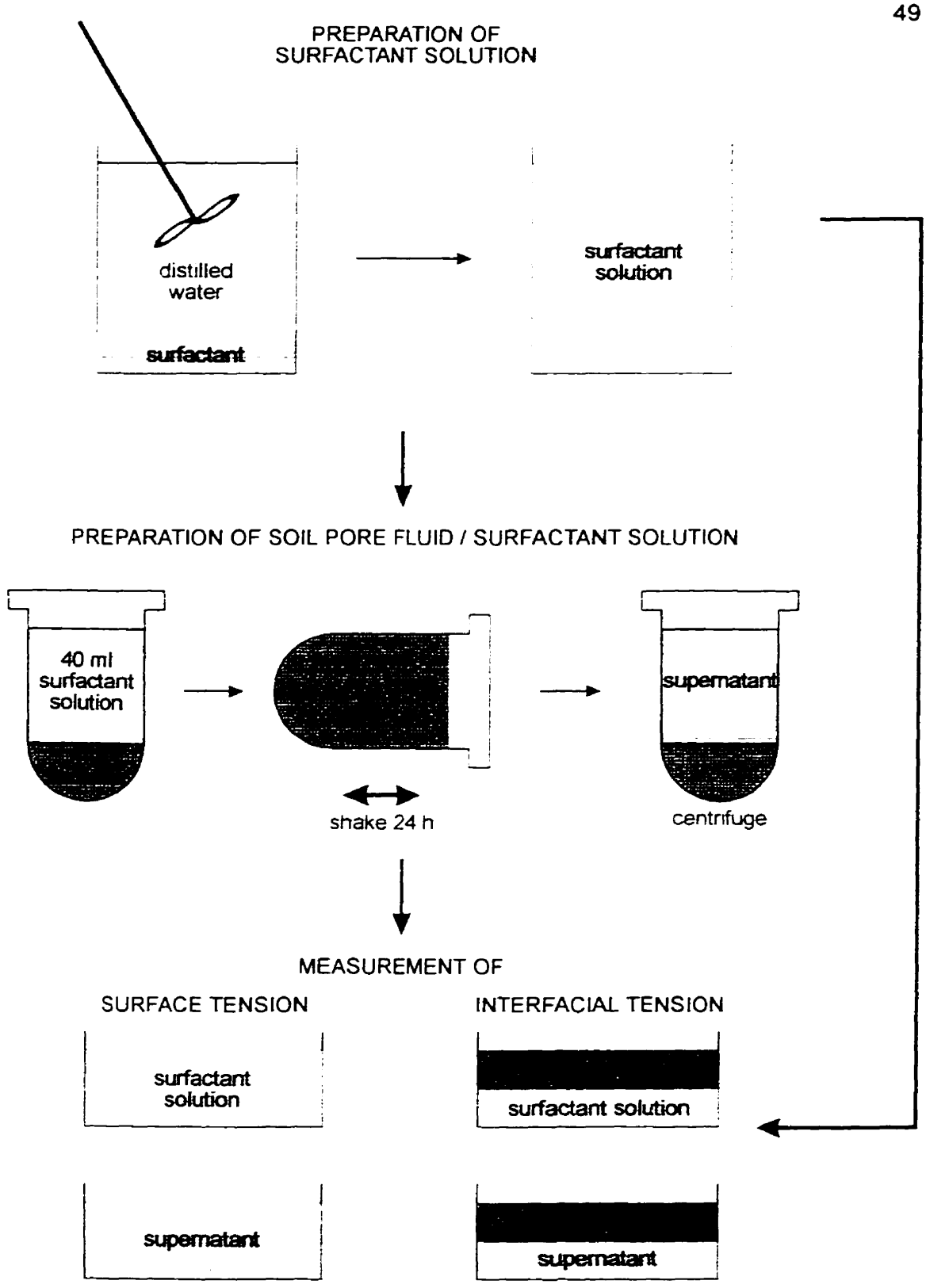

Figure 3.4. Schematic diagram of procedure to measure surface and interfacial tensions.

10 mm apart in a plastic container.

3.4.4 Capillary-Moisture Content Relationship

The determination of capillary-moisture relationship was limited to maximum and minimum capillary forces systems, i.e., soil mixtures moulded with distilled water and 6% aqueous surfactant solution respectively. The sand box and ceramic plate were saturated with either distilled water or surfactant solution depending on the system. Twelve samples were prepared for each mixtures, for a total of 24 per system. The general procedure consisted of saturating the samples and increasing the pressure in steps up to pF 3.8 or 4.1 depending on the moulding liquid, and back in a similar fashion to pF 0.0. Samples were normally exposed to a suction/air pressure for one week to ensure that equilibrium conditions were established. At that time, one sample per mixture was removed, weighed and dried to determine moisture content.

CHAPTER 4

RESULTS AND DISCUSSION

The results of the experimental study are presented and discussed in detail in this chapter. The first two sections deal with the effect of the surfactant solutions on phases interaction and soil behaviour in relation to fluid movement. The last section of the chapter is concerned with the oil imbibition experiments, with emphasis on the effect of capillary forces.

4.1 EFFECT OF SURFACTANT ON PHASES INTERACTION

Figure 4.1 presents the drainage and spontaneous imbibition curves for the 80/20 and 60/40 mixtures moulded with distilled water and 6% surfactant solution. In all cases, the nonwetting fluid was air since it is more convenient to use. It is acknowledged that more representative data would have been obtained with motor oil. Further, soil suction tests involve only two fluid phases, whereas the oil imbibition experiments include three fluid phases. Consequently, by recognizing the limitations of the methodology used to carry out these tests, a number of appropriate conclusions can nonetheless be drawn, such as the effect of the surfactant on the aqueous soil solution interaction with the solid substrate.

The soil mixtures moulded with 6% surfactant solution, and especially the 60/40 mixture, bulged at around pF 3.0, causing considerable alterations to the fabric of the samples. From visual inspection of the specimens during the test, where a number of

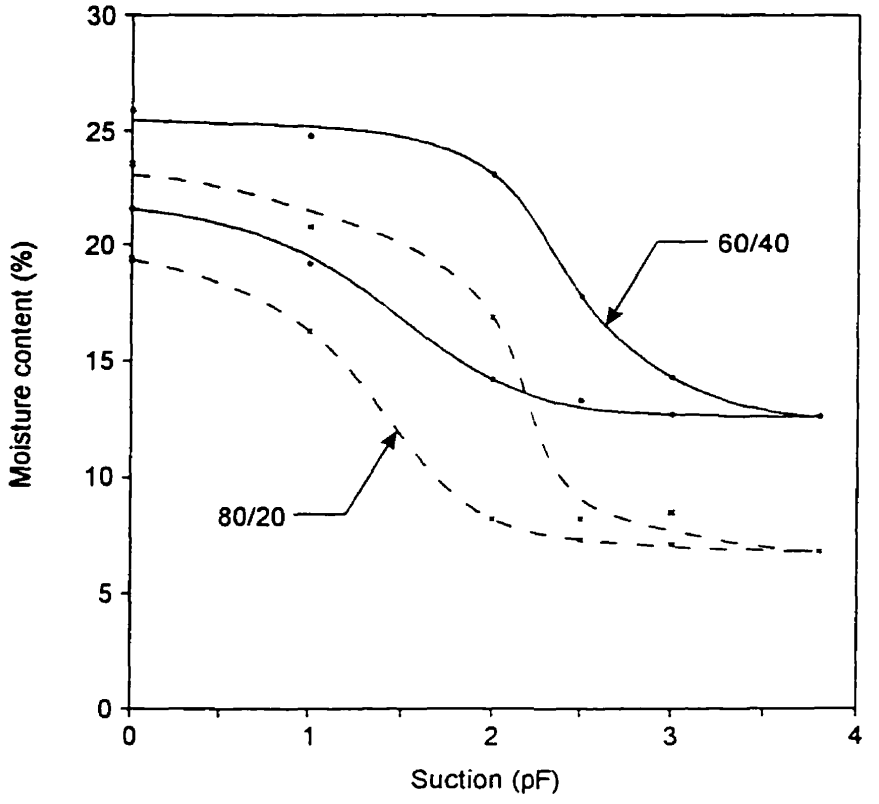

(a)

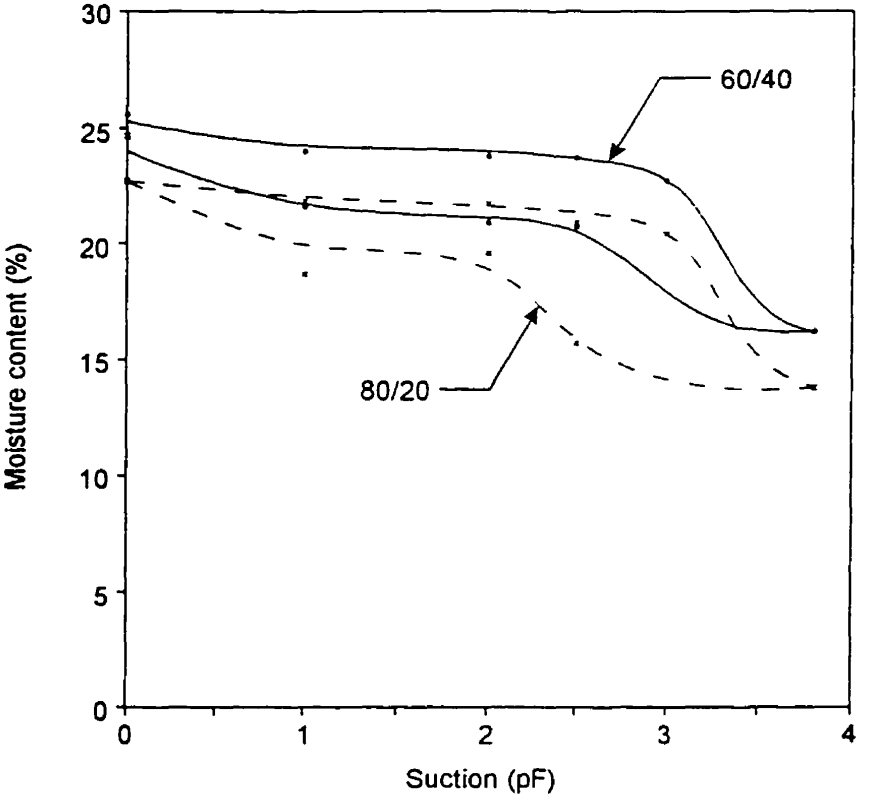

(b)

Figure 4.1. Capillary pressure curves for soil samples moulded with: (a) distilled water, and (b) 6% surfactant solution.

horizontal cracks were observed, one can hypothesize that the parallel particle orientation created planes of weakness. As the air pressure increased, the particles on both sides of this plane were pushed apart due to higher pore water pressure and reduced internal friction to resist movement. The effect of this occurrence on the capillary pressure curve is difficult to assess, although it is suspected that it caused premature emptying of the voids.

The moisture contents at pF 0.0 are greater than the theoretical saturated value computed using the dry densities of the mixtures and an assumed solid density of 2.65 Mg/m^3. It is also significantly greater than the measured moisture content at the end of the hydraulic conductivity tests, where the soils are at or near 100% saturation. This discrepancy may be caused by volume changes during the soil suction test since the samples are not confined in all directions and kaolinite has a small swelling potential, and/or alterations to the soil fabric during placement of the samples in the lucite retainer rings.

The capillary pressure curves show that at any given suction, the moisture content increases with kaolinite content, irrespective of the moulding liquid. This is attributable to the greater surface activity of kaolinite, which gives the soil a greater capability to retain the soil pore fluid. The higher moisture content at 100% saturation for the 60/40 mixture is mainly due to its greater void ratio.

The shape of the drainage curve reflects a pore size distribution. A porous medium with a uniform pore size will retain most of its solution until the pressure is sufficiently high

to empty the voids, at which point the moisture content drops rapidly over a small pressure increment. On the other hand, a soil medium with a large distribution of pore size will loose its wetting liquid more gradually since the biggest voids empty first and as the pressure is increased the smaller interstices start to empty. The experimental curves show that the moisture content remains relatively constant up to a threshold pressure, known as the air entry point. Beyond this pressure, the moisture content decreases gradually, more so for the 60/40 mixture, suggesting a distribution of pore sizes.

The air entry pressures for the 80/20 and 60/40 mixtures mixed with distilled water are approximately the same at pF 2. The surfactant-moulded mixtures have a higher air entry pressure at about pF 3. This increase can be understood by examining the effect of the surfactant on the charge properties of kaolinite, which in turn affect the soil fabric and interparticle energies of interaction. As explained by Yong et al. (1992), the effective charge of a kaolinite particle is mainly attributable to the edges since there is relatively little, if any, isomorphous substitution in the crystal lattice structure. These edge charges in turn exhibit pH dependent properties. Calculations using the DLVO theory show that the high-pH surfactant solution augments the interparticle energies of interaction (see appendix III), thus making the soil fabric more dispersive and increasing the energy with which water is held in the soil.

According to the USBM method (see Section 2.3), the wetting preference of a porous medium can be determined from the ratio of the area under the drainage curve over the area under the forced imbibition curve (see equations 2.3 and 2.4). The experiments to determine the relationship between capillary pressure and moisture content

did not include forced imbibition. However, from the slope of the spontaneous imbibition curve at the moisture content axis, i.e., being almost perpendicular to the ordinate, one can speculate that in all cases the area under the forced imbibition curve would be small, or at least much smaller than the drainage curve. Consequently, it can be assumed that the soil mixtures are water-wet. Clays are known to be hydrophillic and the mixtures preference for water is therefore to be expected.

The wettability characteristic of the soil mixtures appears to be affected by the addition of surfactant. Although it is not possible to determine whether the ratio of areas (drainage over forced imbibition) increases or decreases, the higher irreducible moisture content and the increased amount of spontaneous imbibition suggest that the surfactant-moulded soils have an enhanced preference for water.

As explained in Chapter 2, the total area under the drainage curve, i.e., the area bounded by the curve and the moisture content axis between the saturated and irreducible moisture contents, represents the external work necessary for the nonwetting fluid to displace the wetting phase from a core. Figure 4.1(a) shows that the total area under the 80/20 drainage curve is marginally greater than the area under the 60/40 curve. On the other hand, more fluid is being displaced in the former case. Hence, the amount of work required to bring both soils at a given moisture content is smaller for the 80/20 mixture. Figure 4.1(b) indicates that the situation is similar when the soils are moulded with surfactant solution, i.e., the total areas are approximately equal, although slightly greater for the 60/40 mixture.

The total area under the drainage curve for the mixtures moulded with surfactant solution is less than for those prepared with distilled water. The moisture content is higher at any given suction for the conditioned mixtures, but the irreducible moisture content is significantly increased, with the overall effect of decreasing the total area. Comparing the areas between common starting and finishing moisture contents shows that more work is required to displace the wetting fluid for soils prepared with the 6% surfactant solution. On the basis of surface tension considerations only, one would expect a decrease in external work required to displace the soil pore fluid. However, the changes to the wettability characteristics of the solid phase with the addition of surfactant, i.e., enhanced energies of interaction, seems to have the dominant effect of increasing the work.

The irreducible moisture content is higher for the mixtures moulded with surfactant solution. As explained previously, this is due to the enhanced wetting preference of the medium, i.e., more water-wet. Additionally, the surfactant solution may have increased the mixed-wettability character of the mixtures by making the kaolinite particles increasingly more water wet than the sand grains. This assumes that the micropores are defined by the clay particles, whereas the macropores are bound by sand grains.

The soil suction results suggest that external work is required for oil to imbibe the saturated soil mixtures. However, as will be seen in the next section, the oil imbibition experiments show that this is not the case, i.e., oil penetrates spontaneously into the porous media. The reason for this discrepancy is the different initial moisture content, the soil mixtures being unsaturated in the imbibition experiments.

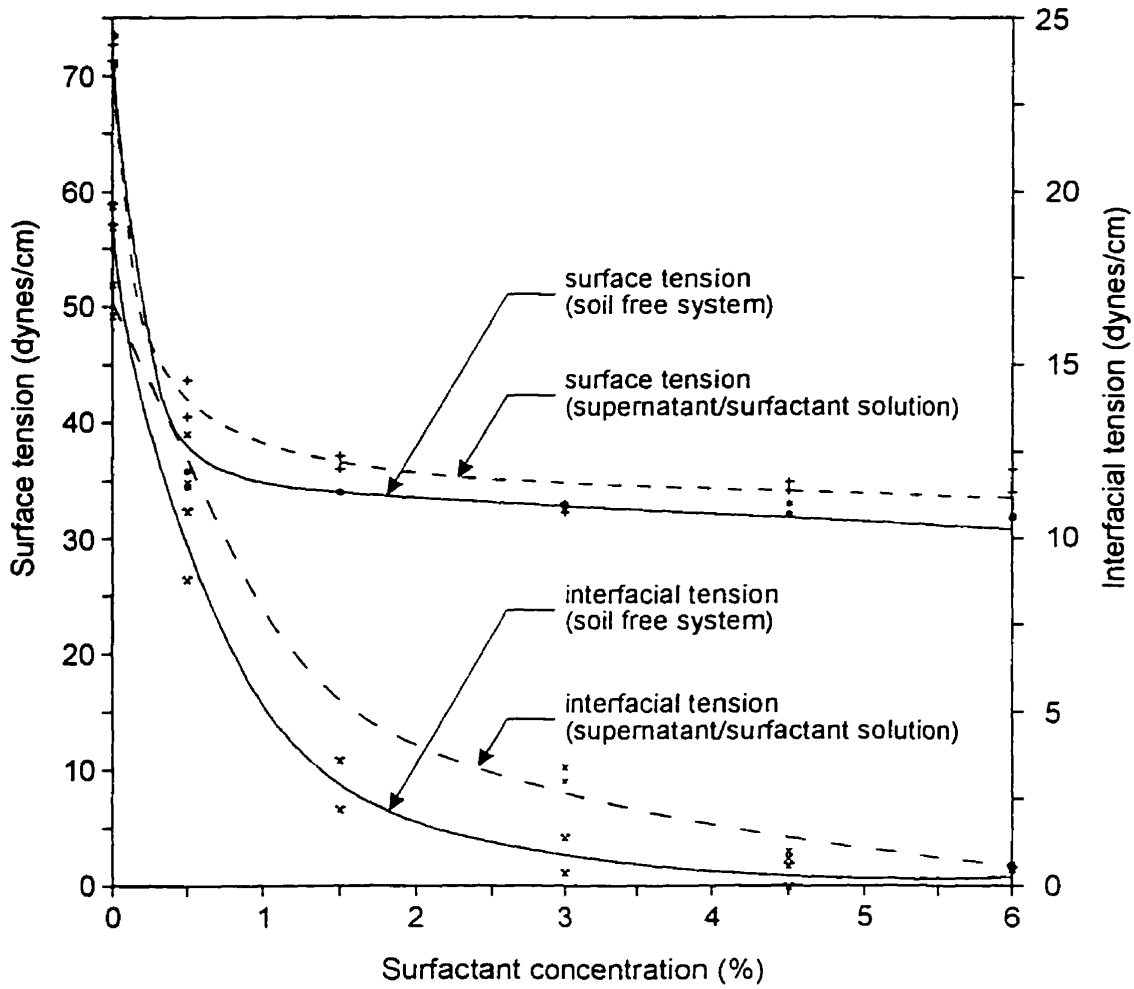

Figure 4.2. Surface and interfacial tensions versus surfactant concentration

The effect of surfactant concentration on surface and interfacial tensions is shown in Figure 4.2. It is evident that the surfactant used for this study served to reduce both properties and that the smallest measurable value was generally reached within the range of concentrations used. The trend observed is consistent with previous work, i.e., an abrupt decrease up to the critical micelle concentration (CMC), followed by a gradual reduction.

The presence of the soil seems to affect the surfactant efficiency, and to a much lesser extent its effectiveness. Rosen (1989) explained that the influence of a surfactant on an interfacial phenomenon is a function of its concentration at the air/liquid or liquid/liquid interface. A possible explanation for the decrease in efficiency is the adsorption of surfactant molecules on the soil surface via water bridging and/or cation bridging with the anionic part of the molecule and/or London-van der Waals dispersion forces with the nonpolar moiety. This reduces the concentration of monomeric molecules in the bulk solution and thus at the fluids interface. Hence, adsorption on the solid phase increases the solution concentration at which saturation occurs at the fluids interface.

In a study on the sorption of nonionic organic compounds in soil-water systems, Sun et al. (1995) found that the effectiveness of a nonionic surfactant is enhanced in soil-water systems, whereas the efficiency seems to be reduced. Therefore, the effect of a solid phase on interfacial phenomena appears to depend on the type of surfactant.

The surfactant is less effective and less efficient with oil than with air. Although the oil/aqueous solution interfacial tension is always smaller, the total reduction is only about

half of the decrease with air as the non-aqueous phase. This observation is consistent with Rosen (1989) who reported that the effectiveness increases with the interfacial tension between the two phases.

By considering the interfacial tensions between air, oil and water, and the energies of interaction with the solid phase, it is possible to qualitatively scale the air-oil, oil-water and oil-surfactant capillary pressure curves from the air-water and air-surfactant saturation-capillary pressure relations. For the air-oil pair of fluids, it is expected that the curves (80/20 and 60/40) would be lower than the air-water curves, i.e., the wetting phase saturation at any capillary pressure would be lower for air-oil. The lower energies of interaction between oil and the solid phase and the lower air-oil interfacial tension reduce the amount of work required by the air to displace the oil and decrease the driving force for spontaneous imbibition. It is also anticipated that the oil-water curves would be lower than the air-water saturation-capillary pressure relations. The higher energies of interaction between the nonwetting fluid (oil) and solid phase, and the lower interfacial tension between the pair of fluids (oil-water) cause this reduction. Similarly, it is expected that the oil-surfactant curves would be lower than the air-surfactant curves.

4.2 EFFECT OF SURFACTANT ON HYDRAULIC CONDUCTIVITY

The hydraulic conductivities of the sand/kaolinite mixtures, obtained with distilled water as the permeant, were evidently influenced by the moulding liquid. The range of hydraulic conductivity, K, for the 80/20 mixture is from 1.3×10^{-6} m/s when moulded with distilled water to 4.0×10^{-8} m/s when prepared with 6% surfactant solution. The hydraulic conductivity varies in a similar fashion for the 60/40 mixture. Values range from 1.0×10^{-8}

m/s with distilled water to 2.5 x 10^{-9} m/s with 6% surfactant solution. This decrease in K was also observed by Suarez et al. (1984) who passed permeants of various pH and electrolyte concentration through air-dry natural clay soils compacted in plastic cylinders.

Soil piping was observed in the top half of the cell at the very beginning of the experiment with the 80/20 mixture moulded with 6% surfactant solution. This possibly caused partial obstruction of the pores downstream. According to Abdul et al. (1991), dispersion of colloidal solids by the surfactant causes this phenomenon. They found that dispersion generally increases with surfactant concentration. Yong et al. (1991) further found that clay migration decreases as the ratio of clay to sand increases. Although soil piping was not observed during other permeability experiments, it is nonetheless possible that clay migration occurred. The magnitude of the decrease for the 80/20 mixture is quite suspicious considering the lower surface activity of sand and the much smaller decrease for the 60/40 mixture. This suggests that clay migration was more important for the lower clay content soil, which is consistent with observations made by Yong et al. (1991).

The phenomenon of soil piping has also been the focus of much research in geotechnical engineering due to the failure of a number of earth dams. According to Ludwig (1979), when the interparticle forces of repulsion exceed those of attraction, clay particles are detached and go into suspension. If water is flowing, the detached clay particles are carried away and piping occurs. The major factor governing a clay's susceptibility to dispersive piping is the quantity of dissolved sodium cations in the pore solution relative to the quantities of divalent cations, such as magnesium and calcium. Further, a hydraulic conductivity greater than 10^{-7} m/s is required to initiate the

phenomenon. It is therefore obvious that the surfactant used for this study promotes this phenomenon by increasing the net repulsive forces, as demonstrated by the soil suction test and calculations using the DLVO theory (appendix III), and the proportion of dissolved sodium ions as it contains sodium xylene sulphonate and trisodium n-hydroxyethyl ethylenediamine triacetate.

The lower hydraulic conductivity of surfactant-conditioned soil mixtures can be explained by the effect of the moulding liquid on the soil fabric. The surfactant solutions have a higher electrolyte concentration and pH than distilled water. As explained previously, the cation exchange capacity (CEC) of kaolinite is attributable largely to the edges of the particle and exhibit pH dependent charge properties. Hence, chemicals with high pH, such as the surfactant solutions used in this study, increase the net negative charge on the clay particles with an associated increase in repulsive forces. Although the higher electrolyte concentration depresses the double layer and hence reduces the repulsive forces, the pH effect appears to be dominant. Under those conditions, there is greater tendency for the particles to be parallel causing the channels to be smaller and the permeability to decrease.

It is tempting to conclude that the passage of distilled water marginally restores the soil fabric. This impression is further enhanced by additional experiments carried out on surfactant-conditioned mixtures permeated with moulding liquids, e.g., 3% surfactant solution used as permeant with mixtures moulded with same solution. Table 4.1, which summarizes the results, shows that permeation with distilled water increases the hydraulic conductivity, but not to the level of water-moulded soils. However, the duration of the

experiments, although sufficient to establish equilibrium conditions, may not have been long enough to reverse the effects of the surfactant on the soil fabric. The hydraulic conductivity of the 80/20 mixture moulded with 6% surfactant solution is higher than for the same moulded with 3% surfactant solution. This is contrary to the general trend where K decreases as the concentration of surface-active agent increases. This discrepancy is simply attributed to experimental variations. Finally, during these additional experiments, the effluent had a noticeable blue tint, suggesting the partial dissolution of the sand and/or clay particles. This is not surprising considering the high pH of the surfactant solutions.

Table 4.1. Summary of calculated hydraulic conductivities

	Hydraulic conductivity (m/s)			
	80/20		60/40	
	D.W.	S.S.	D.W.	S.S.
Moulded with D.W.	1.3×10^{-6}	—	1.0×10^{-8}	—
Moulded with 3% S.S.	2.0×10^{-7}	8.5×10^{-8}	5.0×10^{-9}	4.5×10^{-9}
Moulded with 6% S.S.	4.0×10^{-8}	1.2×10^{-7}	2.5×10^{-9}	2.2×10^{-9}

It is anticipated that the use of oil as the permeant in the unsaturated mixtures, i.e., no permeation with distilled water to saturate the soils prior to the passage of oil, would yield higher hydraulic conductivities. Calculations in appendix III show that the average thickness of the water layer surrounding the particles of the unsaturated soils is

less than the thickness of the diffuse ion layer of the same soils when saturated with distilled water. Obviously, it is assumed that the hydrodynamic immobilized water layer corresponds to the water layer and diffuse ion layer respectively. The effect of increasing the channel width on K is greater since, according to Poiseuille equation, the flow velocity is proportional to the square of the radius of the flow channel, whereas it is inversely proportional to the permeant viscosity.

4.3 OIL IMBIBITION

4.3.1 Oil Content Variations

Considering the low initial moisture content of the soil mixtures, it is believed that the aqueous phase lines the walls of the larger pores and fills the smaller voids. Therefore, voids of a minimum size contain both air and soil solution. Under those conditions, oil imbibition in the unsaturated pores produces a favourable system energy change as it displaces air to contact the soil solution as a result of the lower interfacial tension with the aqueous phase.

Figures 4.3 and 4.4 present the oil concentration profiles. For the 80/20 mixture, the rate of movement and oil content increase as the surfactant concentration in the moulding liquid augments. It is hypothesized that the surfactant causes a redistribution of air and soil solution in the interstices, whereby a larger range of small voids are filled with the latter fluid. Since the overall moisture remains constant, the larger pores must contain less soil solution. The net effect of this redistribution would be to increase the effective pore volume through which oil can migrate, thus increasing the rate of movement and oil content. Clay migration is not believed to be occurring during oil imbibition since no head

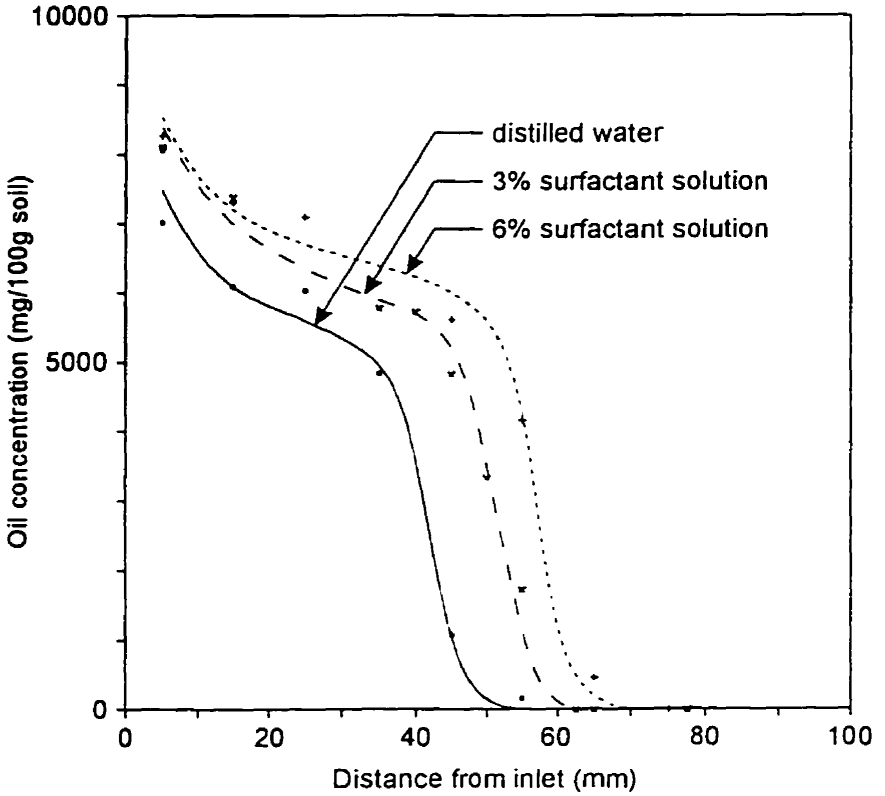

(a)

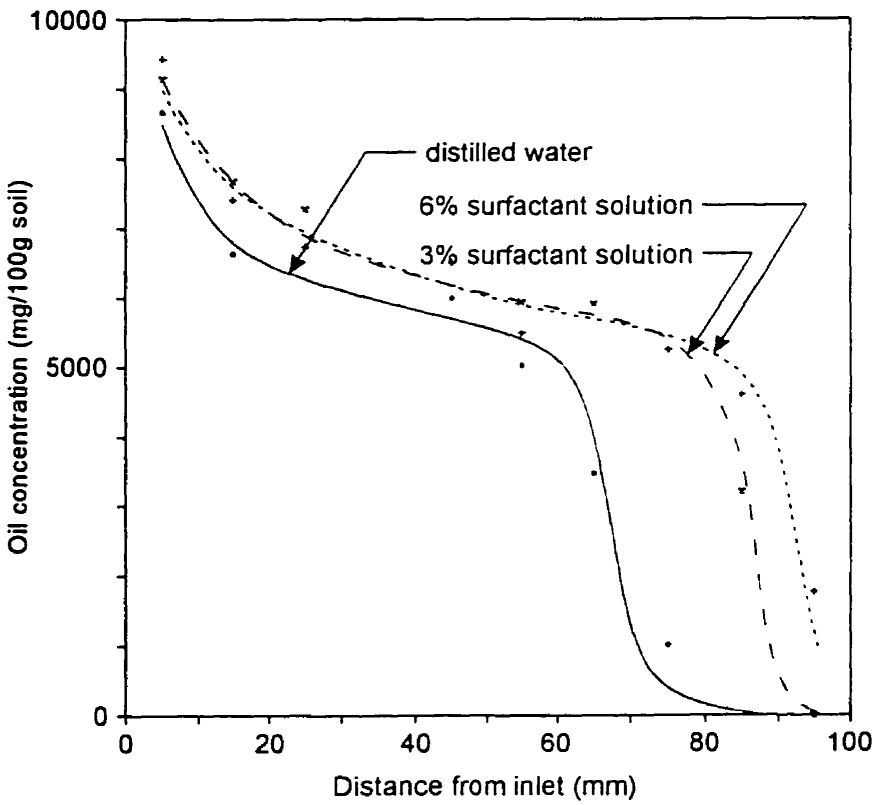

(b)

Figure 4.3. Oil concentration profile for 80/20 mixture after: (a) 1 day, (b) 2 days, and (c) 3 days (next page).

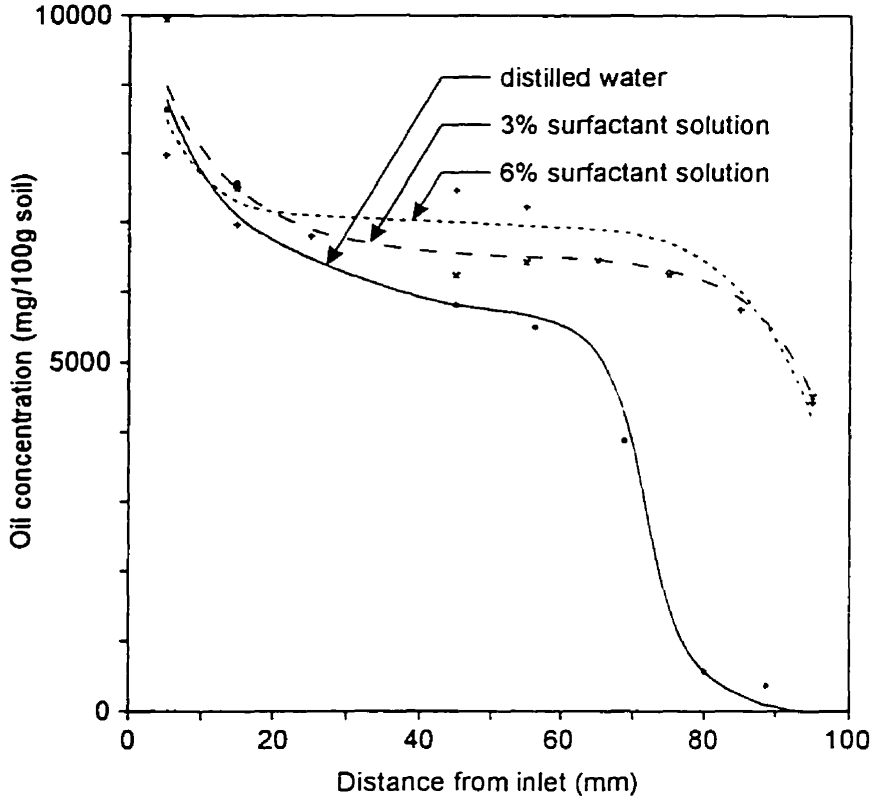

(c)

Figure 4.3. continued

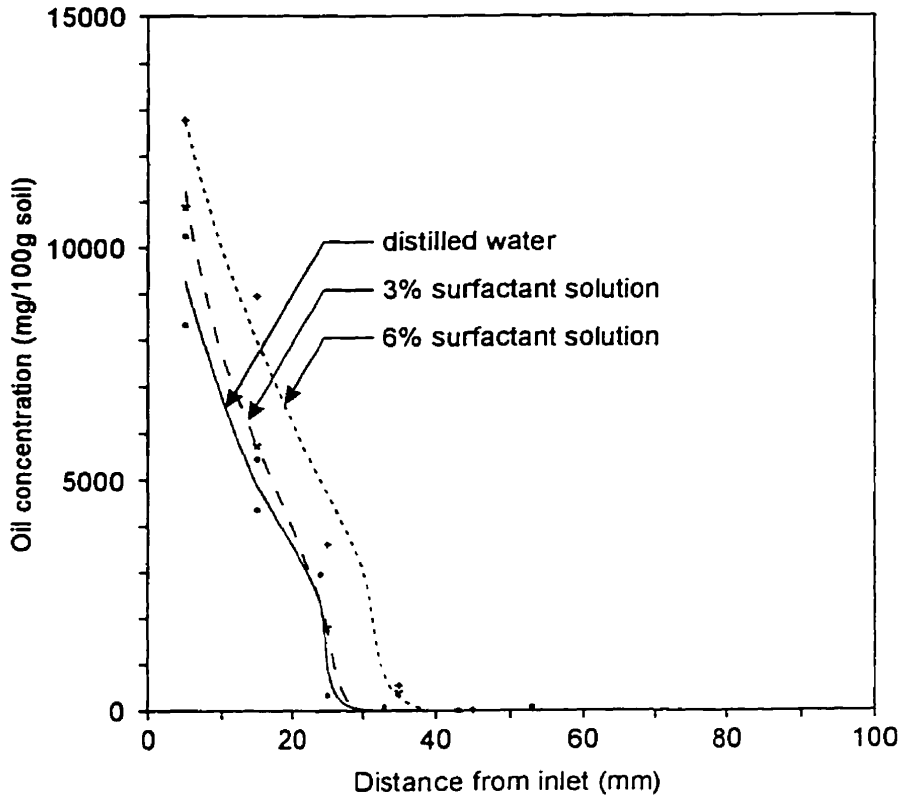

(a)

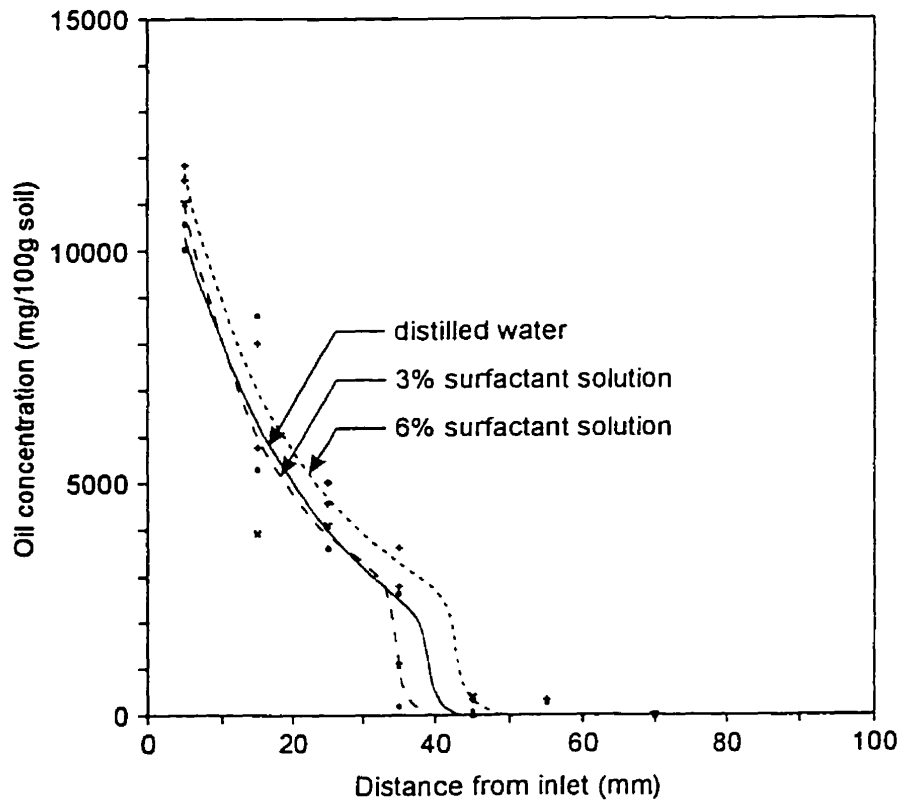

(b)

Figure 4.4. Oil concentration profile for 60/40 mixture after: (a) 3 days, (b) 5 days, and (c) 10 days (next page).

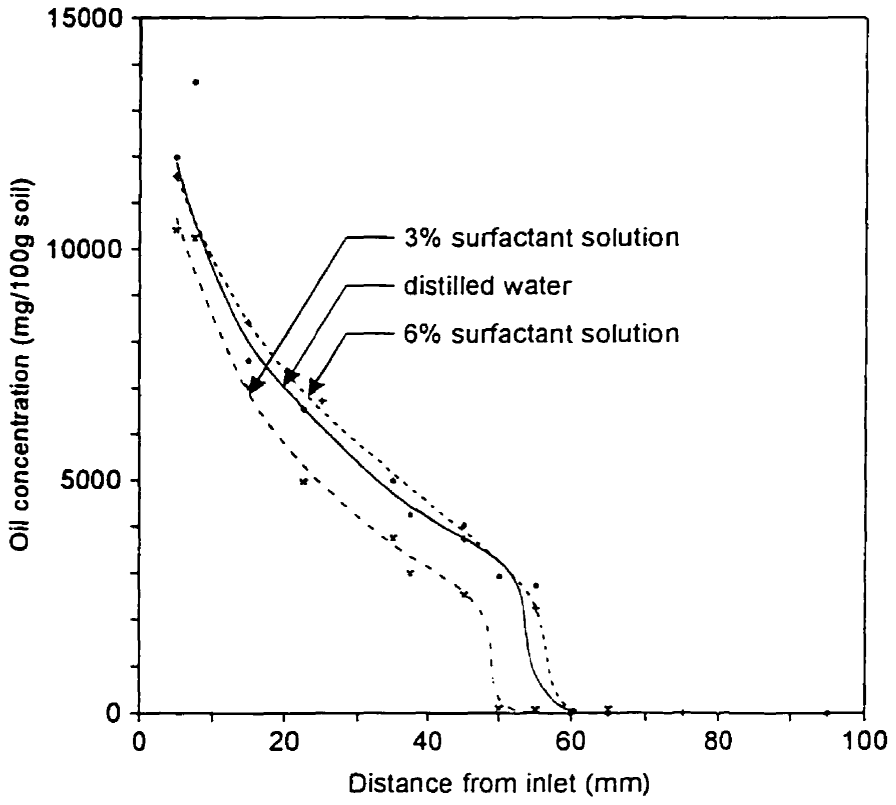

(c)

Figure 4.4. continued

is applied.

For the 60/40 mixture, the rate of movement and oil concentration also increase but to a much smaller extent. As discussed previously, although the void ratio remains constant, the size of pores of these mixtures moulded with surfactant solution decreases due to the greater particle orientation. This partially offsets the effective pore volume increase due to fluid redistribution.

The rate of movement decreases with time due to the fact that as oil moves in the interstices it spreads and/or displaces the aqueous solution, eventually causing the formation of wedges in smaller unsaturated pores. These wedges increase the tortuosity of the oil flow path, thus slowing down the migration. The effective pore size that the oil can occupy is marginally affected, explaining why the oil content at the front remains relatively constant with time. Behind the front, the oil content increases with time due to the enlargement of the channels through which oil moves as a result of the displacement of the wetting phase by viscous forces.

Interfacial tension also controls to a certain extent the rate of oil migration. The tortuosity of the flow path is expected to decrease with a reduction in interfacial tension between the fluid phases. It is difficult to assess the importance of this factor relative to enhanced wettability preference. However, it is suspected that in this study, the reduction in interfacial tension is not sufficient to be the controlling factor. Whether it can be in ultralow interfacial tension systems remains to be investigated.

4.3.2 Water Content Variations

Although the initial moisture contents of the mixtures were below the irreducible wetting phase saturations determined with the suction tests, the moulding liquids were nonetheless displaced by oil during imbibition. This is due to the viscous forces, which are nonexistent during static soil suction tests, and the lower oil-water interfacial tension that permits the displacement of the wetting phase by oil in smaller pores.

The moisture content near the inlet generally decreases with time for the 80/20 mixture, whereas it remains relatively constant for the 60/40 soil. This is probably due to the higher suction in the 60/40 mixture that accelerates the redistribution of moisture. Further, the minimum moisture content is generally lower for soils moulded with surfactant solutions due to the lower interfacial tension.

Figure 4.5 displays typical moisture content profiles for both mixtures moulded with distilled water. It shows that oil displaces the wetting phase via viscous forces. Moisture movement is also induced by suction potential gradient due to varying moisture content. It is well known that the potential decreases as the moisture content increases. Therefore, the soil pore fluid will tend to move from a point of high moisture content (lower suction) to a point of lower moisture content (higher suction). The high moisture content at the outlet end may be explained by the fact the soil drew moisture from the saturated filter paper.

4.3.3 Wetting Front Advance

Previous studies have shown that for soils with little or no swelling being

permeated with water there is a linear relationship between the wetting front advance and the square root of time (Wong and Yong, 1973; Arya et al., 1975; Yong and Mohamed, 1992). This permitted the use of the Boltzmann transformation, therefore simplifying the partial differential equation describing the movement of water into a simple ordinary differential equation that can be solved analytically. As can be seen from Figure 4.6, there is a linear relationship between the oil front advance and the square root of time. The location of the oil front was determined by visual inspection at the end of the imbibition experiments.

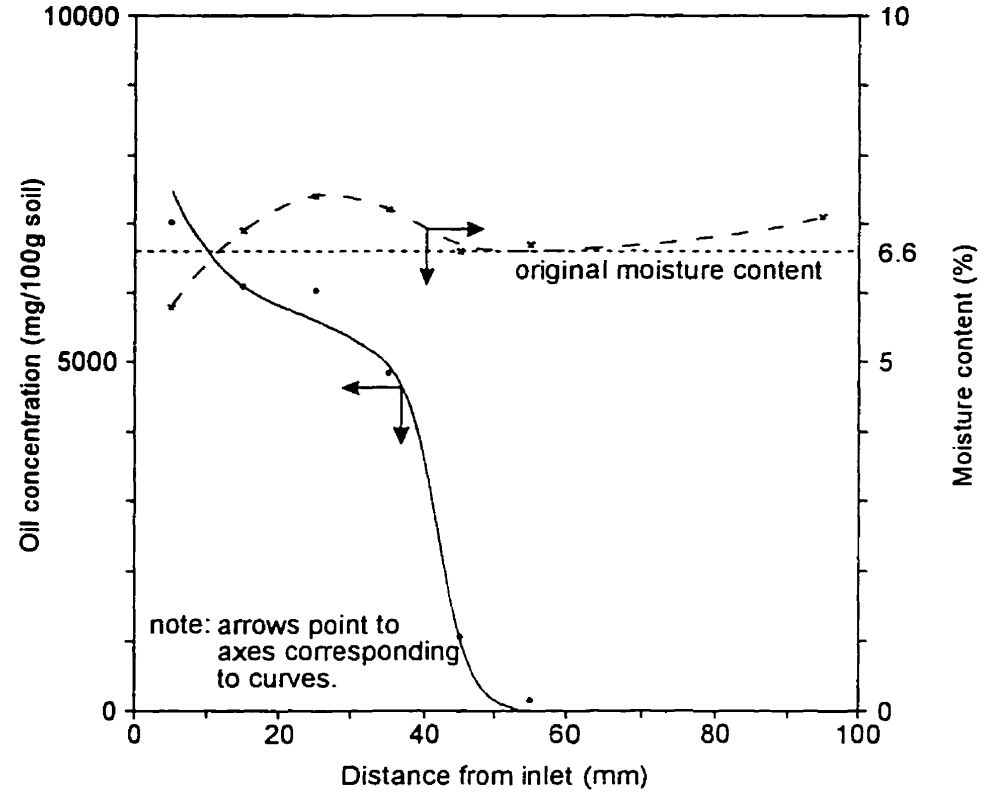

(a)

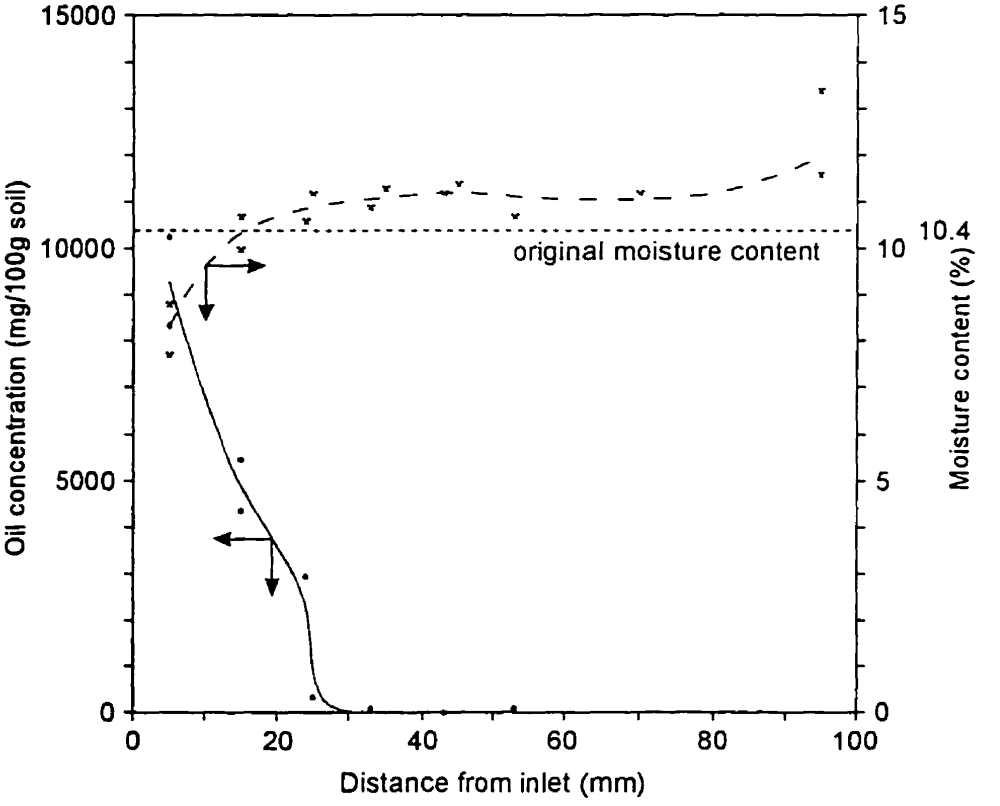

(b)

Figure 4.5. Oil concentration and moisture content profile for: (a) 80/20 moulded with distilled water after 1 day, and (b) 60/40 moulded with distilled water after 3 days.

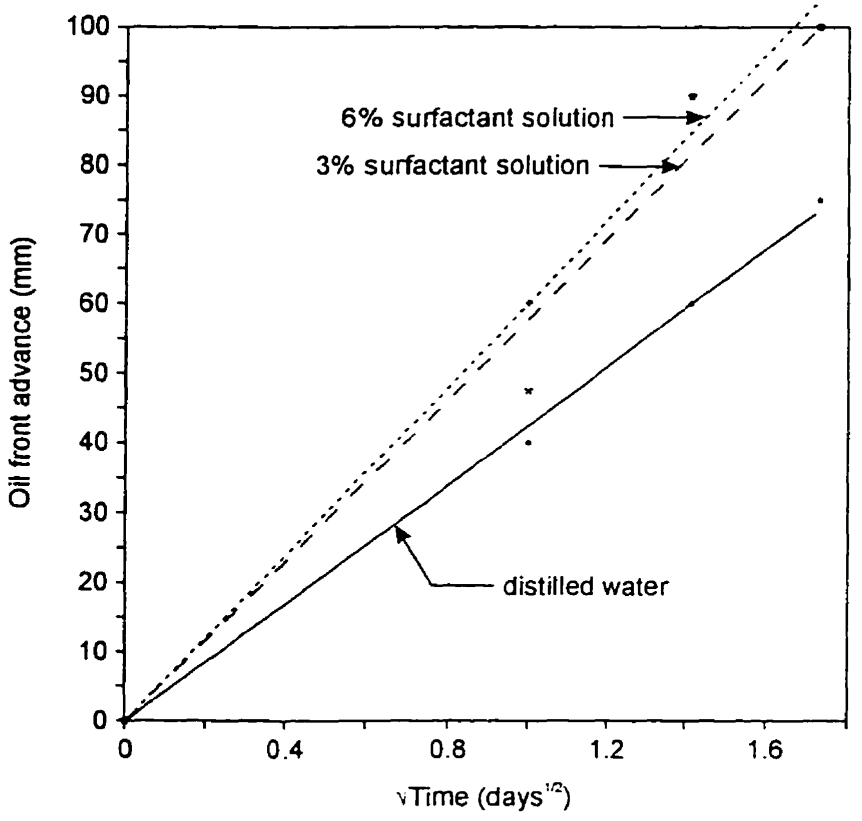

(a)

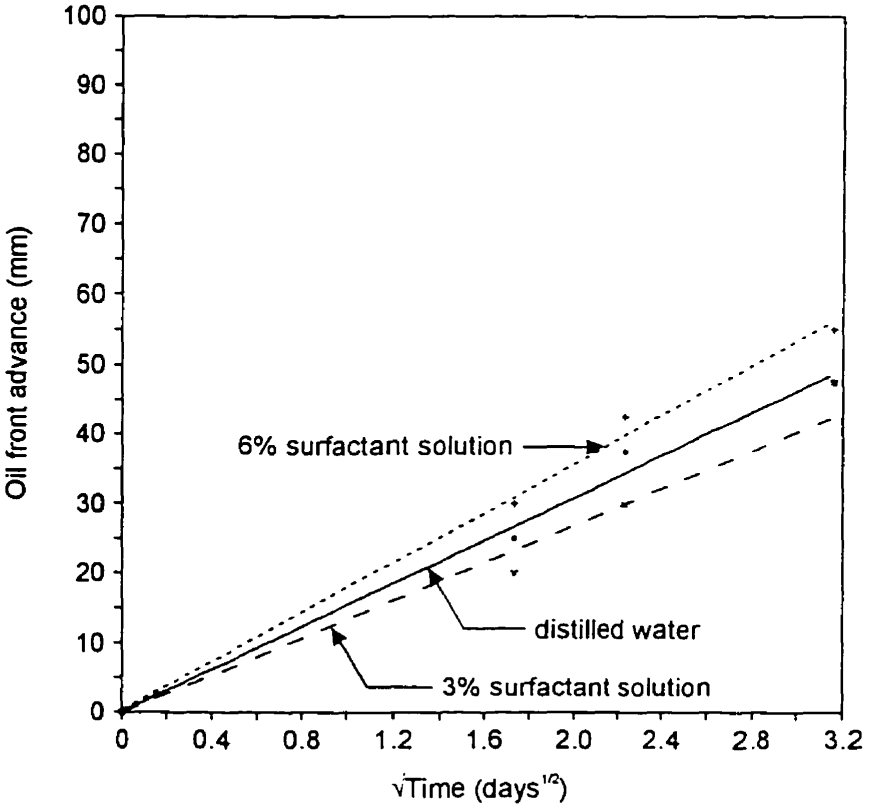

(b)

Figure 4.6. Oil front advance versus square root of time for: (a) 80/20 mixture, and (b) 60/40 mixture.

CHAPTER 5

MODELLING

5.1 INTRODUCTION

As mentioned in the introductory chapter, simulations are essential for the effective management and protection of groundwater resources as well as the remediation of contaminated aquifers. Examples of important applications include (Luckner and Schestakow, 1991):

1. Predicting the migration of point-source and area-source industrial contaminants due to accidental releases, or undetected or unreported leaks.
2. Reducing groundwater contamination due to agricultural practices.
3. Engineering design for the containment of wastes, including specifications for liner requirements, leachate collection systems, and groundwater monitoring networks. It is also employed in the design of long-term remedial action plans for inadequate past practices.
4. In situ treatment of groundwater.

The most important solution methods for mathematical models are analytical and numerical solution methods. Analytical solutions - which include the integration of linear ordinary differential equations; the substitution of variables or the use of transformations, such as Laplace or Boltzmann transformation, to solve partial differential equations; and spatial and temporal superposition of basic solutions - have a number of advantages (Javandel et al., 1984; Luckner and Schestakow, 1991):

1. They show the effect of parameters or boundary and initial conditions directly in the results.
2. They avoid numerical approximation errors.
3. They are the most economical.
4. Experienced modellers and complex numerical codes are not required.

Unfortunately, these methods are limited to certain idealized conditions that may not be applicable to a specific problem due to spatial or temporal variations and/or complex initial and boundary conditions.

It is therefore desirable to obtain a general analytical solution of the flow equation developed in Chapter 2, equation 2.10. However, by considering the diffusivity as a function of oil content, the flow equation becomes a nonlinear partial differential equation for which there is no general solution. Numerical methods, such as finite difference and finite element, allow the solution of such complex equations under various conditions. Generally, numerical methods approximate differential equations with algebraic equations relating unknown variables at discrete nodal points and at different times. The difficulties with numerical solutions are lack of accuracy due to truncation errors, and stability and convergence problems, all of which can require a great deal of efforts and computational time to overcome.

Past attempts to model the movement of NAPLs either overlooked important processes that occurred during multiphase transport or were so complex that they became practically inaccessible to persons other than the authors. The purpose of this chapter is

to develop an approach that is conceptually correct while remaining simple.

5.2 GOVERNING EQUATIONS

Unsaturated fluid flow in soils satisfying the physical condition of little or no volume change is generally described by an equation analogous to the heat flow equation. The formulation for analysis of flow presumes that Darcy's equation holds for unsaturated flow. Hence, generalizing the hydraulic gradient, grad h, and replacing it with the soil water potential gradient, grad Ψ, the Darcy equation is written as:

$$q = - K \, \text{grad}\, \Psi \tag{5.1}$$

where:

q = vector flow velocity

$$\text{grad}\, \Psi = \left(\frac{\partial}{\partial x} \bar{i} + \frac{\partial}{\partial y} \bar{j} + \frac{\partial}{\partial z} \bar{k} \right) \Psi$$

The negative sign in equation 5.1 accounts for the fact that oil flows in the direction of decreasing potential. The equation of continuity, which states that the flow of oil into or out of a unit of soil equals the rate of change in oil content, implicitly indicates that the system is preserved, i.e., no volume change. Thus:

$$\text{div}\, q = - \frac{\partial \theta}{\partial t} \tag{5.2}$$

where:

$$\text{div}\, q = \left(\frac{\partial}{\partial x} \bar{i} + \frac{\partial}{\partial y} \bar{j} + \frac{\partial}{\partial z} \bar{k} \right) q$$

θ = volumetric oil content

Substitution of equation 5.1 into equation 5.2 yields the general three-dimensional

diffusion equation. Thus

$$\frac{\partial\theta}{\partial t} = \text{div}(K \ \text{grad}\,\Psi) \qquad \textbf{(5.3)}$$

For horizontal fluid flow, the gravity potential, Ψ_g, representing gravitational forces is zero. If Ψ is a unique function of θ, equation 5.3 can be reduced to:

$$\frac{\partial\theta}{\partial t} = \frac{\partial}{\partial x}\left(K \frac{\partial\Psi}{\partial\theta} \frac{\partial\theta}{\partial x}\right) \qquad \textbf{(5.4)}$$

where x is the horizontal coordinate axis.

Solution of equation 5.4 is facilitated by introducing the diffusivity coefficient of oil $D(\theta) = K(\theta)\ (\partial\Psi / \partial\theta)$, which makes the equation analogous to those describing thermal diffusion of heat.

$$\frac{\partial\theta}{\partial t} = \frac{\partial}{\partial x}\left(D(\theta)\frac{\partial\theta}{\partial x}\right) \qquad \textbf{(5.5)}$$

5.3 CALCULATION OF OIL DIFFUSIVITY

As demonstrated in Chapter 4, there is a linear relationship between x, the distance of the wetting front from the source of fluid intake, and $\sqrt{t}$, the square root of time taken by the oil front to reach x. By resorting to a similarity solution technique, invoking the Boltzmann transformation:

$$\lambda = \frac{x}{\sqrt{t}} = \lambda(\theta) \qquad \textbf{(5.6)}$$

it becomes possible to reduce equation 5.5 to an ordinary differential equation:

$$\frac{\lambda}{2}\frac{d\theta}{d\lambda} = \frac{d}{d\lambda}\left(D(\theta)\frac{d\theta}{d\lambda}\right) \qquad \textbf{(5.7)}$$

subject to the usual boundary conditions:

$$\text{at } t = 0 \text{ and } 0 < x < \infty \text{ (thus } \lambda = \infty), \ \theta = \theta_i$$

$$\text{at } t > 0 \text{ and } x = 0 \text{ (thus } \lambda = 0), \ \theta = \theta_0$$

The diffusivity coefficient can be calculated from an experimentally measured oil profile that is divided into n equal parts (Wong and Yong, 1973), as shown in Figure 5.1.

$$\frac{\theta_0 - \theta_i}{n} = \Delta\theta \quad \text{and} \quad \theta_r = (n - r)\,\Delta\theta + \theta_i \qquad \textbf{(5.8)}$$

Since the part of the curve between A and B in Figure 5.1 is continuous and differentiable, from the Mean Value Theorem, there will be a point C in between A and B such that the tangent at C is equal to the slope of the straight line joining A and B, i.e.:

$$\left(\frac{d\theta}{dx}\right)_{\theta_c} = -\frac{\Delta\theta}{x(\theta_{r+1}) - x(\theta_r)} \qquad \textbf{(5.9)}$$

By taking $\Delta\theta$ sufficiently small, C can be taken approximately as the point [$x(\theta_{r+½})$, $\theta_{r+½}$] on the part of the curve between A and B. Integrating equation 5.7 with respect to λ, with θ varying from θ_i to θ_c gives the diffusivity at θ_c :

$$D(\theta_c) = \frac{1}{2}\left(\frac{d\lambda}{d\theta}\right)_{\theta_c} \int_{\theta}^{\theta_c} \lambda \, d\theta$$

$$= -\frac{1}{2t}\left(\frac{dx}{d\theta}\right)_{\theta_c} \int_{\theta}^{\theta_c} x \, d\theta \qquad \textbf{(5.10)}$$

Since θ_c is approximately equal to $\theta_{r+½}$, it follows that $D(\theta_c) = D(\theta_{r+½})$; substituting equation 5.9 into equation 5.10 gives:

$$D(\theta_{r+½}) = \frac{x(\theta_{r+1}) - x(\theta_r)}{2t\ \Delta\theta} \int_{0}^{\theta_{n-½}} x \, d\theta$$

$$= \frac{x(\theta_{r+1}) - x(\theta_r)}{2t\ \Delta\theta} \cdot \sum_{j=n-1}^{j=r} x(\theta_j)\Delta\theta + R \qquad \textbf{(5.11)}$$

where:

$$R = \int_{\theta_1}^{\theta_{n-½}} x \, d\theta = x(\theta_1)(\theta_{n-½} - \theta_1)$$

The maximum error (E_{max}) introduced in the calculation of $D(\theta_c)$ by taking C as the point [$x(\theta_{r+½})$, $\theta_{r+½}$] is given by:

$$E_{max} = \pm \frac{\left(\frac{x(\theta_{r+1}) - x(\theta_r)}{2\ \Delta\theta}\right)\left(\frac{x(\theta_r)\ \Delta\theta}{2}\right)}{t} \qquad \textbf{(5.12)}$$

$$= \pm \frac{1}{4}\frac{(x(\theta_{r+1}) - x(\theta_r))\ x(\theta_r)}{t}$$

Using the experimentally determined oil concentration-distance curves, the diffusivities were calculated as per the following general procedure:

1. The oil concentration in mg/100 g of dry soil was converted to volumetric oil content with the equation given below:

$$\theta = \frac{C_{oil}}{100} \times \frac{\rho_d}{\rho_{oil}} \qquad (5.13)$$

where C_{oil} is the oil concentration, ρ_d is the soil dry density and ρ_{oil} is the oil density. The volumetric oil content versus distance curve was then constructed and divided into n equal intervals, $\Delta\theta$, as shown in Figure 5.1.

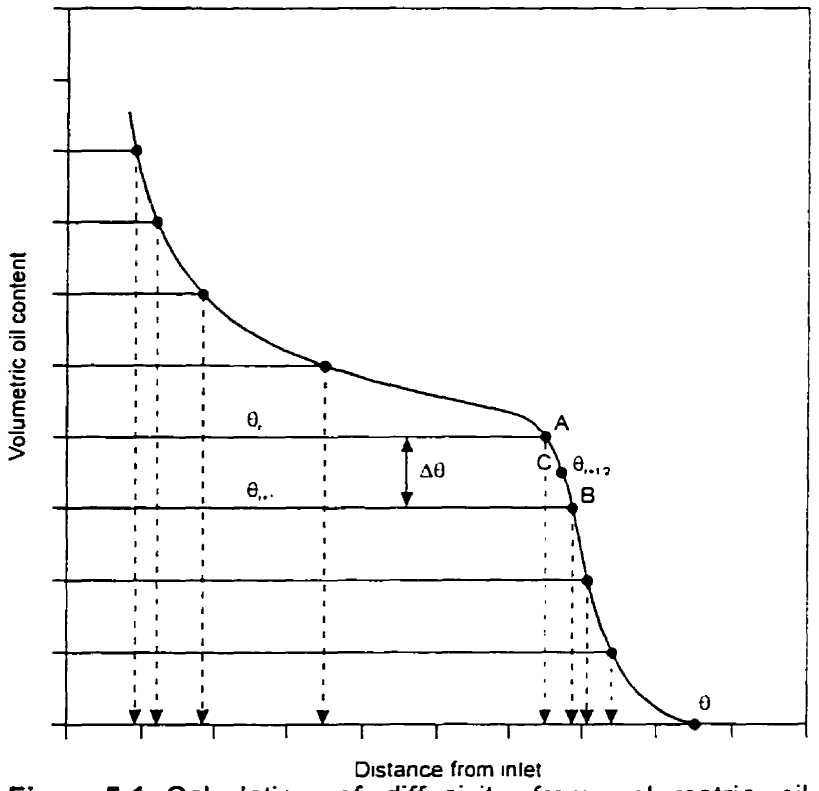

Figure 5.1. Calculation of diffusivity from volumetric oil content profile.

2. The distances, x(θ), corresponding to the volumetric oil contents were determined.

3. By inputting the above data in equation 5.11, the diffusivities were computed.

Because of the iterative nature of the calculations, a program written in Turbo Pascal (see Appendix IV) was used to obtain D and the corresponding θ. Figure 5.2 presents the flow chart of the program.

5.4 DETERMINATION OF DIFFUSIVITY FUNCTION

The commercial program Tablecurve was employed to determine the diffusivity function and parameters that best express the relation between the calculated diffusivities and volumetric oil contents. It was found that the following general diffusivity equation correlates well with the computed data:

$$D(\theta) = a + b e^{f(\upsilon)} \qquad \textbf{(5.14)}$$

The calculated 3 day diffusivities for the 80/20 mixtures moulded with surfactant solutions were markedly different from the 1 and 2 day diffusivities. It is believed that the oil reached the downstream end plate before 3 days, thus explaining the different results. The diffusivities obtained with these 3 day experiments were not utilized to determine the diffusivity function. Instead, the D obtained with the shorter duration experiments were combined to determine average parameters that could be used to simulate the 3 day oil imbibition.

For the 80/20 mixtures, the function f(θ) that generally gives the best fit is:

$$f(\theta) = 1 + \frac{c - \theta}{d} - e^{\frac{c - \upsilon}{d}} \qquad \textbf{(5.15)}$$

The unknown function parameters a, b, c, and d were also determined and the

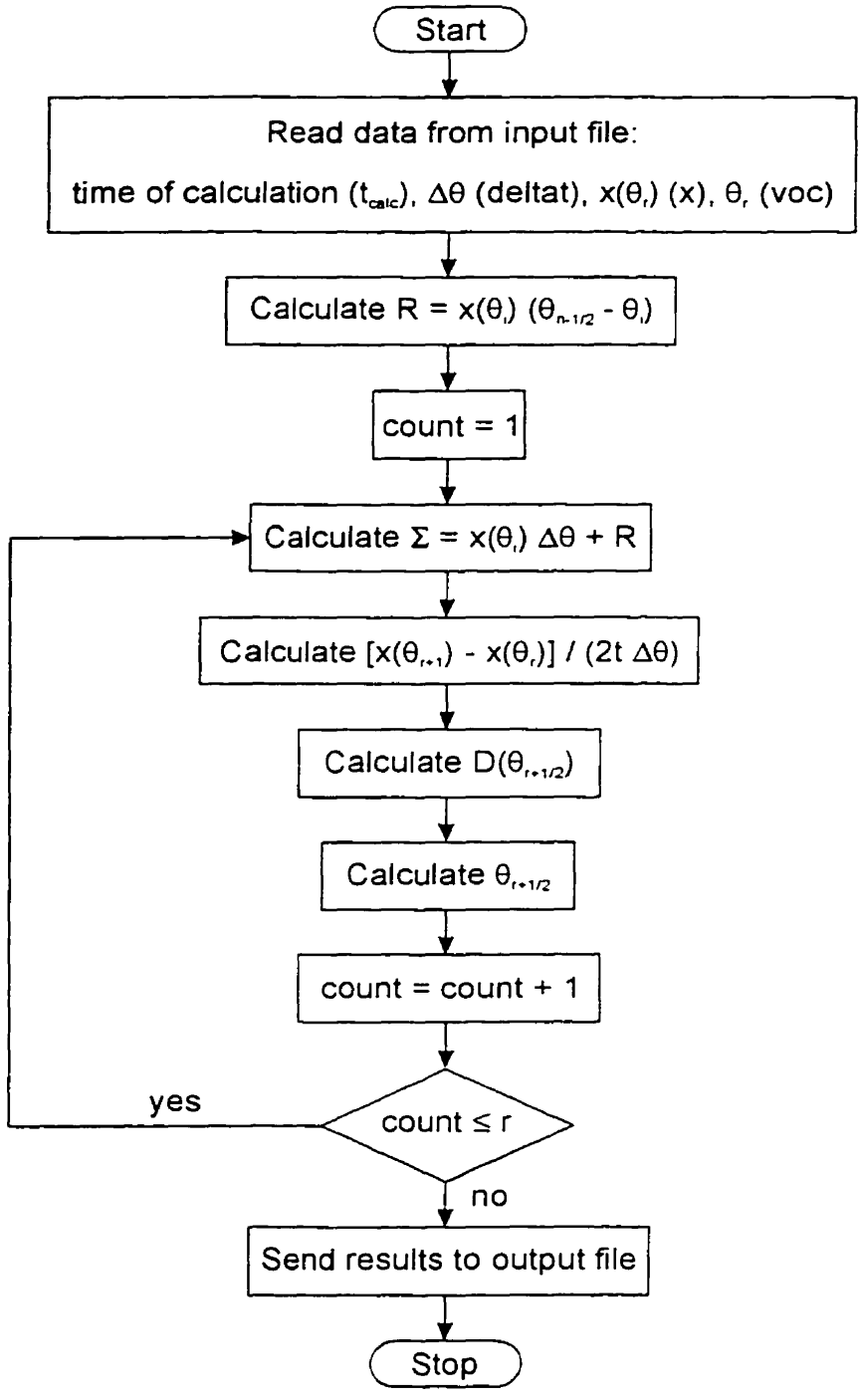

Figure 5.2. Calculation of diffusivity program flow chart.

values are summarized in Table 5.1. Figure 5.3 illustrates the D-θ relationship for the 80/20 mixture. It can be seen that the diffusivity remains constant at a value equal to 'a' up to a threshold oil content of about 8%. It then increases to a maximum value at a θ of about 12% before decreasing back to a minimum value equal to 'a'. This minimum D decreases with time, i.e., $D_{min.\ 1\ day} > D_{min.\ 2\ days} > D_{min.\ 3\ days}$, but increases with the concentration of surfactant, i.e., $D_{min.\ DW} < D_{min.\ 3\%} < D_{min.\ 6\%}$. The threshold oil content slightly increases with surfactant concentration. There is no apparent relation between time and maximum D, whereas it increases with surfactant concentration, i.e., $D_{max.\ DW} < D_{max.\ 3\%} < D_{max.\ 6\%}$. Furthermore, the oil content at maximum diffusivity increases marginally with the surface-active agent concentration, i.e., $\theta_{Dmax\ DW} < \theta_{Dmax\ 3\%} < \theta_{Dmax\ 6\%}$.

For the 60/40 mixtures, the function f(θ) that generally gives the best fit is:

$$f(\theta) = -0.5 \times \left(\frac{\ln(\theta/c)}{d}\right)^2 \qquad \textbf{(5.16)}$$

Table 5.2 summarizes the values of the parameters a, b, c and d for the 60/40 mixtures. On a number of occasions the parameter 'a' is negative. This parameter represents the point where the function intersects the y axis, i.e., the value of D at $\theta = 0$. A negative value for 'a' indicates that the diffusivity function becomes negative before it reaches the ordinate. Obviously a negative D has no physical meaning and the function needs to be bounded, i.e., the diffusivity is zero below the threshold volumetric oil content.

Figure 5.4 plots the diffusivity function for the 60/40 mixture. In this case, it is more difficult to draw conclusions since there are always exceptions to the observed

Table 5.1. Calculated parameters of the diffusivity function for 80/20 mixtures.

Moulding liquid	Duration	Parameters				
		a ($x10^{-9}$)	b ($x10^{-8}$)	c ($x10^{-1}$)	d ($x10^{-2}$)	r^2
Distilled water	1 day	1.3182	2.2969	1.1101	1.3871	0.9991
	2 days	1.1723	3.1282	1.1734	1.4964	0.9965
	3 days	0.9446	2.3557	1.1750	1.5134	0.9992
3% surf. sol.	1 day	2.3109	3.2355	1.2411	1.5215	0.9922
	2 days	2.1518	4.6470	1.2205	1.6396	0.9870
	3 days[1]	2.3162	3.9128	1.2301	1.6010	N/A
6% surf. sol.	1 day	1.9903	5.7074	1.2780	1.2427	0.9990
	2 days	1.4053	4.1482	1.1935	1.8185	0.9974
	3 days[1]	2.3375	4.7726	1.2507	1.4404	N/A

[1] Parameters obtained by combining the data for 1 and 2 days.

Table 5.2. Calculated parameters of the diffusivity function for 60/40 mixtures.

Moulding liquid	Duration	Parameters				
		a	b	c	d	r^2
Distilled water	3 days	-3.0560E-10	9.4098E-10	1.0755E-1	9.4634E-1	0.8535
	5 days	-2.3128E-7	2.3218E-7	8.3476E-2	1.2796E1	0.9476
	10 days	1.3758E-12	1.1821E-9	9.8298E-2	4.7207E-1	0.8931
3% surf. sol.	3 days	1.2939E-10	5.8616E-10	1.1018E-1	4.3051E-1	0.9871
	5 days	7.3137E-11	9.0030E-10	8.6545E-2	4.3975E-1	0.7900
	10 days	-4.6809E-12	9.1832E-10	8.3640E-2	5.5581E-1	0.8844
6% surf. sol.	3 days	6.8012 E-12	1.0676E-9	1.3973E-1	5.8382E-1	0.9719
	5 days	-1.3779E-10	1.4058E-9	8.8989E-2	6.0261E-1	0.8811
	10 days	-1.8290E-12	1.2374E-9	1.0680E-1	5.2809E-1	0.9742

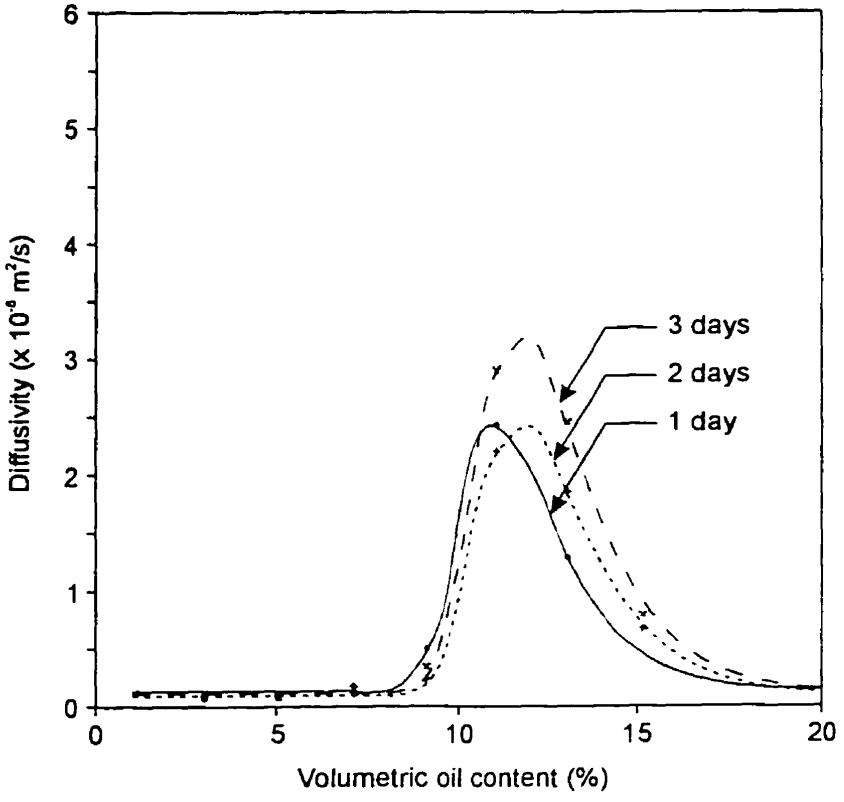

(a)

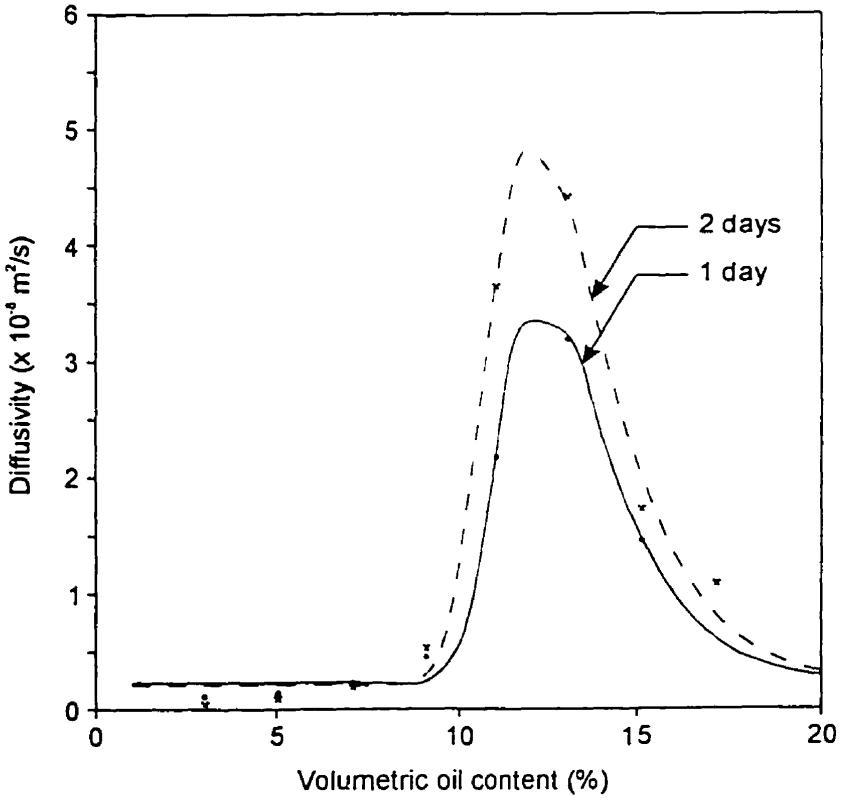

(b)

Figure 5.3. Diffusivity versus volumetric oil content for 80/20 mixture moulded with: (a) distilled water, (b) 3% surfactant solution, and (c) 6% surfactant solution (next page).

(c)

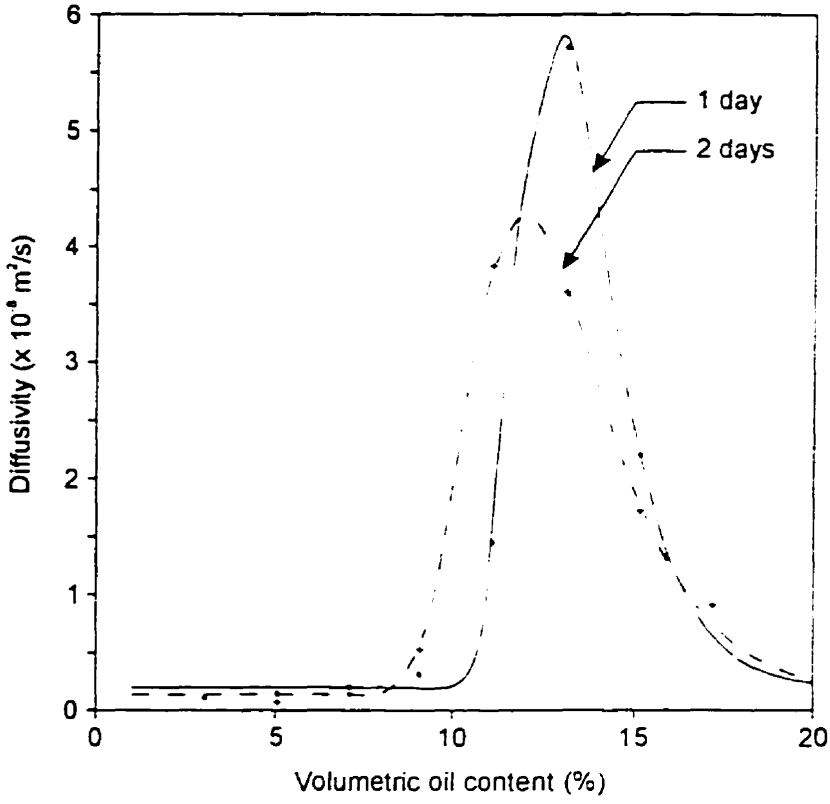

Figure 5.3. continued

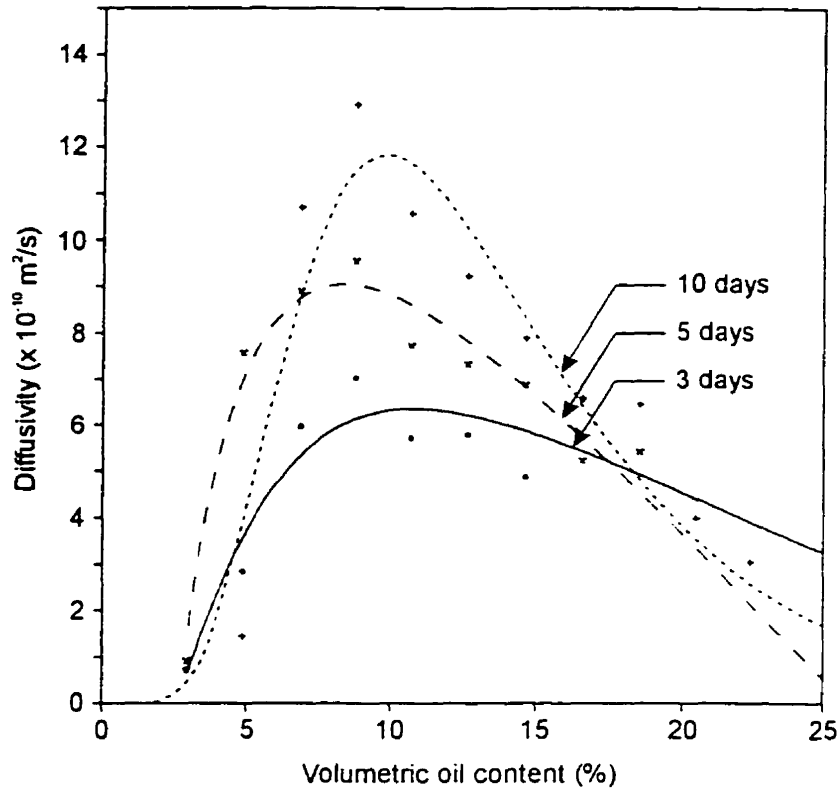

(a)

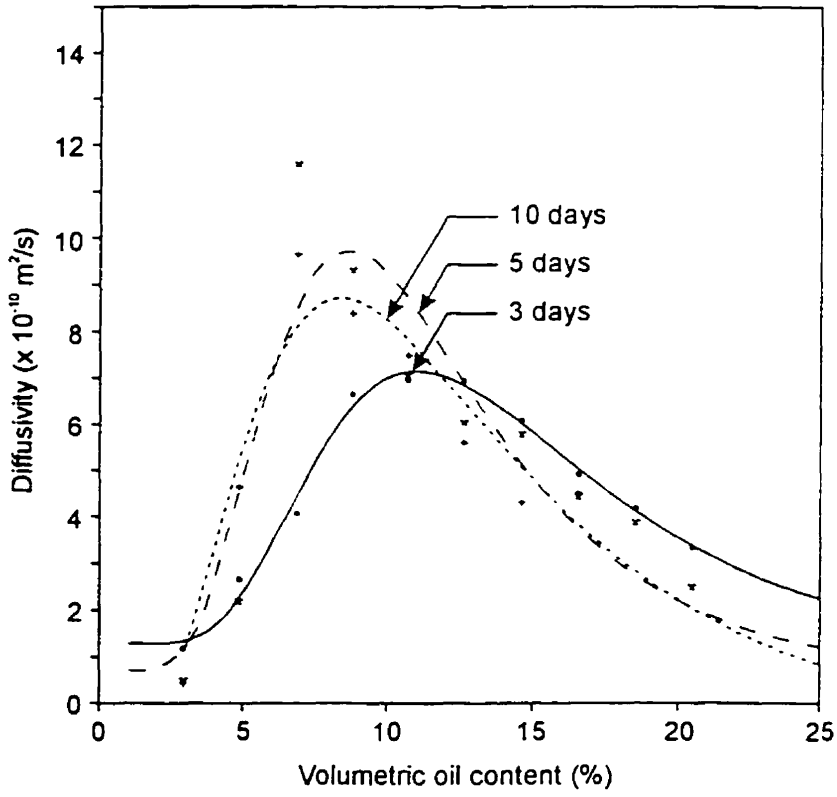

(b)

Figure 5.4. Diffusivity versus volumetric oil content for 60/40 mixture moulded with: (a) distilled water, (b) 3% surfactant solution, and (c) 6% surfactant solution (next page).

(c)

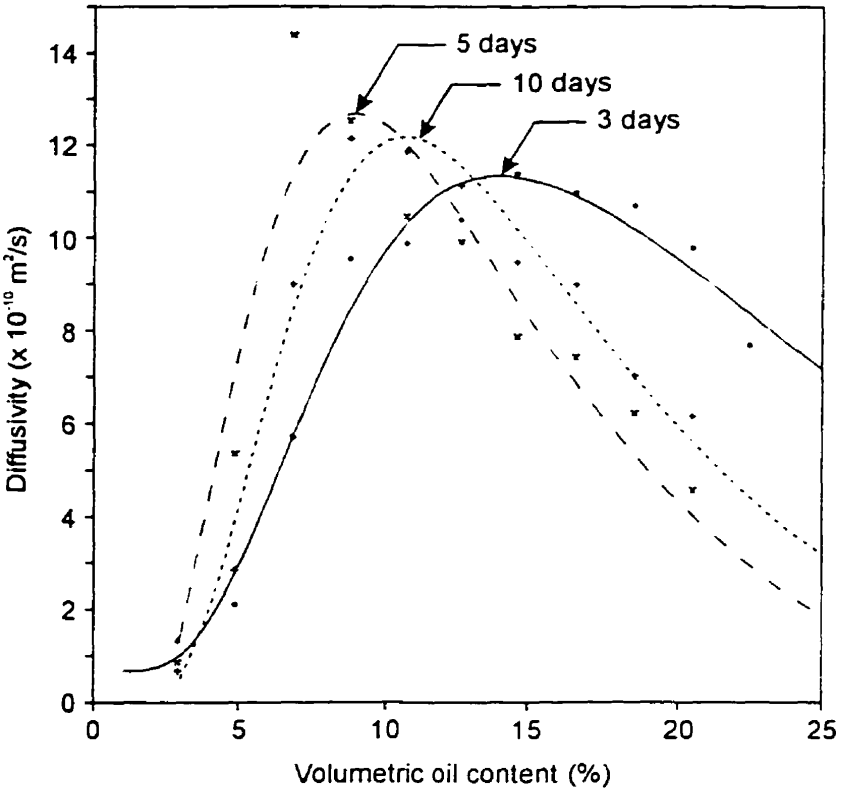

Figure 5.4. continued

trends. Similarly to the 80/20 soil, the diffusivity reaches a peak value at around an oil content of 9% and decreases back immediately, at a slower rate, to low values. Generally, there is no plateau at low θ, as was observed for the 80/20 mixture. The threshold oil content at which D becomes positive never exceeds 3%. Again, there is no apparent relation between time and D_{max}, except that it is consistently lower at 3 days. Generally, the maximum diffusivity increases with surfactant concentration and this occurs, by and large, at increasing oil content, i.e., $D_{max\ DW} < D_{max,\ 3\%} < D_{max\ 6\%}$ and $\theta_{Dmax\ DW} < \theta_{Dmax\ 3\%} < \theta_{Dmax,\ 6\%}$.

5.5 MODEL CALIBRATION/SIMULATION

According to Abriola (1984), the majority of oil models have used finite difference discretization of the governing equations because of the simplicity of the concept and ease of application.

The finite difference method approximates the differential operators by difference operators determined by means of a Taylor series expansion. Dividing time, t, and distance, x, into j and i intervals respectively, equation 5.5 becomes (Wong, 1973):

$$\frac{(\theta_i^{j+1} - \theta_i^j)}{\Delta t} = \frac{[D(\theta_{i+1}^j) + D(\theta_i^j)]\,[\theta_{i+1}^j - \theta_i^j] - [D(\theta_i^j) + D(\theta_{i-1}^j)]\,[\theta_i^j - \theta_{i-1}^j]}{2(\Delta x)^2} \quad \textbf{(5.17)}$$

For stability requirements,

$$D_{max}\,\frac{\Delta t}{(\Delta x)^2} \leq \frac{1}{2}$$

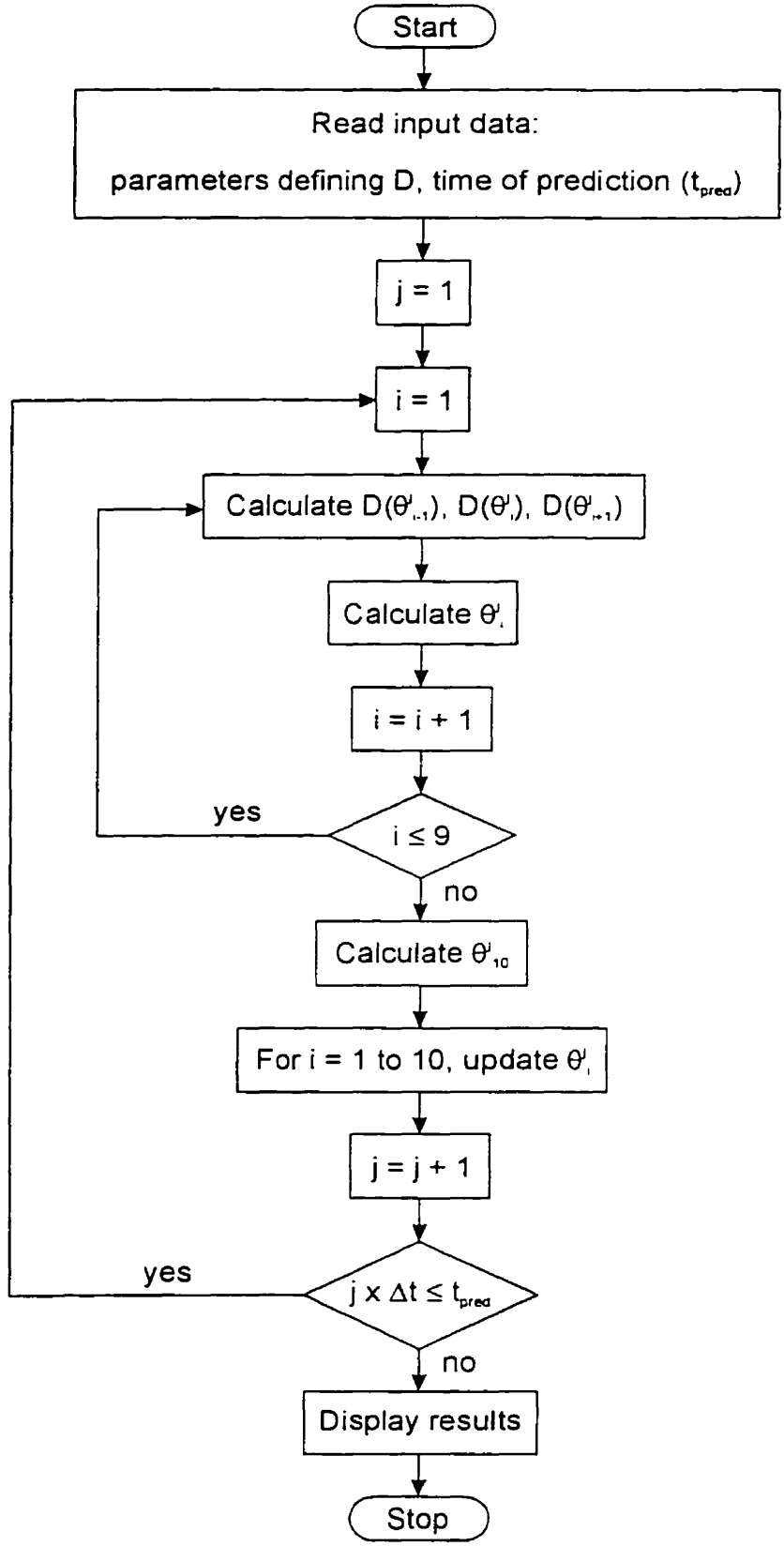

Figure 5.5. Volumetric oil content prediction program flow chart.

where D_{max} is the maximum diffusivity value.

Calibration/simulation was performed using a Turbo Pascal computer program (see appendix IV) with the flow chart shown in Figure 5.5. The exercise was carried out with a uniform rectangular grid having time steps of 60 seconds and space increments of 10 mm (Figure 5.6).

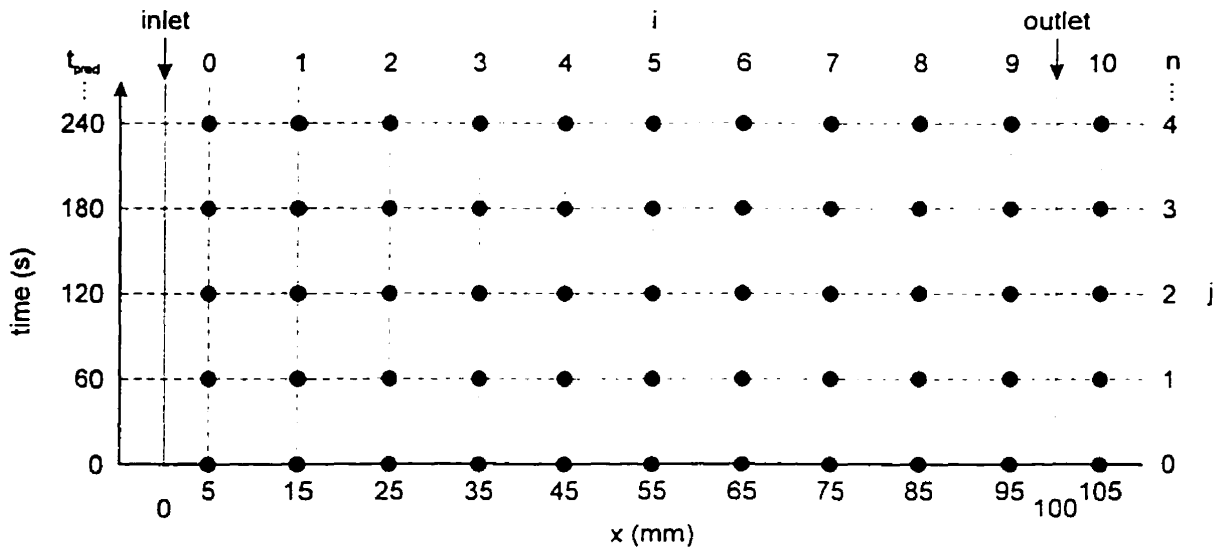

Figure 5.6. Grid used for oil migration simulation.

The following initial and boundary conditions were used:

at $t = 0$ and $x > 5$ (thus from $i = 1$ to 10), $\theta = 0$

at $t \geq 0$ and $x = 5$ (thus $i = 0$), $\theta = \theta_0$

at $t > 0$ and $x = 100$, $D\, \partial\theta / \partial x = 0$

where the latter condition implies that θ_{10} is always equal to θ_9.

The calibration/simulation was carried out for all oil imbibition experiments using the parameter values in Tables 5.1 and 5.2. For a number of 60/40 mixtures, a negative D is obtained at low volumetric oil content. As previously mentioned, this has no physical

meaning, and the computer program makes the diffusivity function equal to zero when a negative value is computed. Further, it is not feasible to determine D with the function for the 60/40 mixtures when θ is zero. Again, the computer program deviates from the mathematical model by making the diffusivity equal to 'a' when it is positive, or zero when 'a' is negative. Figures 5.7 and 5.8 show the comparison between experimental oil concentrations (points) and simulated curves. From these figures, it can be seen that:

1. For the 80/20 mixture, the simulations slightly underestimate the oil concentration, irrespective of the moulding liquid. The greatest errors generally occur near the oil front - the concentration at the top of the near vertical portion of the curve is often lower than the experimental value.
2. With the diffusivity function used for the 80/20 mixture, the model is capable of reproducing the shape of the experimental curves, i.e., a horizontal S-shape curve.
3. For the 60/40 mixture, the simulations match more closely the experimental oil concentrations.
4. The model does not exactly reproduce the shape of the experimental curve for the 60/40 mixture. The simulated curve does not have a near vertical portion that corresponds to the oil front.

5.6 PREDICTION

With the known diffusivity function for each group of soil and using equation 5.17, it is possible to obtain an oil concentration profile at any time. In this regard, the Turbo Pascal computer program used for calibration/simulation was again employed to predict

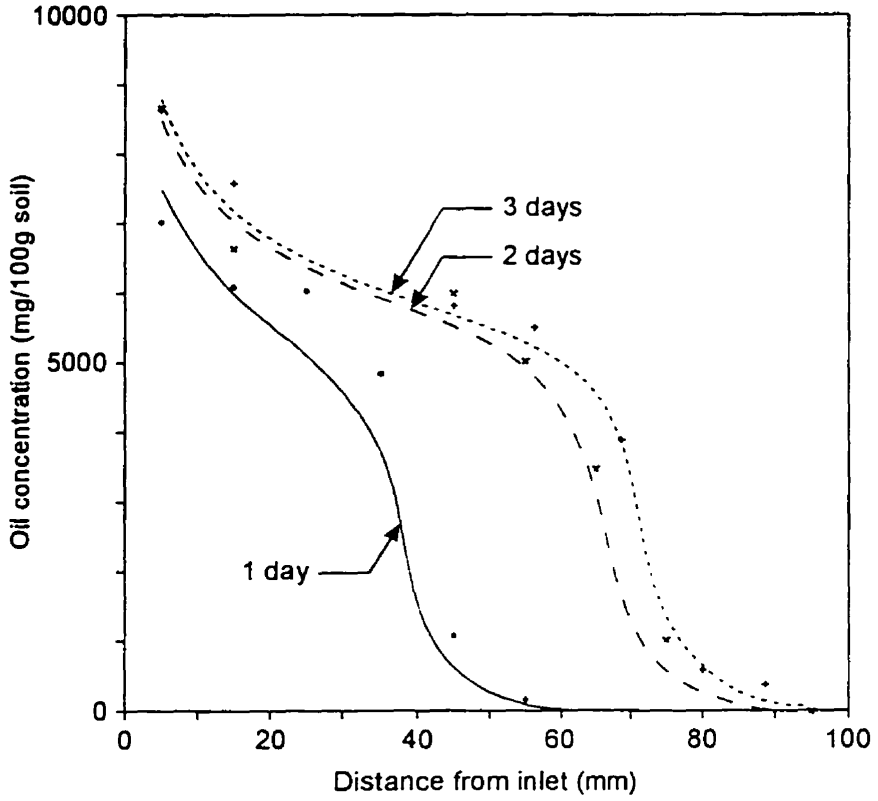

(a)

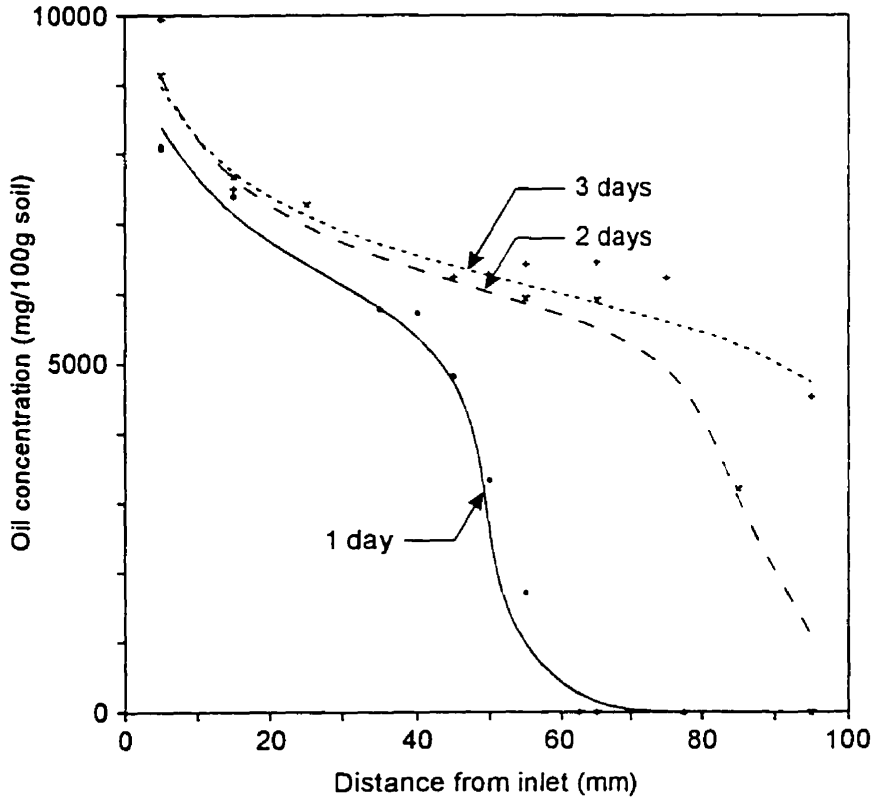

(b)

Figure 5.7. Comparison of simulated and experimental oil concentration profiles for 80/20 mixture moulded with: (a) distilled water, (b) 3% surfactant solution, and (c) 6% surfactant solution (next page).

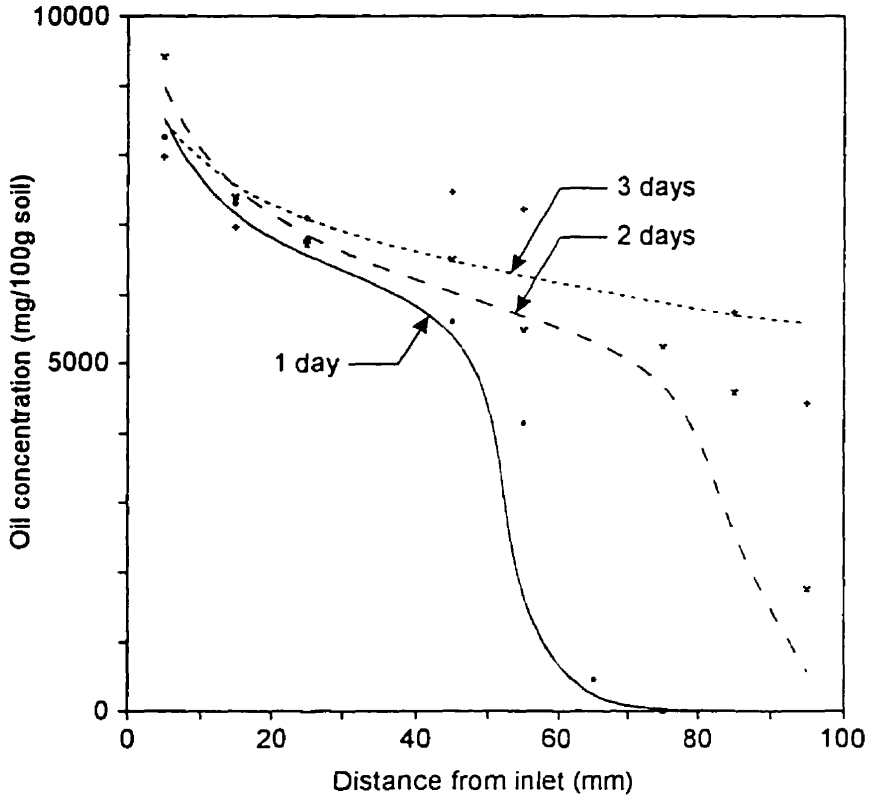

(c)

Figure 5.7. continued

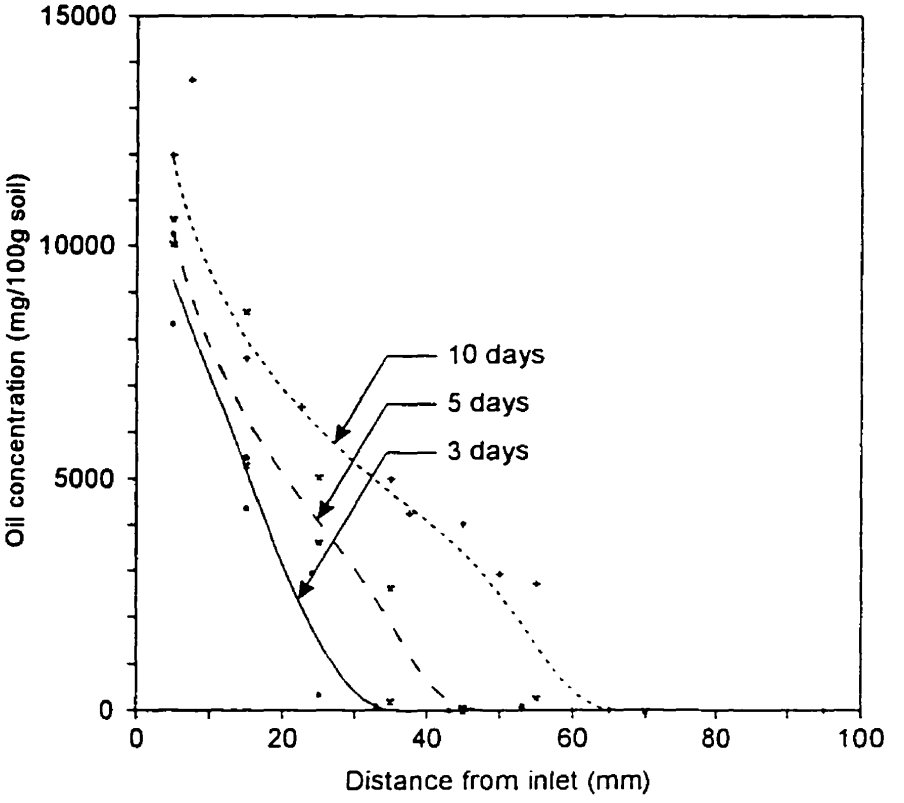

(a)

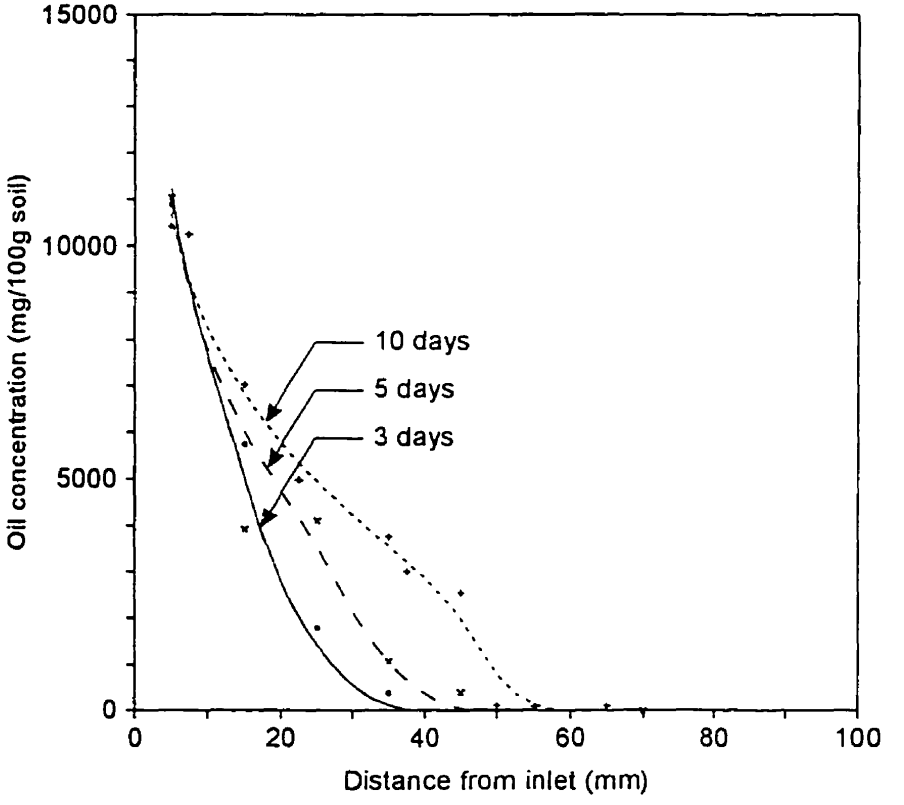

(b)

Figure 5.8. Comparison of simulated and experimental oil concentration profiles for 60/40 mixture moulded with: (a) distilled water, (b) 3% surfactant solution, and (c) 6% surfactant solution (next page).

(c)

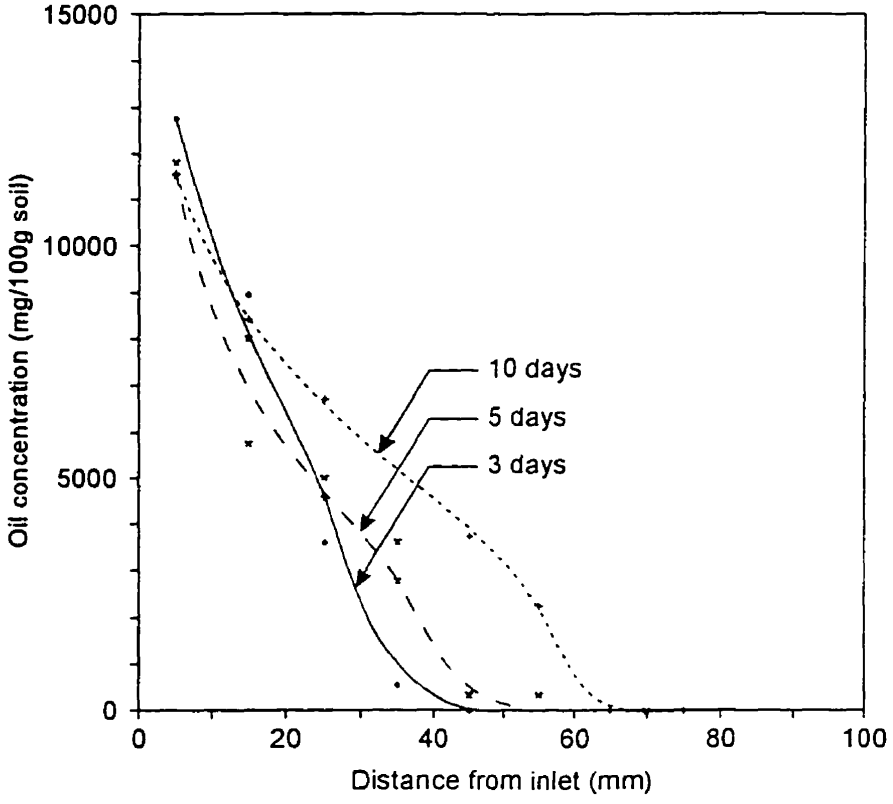

Figure 5.8. continued

the time required to saturate the soil mixtures with oil. For this exercise, average values were used for the parameters of the diffusivity function. Figure 5.9 shows the oil concentration profile curves obtained with the model. For the 80/20 mixture, the time required to saturate the soil decreases significantly with the addition of surfactant. It takes approximately 125 days for the mixture moulded with distilled water, whereas the time is reduced to 65 days for surfactant-moulded soils. For the 60/40 mixture, the saturation time remains constant at approximately 500 days.

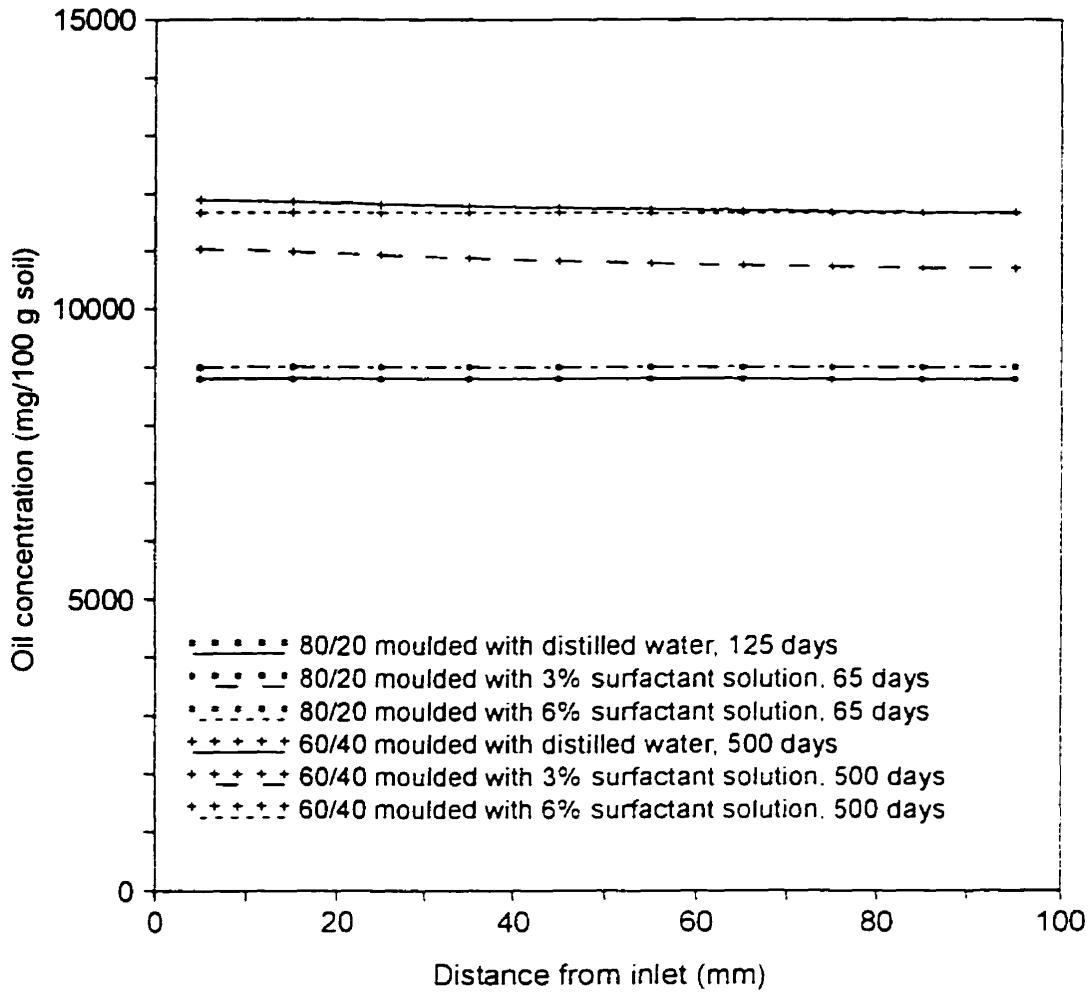

Figure 5.9. Predicted oil concentration profile curves.

CHAPTER 6

SUMMARY AND CONCLUSIONS

The main focus of this study was to investigate the effect of capillary forces on the migration of motor oil in an unsaturated soil. Oil imbibition experiments and characterization work were carried out to understand the processes that occur during multiphase flow. The observations and conclusions of this study, and their relation to the stated objectives and questions of Chapter 1 are presented in this chapter, followed by suggestions for future work.

6.1 SUMMARY

Due to its high pH, the surfactant used in this study increased the energies of interaction between kaolinite particles, thus making soil fabric more dispersive and increasing the energy with which water is held. This, in turn, had a number of repercussions on soil properties, such as wettability and permeability. It was found that the surfactant-moulded soils had an enhanced preference for water. With respect to soil permeability, it was found that the hydraulic conductivity of the mixtures decreased as the concentration of surfactant in the soil pore fluid increased.

The surfactant also reduced both surface and interfacial tensions. The presence of surface-active minerals in the soil seems to adversely affect the surfactant efficiency and effectiveness.

The rate of oil migration generally increased with the addition of surfactant to the soil pore fluid. This increase was not as evident for the 60/40 mixture. It is hypothesized that the surfactant caused a redistribution of air and soil pore solution in the interstices of the unsaturated soils. The net effect of this redistribution would be to increase the effective pore volume through which oil can migrate. It is also believed that the reduction in interfacial tension contributed to this accelerated migration by reducing the tortuosity of the flow path.

A linear relationship between the oil front advance and the square root of time was observed in all cases.

The diffusivity and corresponding volumetric oil content were determined from the experimentally obtained oil concentration profile curves. This relationship was then used to derive a diffusivity function. Generally, the function correlated well with the computed points. The simulations showed that the diffusivity function for the 80/20 mixture slightly underestimates the oil concentration but is capable of adequately reproducing the shape of the profile curve. For the 60/40 mixture, there was a better correlation between simulated and experimental curves, but the shape of the curve was not accurately reproduced.

6.2 CONCLUSIONS

1. To ensure that consistent results are obtained, it is vital to remove all the air in the inlet porous stone at the beginning of the oil imbibition experiments. This occurrence can cause large variations in the rate of movement of oil and

may explain the inconsistent results obtained with the 60/40 mixture. The removal of air is accomplished by opening the air vent while the oil fills the tube and saturates the porous stone. The vent can be closed after oil flows out of the vent. It may take more than one attempt to successfully remove all the air. When no air bubbles are trapped in the porous stone, it is of uniform dark colour, while lighter spots can be seen when air is present.

2. The measurement of oil content by the Soxhlet extraction method is difficult and occasionally gives erratic results.
3. Oil spontaneously imbibes into an unsaturated soil due to a favourable system energy change.
4. Capillary forces reduce the rate of movement of oil in an unsaturated soil by limiting the microscopic displacement efficiency. Their effect seems to be attenuated as the clay content increases.
5. The simulation of oil migration with the finite difference form of the classical diffusion equation generally compares well with experimental results. The inclusion of terms in the model that represent other mechanisms that occur during multiphase flow, such as adsorption and biodegradation, may further improve the results.
6. The diffusivity function determines the shape of the oil concentration profile curve.
7. The surfactant used for this study reduces the soil's ability to convey fluids due to its effect on soil fabric. This may be considered beneficial or detrimental depending on the use of the surfactant, i.e., to have a barrier that slows down the movement of contaminant or to clean the soil and

groundwater.

8. The surfactant also increases the soil solid phase preference for water.
9. The surfactant can promote the migration of fines depending on surfactant concentration and clay content. Soil piping is considered detrimental to the soil flushing process since it reduces the effectiveness of the technique by clogging the pores and reducing the ability of the soil to convey fluids.
10. The surfactant reduces interfacial tension but not to the extent of producing ultralow interfacial tension. It alters the soil original wettability. It may therefore be more appropriate to refer to the product as an alkaline agent.
11. The surfactant/alkaline agent acts on the displacement efficiency at the pore scale via interfacial tension reduction and wettability alteration. However, due to its tendency to promote soil piping and detrimental effect on soil permeability, this product may not be appropriate for soil flushing operations.

6.2 SUGGESTIONS FOR FURTHER STUDIES

Further studies on the following items are suggested:

1. To examine how the addition of surfactant affects the wetting preference of the sand and kaolinite individually. Determine the type of wettability of the sand/kaolinite mixtures, i.e., uniform, fractional or mixed wettability, and investigate how the surfactant affects the type of wettability.
2. To examine the effect of initial moisture content on the capillary pressure curve (oil-moulding liquid) and the work required by the oil to displace both the moulding liquid and air from the voids.

3. To determine the extent of clay migration of surfactant-moulded soils during oil imbibition.
4. To determine the importance of capillary forces when oil flows under various pressure heads. Also examine how it affects the diffusivity function.
5. To examine the effects of heterogeneities on the migration of oil.
6. To examine the effect of initial moisture content on the migration of oil.
7. To determine the extent of adsorption of oil on the solid phase and modify the mathematical model to take this mechanism into account.
8. The addition of surfactant can affect the microbial system, and may either enhance or inhibit the rate and extent of biodegradation. Examine the effects of this surfactant solution on biodegradation.

CHAPTER 7

REFERENCES

Abdul, A.S., Gibson, T.L., and Devi, N.R., (1991), "Selection of surfactants for the removal of petroleum products from shallow sandy aquifers", *Ground Water*, **26**(6): 920-926.

Abriola, L.M., (1984), "Multiphase migration of organic compounds in a porous medium. A mathematical model", in: *Lecture Notes in Engineering*, edited by C.A. Brebbia and S.A. Orszag, Springer-Verlag, Berlin, 232 p.

Acar, Y.B., Hamidon, A., Field S.D., and Scott, L., (1985), "The effect of organic fluids on hydraulic conductivity of compacted kaolinite", in: *Hydraulic barriers in soil and rock*, edited by A.I. Jonhson, R.K. Forbel, N.J. Cavalli, and C.B. Peterson, American Society for Testing and Materials, Special Technical Publication 874, pp. 171-187.

Anderson, D.C., Brown, K.W., and Thomas, J.C., (1985), "Conductivity of compacted clay soils to water and organic liquids", *Waste Management and Research*, **3**(4): 339-349.

Anderson, W.G., (1986a), "Wettability literature survey - Part 1: rock/oil/brine interactions and the effects of core handling on wettability", *Journal of Petroleum Technology*, pp. 1125-1144.

Anderson, W.G., (1986b), "Wettability literature survey - Part 2: wettability measurements", *Journal of Petroleum Technology*, pp. 1246-1262.

Anderson, W.G., (1987a), "Wettability literature survey - Part 4: effects of wettability on capillary pressure", *Journal of Petroleum Technology*, pp. 1283-1300.

Anderson, W.G., (1987b), "Wettability literature survey - Part 5: the effects of wettability on relative permeability", *Journal of Petroleum Technology*, pp. 1453-1468.

Arya, L.M., Farrel, D.A., and Blake, G.R., (1975), "A field study of soil water depletion patterns in presence of growing ceylon roots: I. Determination of hydraulic properties of the soil", *Soil Science Society of America Journal*, **39:** 424-430.

Bavière, M., (1991), "Preface", in: *Basic concepts in Enhanced Oil Recovery Processes*, edited by M. Bavière, Elsevier Scientific Publishing Company, New York, pp. v-viii.

Boyd, S.A., Mortland, M.M., and Chiou, C.T., (1988), "Sorption characteristics of organic compounds on hexadecyltrimethylammonium-smectite", *Soil Science Society of America Journal*, **52**:652-657.

Brown, K.W., Thomas, J.C., and Green, J.W., (1984), "Permeability of compacted soils to solvent mixtures and petroleum products", *Land Disposal of Hazardous Waste, Proceedings of the 10th Annual Research Symposium*, EPA-600/9-84-007, Ft. Washington, PA, pp.124-137.

Brown, K.W., Thomas, J.C., and Green, J.W., (1986), "Field cell verification of the effects of concentrated organic solvents on the conductivity of compacted soils", *Hazardous Waste and Hazardous Materials*, **3**(1): 1-19.

Brown, C.L., Pope, G.A., Abriola, L.M., Sepehrnoori, K., (1995), "Simulation of surfactant-enhanced aquifer remediation", *Water Resources Research*, **30**(11): 2959-2977.

Bruce, R.R., and Klute, (1956), "The measurement of Soil Moisture Diffusivity", *Soil Science Society of America Journal*, **20:** 458-462.

Cabral, A.R., (1992), *A study of compatibility to heavy metal transport in permeability testing*, Ph.D Thesis, McGill University.

Calhoun, Jr., J.C., (1951), "Criteria for determining rock wettability", *Oil & Gas Journal*, **50**(1): 151.

Calhoun, Jr., J.C., (1953), *Fundamentals of Reservoir Engineering*, University of Oklahoma Press, 417 p.

Carcoana, A., (1992), *Applied Enhanced Oil Recovery*, Prentice Hall, Englewood Cliffs, 292 p.

Caudle, B.H., Slobod, R.L., and Brownscombe, E.R., (1951), "Further developments in the laboratory determination of relative permeability", *Transactions American Institute of Mining, Metallurgical, and Petroleum Engineers*, **192:** 145-150.

Childs, E.C., and George, N.C., (1950a), *Transactions 4th International Congress of Soil Science*, 1:60.

Childs, E.C., and George, (1950b), Proceedings Royal Society of London Series A., 201:392.

Chilingar, G.V., and Yen, T.F., (1983), "Some notes on wettability and relative permeabilities of carbonate reservoir rocks, II", *Energy Sources*, **7**(1): 67-75.

Clementz, D.M., (1976), "Interaction of Petroleum Heavy Ends with Montmorillonite", *Clays and Clay Minerals*, **24:** 312-319.

Collins, S.H., and Melrose, J.C., (1983), "Adsorption of asphaltenes and water on reservoir rock minerals", paper SPE 11800 presented at the 1983 SPE International Symposium on Oilfield and Geothermal Chemistry, Denver, June 1-3, pp. 249-254.

Craig, F.F., (1971), *The Reservoir Engineering Aspects of Waterflooding*, Monograph series, Society of Petroleum Engineers, Richardson.

D'Arcy, H., (1856), *Les Fontaines Publiques de la Ville de Dijon*, Dalmont, Paris.

Donaldson, E.C., and Thomas, R.D., (1971), "Microscopic observations of oil displacement in water-wet and oil-wet systems", paper SPE 3555 presented at the 1971 SPE Annual Meeting, New Orleans, Oct. 3-6.

Fatt, I., and Klikoff, W.A., (1959), "Effect of fractional wettability on multiphase flow through porous media", *Transactions American Institute of Mining, Metallurgical, and Petroleum Engineers*, **216:** 426-432.

Fernandez, F., and Quigley, R.M., (1985), "Hydraulic conductivity of natural clays permeated with simple liquid hydrocarbons", *Canadian Geotechnical Journal*, **22:** 205-214.

Fernandez, F, and Quigley, R.M., (1988), "Viscosity and dielectric constant controls on the hydraulic conductivity of clayey soils permeated with water-soluble organics", *Canadian Geotechnical Journal*, **25:** 582-589.

Galvez, R. (1989), *Clay suspension as a buffering system for accumulation of lead as a soil pollutant*, M.Eng. Thesis, McGill University.

Gaudin, A.M, (1957), *Flotation*, 2nd ed., McGraw-Hill Book Co. Inc., New York, 573 p.

Green, W.J., Lee, G.F., and Jones, R.A., (1981), "Clay-soils permeability and hazardous waste storage", *Journal Water Pollution Control Federation*, **53**(8): 1347-1354.

Greenberg, A., Clesceri, L., and Eaton, A., (1992), *Standard Methods for the Examination of Water and Wastewater*, 18th ed., American Public Health Association, Washington, pp. 5.27-5.29.

Hansbo, S., (1960), "Consolidation of clay with special reference to influence of vertical sand drains", *Proceedings no. 18*, Swedish Geotechnical Institute, pp. 45-50.

Hasbach, A., (1993), "Moving beyond pump-and-treat", *Pollution Engineering*, **25**(3): 36-39.

Hillel, D., (1989), "Movement and retention of organics in Soil: a review and critique of modeling", in: *Petroleum Contaminated Soils*, vol. 1, edited by P.T. Kostecki and E.J. Calabrese, Lewis Publishers, pp.81-86.

Hoffman, R.W., and Brindley, G.W., (1960), "Adsorption of nonionic aliphatic molecules from aqueous solutions on montmorillonite. Clay organic studies II", *Geochimica et Cosmochimica Acta*, **20:** 15-29.

Javandel, I., Doughty, C., and Tsang, C.-F., (1984), *Groundwater Transport: Handbook of Mathematical Models*, American Geophysical Union, Washington, D.C., 228 p.

Jennings, H., Y., Jr., (1957), "Surface properties of natural and synthetic porous media", *Producers Monthly*, **21**(5): 20-24.

Klute, A., (1952),"Some theoretical aspects of the flow of water in unsaturated soils", *Soil Science Society of America Proceedings*, **16:** 144-148.

Leverett, M.C., (1938), "Flow of oil-water mixtures through unconsolidated sands", *Transactions American Institute of Mining, Metallurgical, and Petroleum Engineers*, **132:** 149-171.

Lorenz, P.B., Donaldson, E.C., and Thomas, R.D., (1974), "Use of centrifugal measurements of wettability to predict oil recovery", report 7873, United States Bureau of Mines, Bartlesville Energy Technology Center.

Ludwig, H., (1979), *A Study of Some Aspects of Dispersive Clay Particle Interaction*, M.Eng. Thesis, McGill University.

Mackay, D.M., Roberts, P.V., and Cherry, J.A., (1985), "Transport of organic contaminants in groundwater", *Environmental Science & Technology*, pp.384-392.

Mann, M.J., (1993), *Innovative Site Remediation Technology - Soil Washing/Soil Flushing*, volume 3, edited by W.C. Anderson, American Academy of Environmental Engineers, Annapolis.

Marle, C.M., (1991), "Oil entrapment and mobilization", in: *Basic Concepts in Enhanced Oil Recovery Processes*, edited by M. Bavière, Elsevier Scientific Publishing Company, New York, pp. 3-39.

McCaffrey, F.G., (1973), "The effect of wettability on relative permeability and imbibition in porous media", Ph.D Thesis, University of Calgary.

McCaffrey, F.G., and Bennion, D.W., (1974), "The effect of wettability on two-phase relative permeabilities", *Journal of Canadian Petroleum Technology*, **13**(4): 42-53.

McGhee, J.W., Crocker, M.E., and Donaldson, E.C., (1979), "Relative wetting properties of crude oils in Berea sandstone", report BETC/RI-78/9, Bartlesville Energy Technology Centre, U.S.DOE.

Melrose, J.C., and Brandner, C.F., (1974), "Role of capillary forces in determining microscopic displacement efficiency for oil recovery by waterflooding", *The Journal of Canadian Petroleum Technology*, **13**: 54-62.

Mesri, G., and Olson, R.E., (1971), "Mechanisms controlling the permeability of clays", *Clays and Clay Minerals*, **19**: 151-158.

Meyers, P.A., and Quinn, J.G., (1973), "Association of hydrocarbons and mineral particles in saline solution", *Nature*, **244**: 23-24.

Michaels, A.S., and Lin, C.S., (1954), "Permeability of kaolinite", *Industrial and Engineering Chemistry*, **46**:1239-1246.

Mitchell, J.K., and Madsen, F.T., (1987), "Chemical effects on clay hydraulic conductivity", in: *Geotechnical Practice for Waste Disposal*, ASCE specialty conference, edited by R.D. Woods, American Society of Civil Engineers, New York, pp. 87-116.

Mohammed, L.F., (1995), *Assessment of soil stabilization via oil residue and its environmental implications*, Ph.D Thesis, McGill University.

Mohanty, K.K., and Salter, S.J., (1983), "Multiphase flow in porous media: III. Oil mobilization, transverse dispersion, and wettability", paper SPE 12127 presented at the 1983 SPE Annual Technical Conference and Exhibition, San Francisco, Oct. 5-8.

Morgan, J.T., and Gordon, D.T., (1970), "Influence of pore geometry on water-oil relative permeabilities", *Journal of Petroleum Technology*, pp. 1199-1208.

Morrow, N.R., (1970a), "Physics and thermodynamics of capillary action", *Industrial and Engineering Chemistry*, **62**: 32-56.

Morrow, N.R., (1970b), "Irreducible wetting-phase saturation in porous media", *Chemical Engineering Science*, **25**: 1799-1815.

Morrow, N.R., and Mungan, N., (1971), "Wettability and capillarity in porous media", report RR-7, Petroleum Recovery Research Institute, Calgary.

Morrow, N.R., (1976), "Capillary pressure correlation for uniformly wetted porous media", *Journal of Canadian Petroleum Technology*, **15**(4): 49-69.

Morrow, N.R., McCaffrey, F.G., (1978), "Displacement studies in uniformly wetted porous media", *Wetting, Spreading, and Adhesion*, edited by G.F. Padday, Academic Press, New York.

Mortland, M.M., (1970), "Clay-organic complexes and interactions", *Advances in Agronomy*, **22**: 75-117.

Mortland, M.M., (1986), "Mechanisms of adsorption of non-humic species by clays", in: *Interaction of Soil Minerals with Natural Organics and Microbes*, edited by P.M. Huang, Soil Science Society of America, Madison, Wisconsin, pp. 59-76.

Nielsen, D.R., van Genutchen, M. TH., and Biggar, J.W., (1986), "Water flow and solute transport processes in the unsaturated zone", *Water Resources Research*, pp.89S-108S.

Olsen, H.W., (1962), "Hydraulic flow through saturated clays", *Clays and Clay Minerals*, **9:** 131-161.

Olsen, H.W., (1966),"Darcy's law in saturated kaolinite", *Water Resources Research*, **2**(2): 287-295.

Owens, W.W., and Archer, D.L., (1971), "The effect of rock wettability on oil-water relative permeability relationship", *Journal of Petroleum Technology*, pp. 873-878.

Palmer, C.D., and Johnson, R.L., (1989), "Physical processes controlling the transport of non-aqueous phase liquids in the subsurface", in: *Transport and Fate of Contaminants in the Subsurface*, EPA/625/4-89/019, pp.23-27.

Parker, J.C., (1989), "Multiphase flow and transport in porous media", *Reviews of Geophysics*, **27**(3): 311-328.

Pope, G.A., and Bavière, M., (1991), "Reduction of capillary forces by surfactants",in: *Basic Concepts in Enhanced Oil Recovery Processes*, edited by M. Bavière, Elsevier Scientific Publishing Company, New York, pp. 89-121.

Pope, G.A., and Wade, W.H., (1995), "Lessons from enhanced oil recovery research for surfactant-enhanced aquifer remediation", in: *Surfactant-Enhanced Subsurface Remediation - Emerging Technologies*, edited by D.S. Sabatini, R.C. Knox and J.H. Harwell, ACS Symposium Series 594, Washington, pp. 142-160.

Richards, L.A., (1947), "Pressure-membrane apparatus - construction and use", *Agricultural Engineering*, October, pp. 451-455.

Richardson, J.G., Perkins, F.M., and Osoba, J.S., (1955), "Differences in behavior of fresh and aged east Texas woodbine core", *Transactions American Institute of Mining, Metallurgical, and Petroleum Engineers*, **204:** 86-91.

Rosen, M.J., (1989), *Surfactants and Interfacial phenomena*, 2nd edition, John Wiley & Sons, New York, 431 p.

Sabatini, D.A., Knox, R.C., and Harwell, J.H., (1995), "Emerging technologies in surfactant-enhanced subsurface remediation", in: *Surfactant-Enhanced Subsurface Remediation - Emerging Technologies*, edited by D.A. Sabatini, R.C. Knox and J.H. Harwell, ACS Symposium Series 594, Washington, pp.1-8.

Schmid, C., (1964), "The wettability of petroleum rocks and the results of experiments to study the effects of variations of wettability of core samples", *Erdöl und Kohle-Erdgas-Petrochemie*, **17**(8): 605-609. English translation available from the John Crerar Library, translation no. TT-65-12404.

Schwille, F., (1967), "Petroleum contamination of the subsoil - A hydrological problem", in: *The Joint Problems of the Oil and Water Industries, Proceedings of a Symposium*, edited by P. Hepple, Institute of Petroleum, London, pp. 23-54.

Shah, D.O., (1981), "Introduction", *Surface Phenomena in Enhanced Oil Recovery*, ed. by D.O. Shah, Plenum Press, New York, pp. 1-12.

Singhall, A.K., Mukherjee, D.P., and Somerton, W.H., (1976), Effect of heterogeneous wettability of flow of fluids through porous media", *Journal of Canadian Petroleum Technology*, **15**(3): 63-70.

Somerton, W.H., and Clayton, J.R., (1980), "Role of clays in the enhanced recovery of petroleum", paper SPE 8845 presented at the 1980 SPE/DOE Symposium on Enhanced Oil Recovery, Tulsa, April 20-23, pp. 363-375.

Sposito, G. (1989), *The Chemistry of Soils*, Oxford University Press, New York, 277 p.

Stumm, W., and Morgan J.J., (1981), *Aquatic Chemistry - An Introduction Emphasizing Chemical Equilibria in Natural Waters*, John Wiley & Sons, New York, 780 p.

Suarez, D.L., Rhoades, J.D., Lavado, R., and Grieve, C.M., (1984), "Effect of pH on saturated hydraulic conductivity and soil dispersion", *Soil Science Society of America Journal*, **48**: 50-55.

Sun, S., Inskeep, W.P., and Boyd, S.A., (1995), "Sorption of nonionic organic compounds in soil-water systems containing a micelle-forming surfactant", *Environmental Science & Technology*, **29**: 903-913.

Talash, A.W., and Crawford, P.B., (1961a), "Experimental flooding characteristics of 75 percent water-wet sands", *Producers Monthlty*, **25**(2): 24-26.

Talash, A.W., and Crawford, P.B., (1961b), "Experimental flooding characteristics of unconsolidated sands", paper SPE 36 presented at the 1961 SPE Permian Basin Oil and Gas Recovery Conference, Midland, May 4-5.

Theng, B.K.G., (1974), *The Chemistry of Clay-organic reactions*, John Wiley & Sons, 343 p.

Theng, B.K.G., (1982), "Clay-polymer interactions: summary and perspective", *Clays and Clay Minerals*, **1**(1): 1-10.

Wyckoff, R.D., and Botset, H.G., (1936), "The flow of gas-liquid mixtures through unconsolidated sand", *Physics*, **7**: 325-345.

van Dam, J., (1967), "The migration of hydrocarbons in a water-bearing stratum", in: *The Joint Problems of the Oil and Water Industries, Proceedings of a Symposium*, edited by P. Hepple, Institute of Petroleum, London, pp. 55-88.

van Olphen, H., (1963), *An Introduction to Clay Colloid Chemistry*, John Wiley & Sons, New York, 301 p.

Wong, H.-Y., and Yong, R.N., (1973), "A simple solution of some practical engineering problems concerning unsaturated soils", *Civil Engineering and Public Works Review*, **68:** 759-765.

Wong, H.-Y., (1973), *Unsaturated Flow in Clay Soils*, Ph.D Thesis, McGill University.

Yong, R.N., and Warkentin, B.P., (1975), *Soil Properties and Behaviour*, Elsevier Scientific Publishing Company, Amsterdam, 449 p.

Yong, R.N., (1987), "Problems and issues in land management and waste disposal vis-à-vis groundwater contamination", in: *Proceedings, Montréal Geotechnical Group Workshop on Soil Barriers to Control Groundwater Contamination of Landwaste Disposal Sites*, Montréal, pp.1-21.

Yong, R.N., Mohamed, A.M.O, and El Monayeri, D.S., (1991), "Flow of surfactant fluid in nonaqueous phase liquid-saturated soils during remedial measures", Geotechnical Engineering Congress 1991 GT Div/ASCE, pp. 1137-1147.

Yong, R.N., and Rao, S.M., (1991), "Mechanistic evaluation of mitigation of petroleum hydrocarbon contamination by soil medium", *Canadian Geotechnical Journal*, **28:** 84-91.

Yong, R.N., and Mohamed, A.M.O., (1992), "A study of particle interaction energies in wetting of unsaturated expansive clays", *Canadian Geotechnical Journal*, **29:** 1060-1070.

Yong, R.N., Mohamed, A.M.O., Warkentin, B.P., (1992), *Principles of Contaminant Transport in Soils*, Elsevier Scientific Publishing Company, Amsterdam, 327 p.

Yong, R.N., Mohammed, L.F., and Mohamed, A.M.O., (1994), "Retention and transport of refinery residual petroleum in soil", in: *Analysis of Soils Contaminated with Petroleum Constituents*, edited by T.A. O'Shay and K.B. Hoddinott, American Society for Testing and Materials, Special Technical Publication 1221, pp.89-110.

APPENDIX I

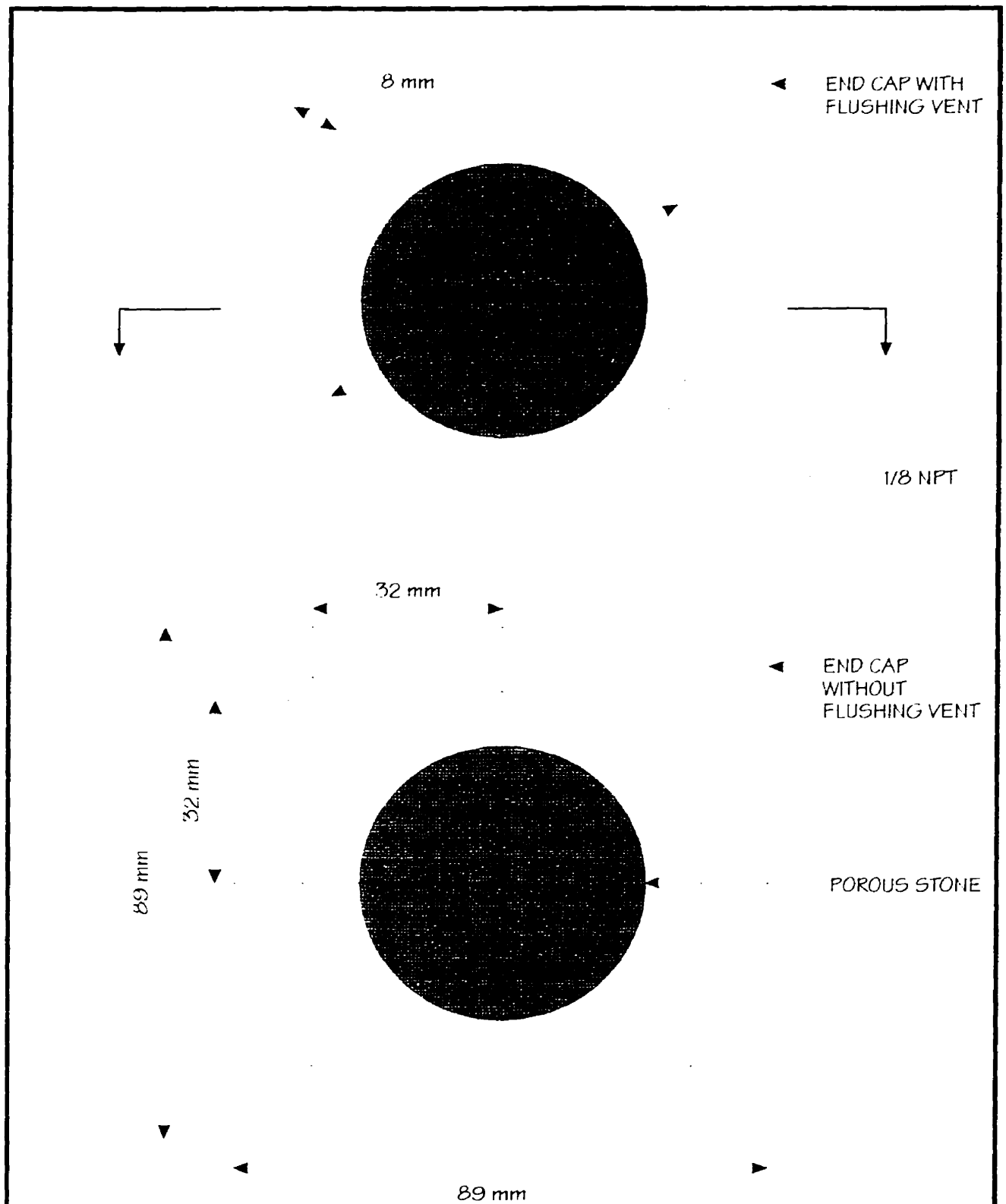

McGILL UNIVERSITY	END CAPS	DRAWN BY RENÉ DESJARDINS
SCALE N.T.S.	TOP VIEW	DATE MARCH 1995

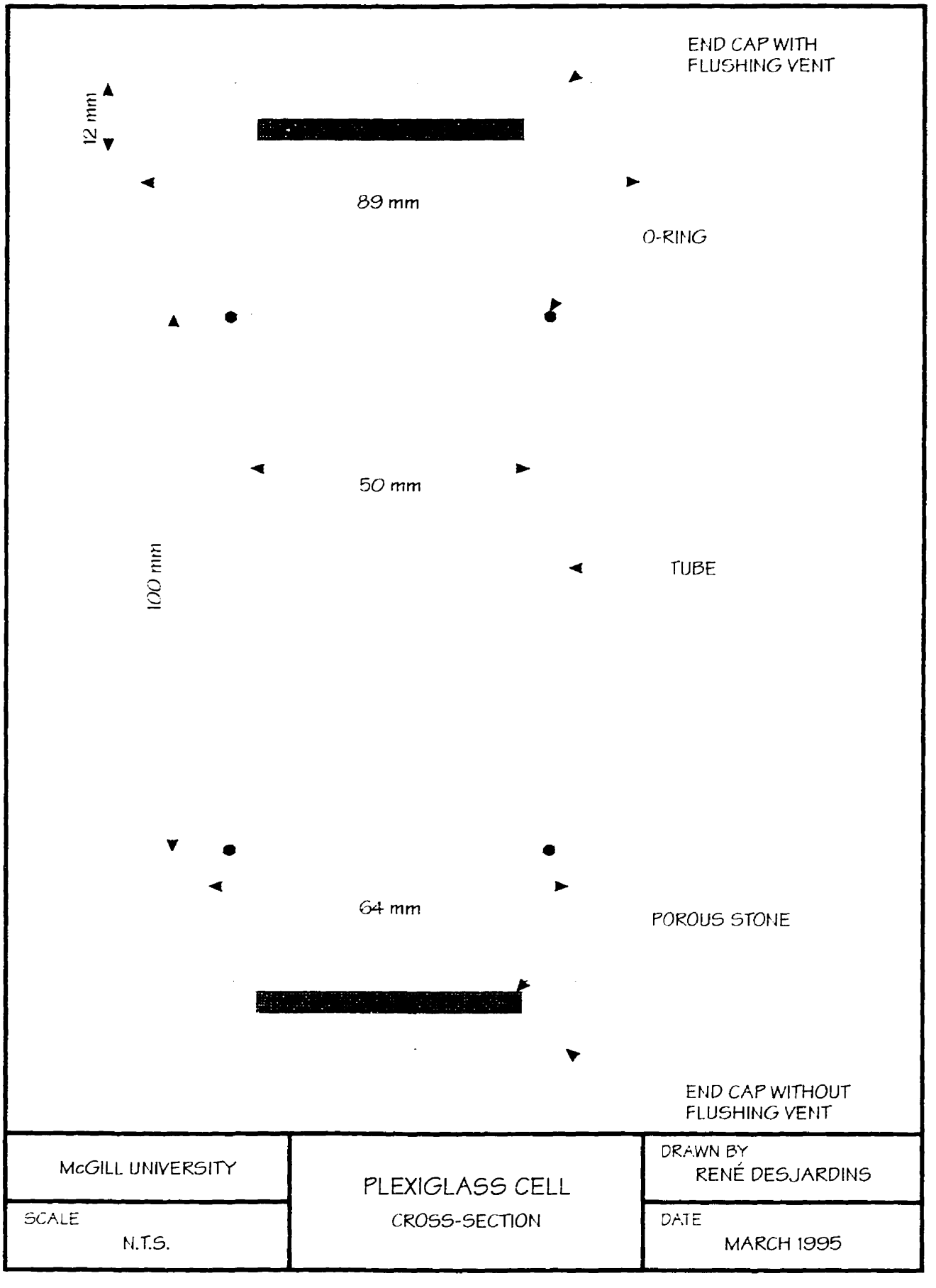

McGILL UNIVERSITY	PLEXIGLASS CELL CROSS-SECTION	DRAWN BY RENÉ DESJARDINS
SCALE N.T.S.		DATE MARCH 1995

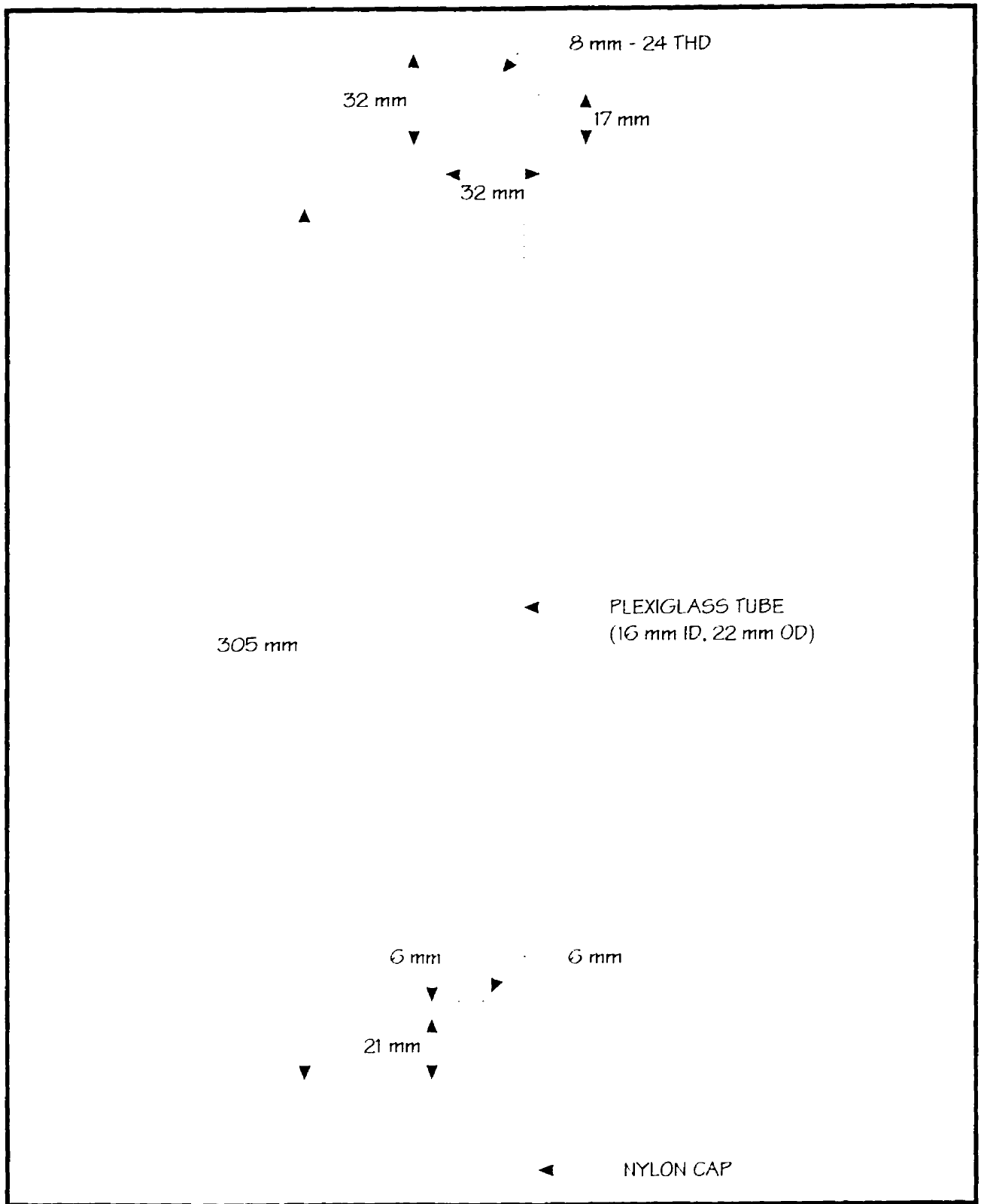

McGILL UNIVERSITY	MARIOTTE FLASK	DRAWN BY RENÉ DESJARDINS
SCALE N.T.S.	SIDE VIEW	DATE MARCH 1995

APPENDIX II

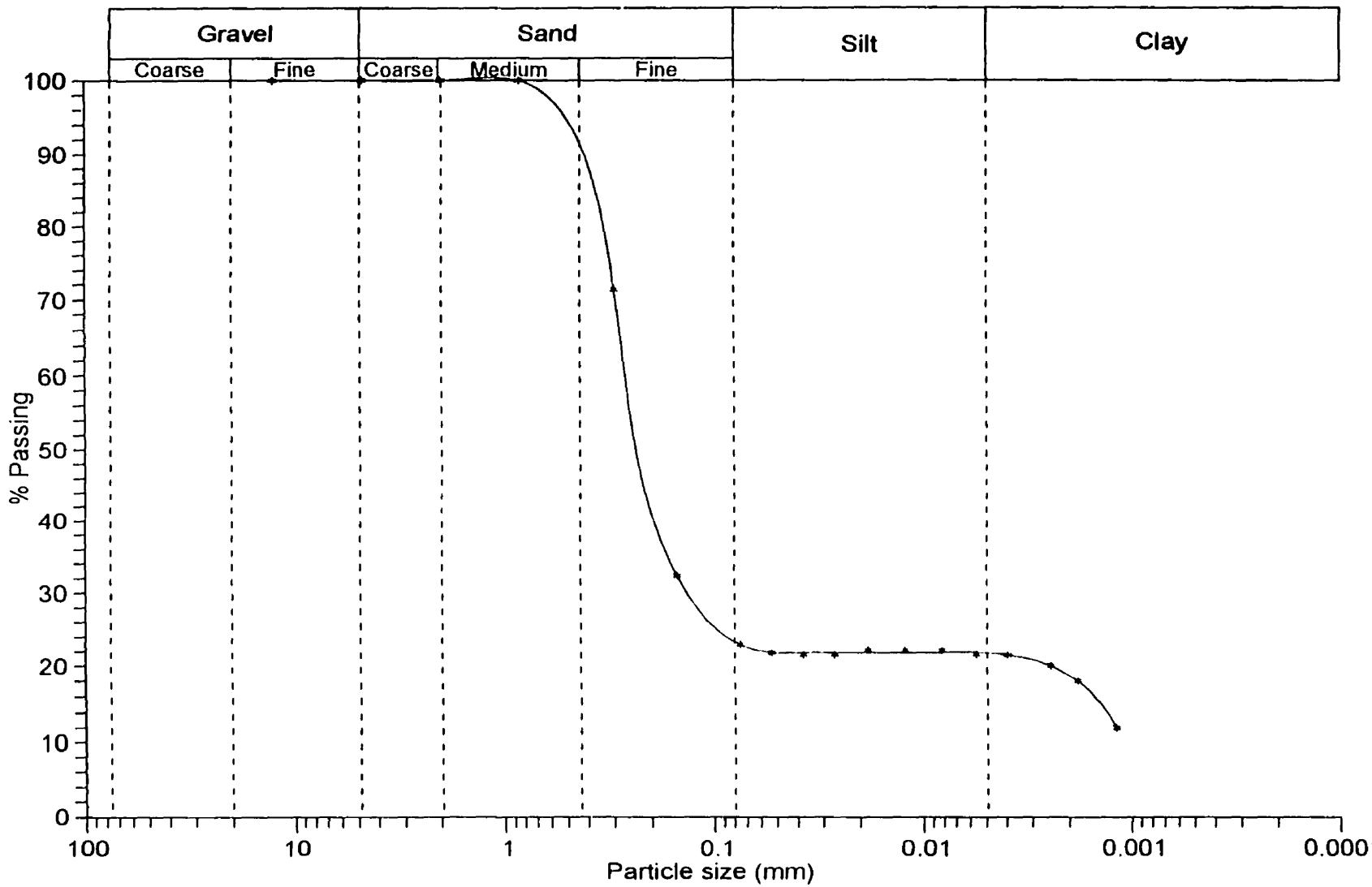

Figure II.1. Particle size distribution for 80% sand and 20% kaolinite.

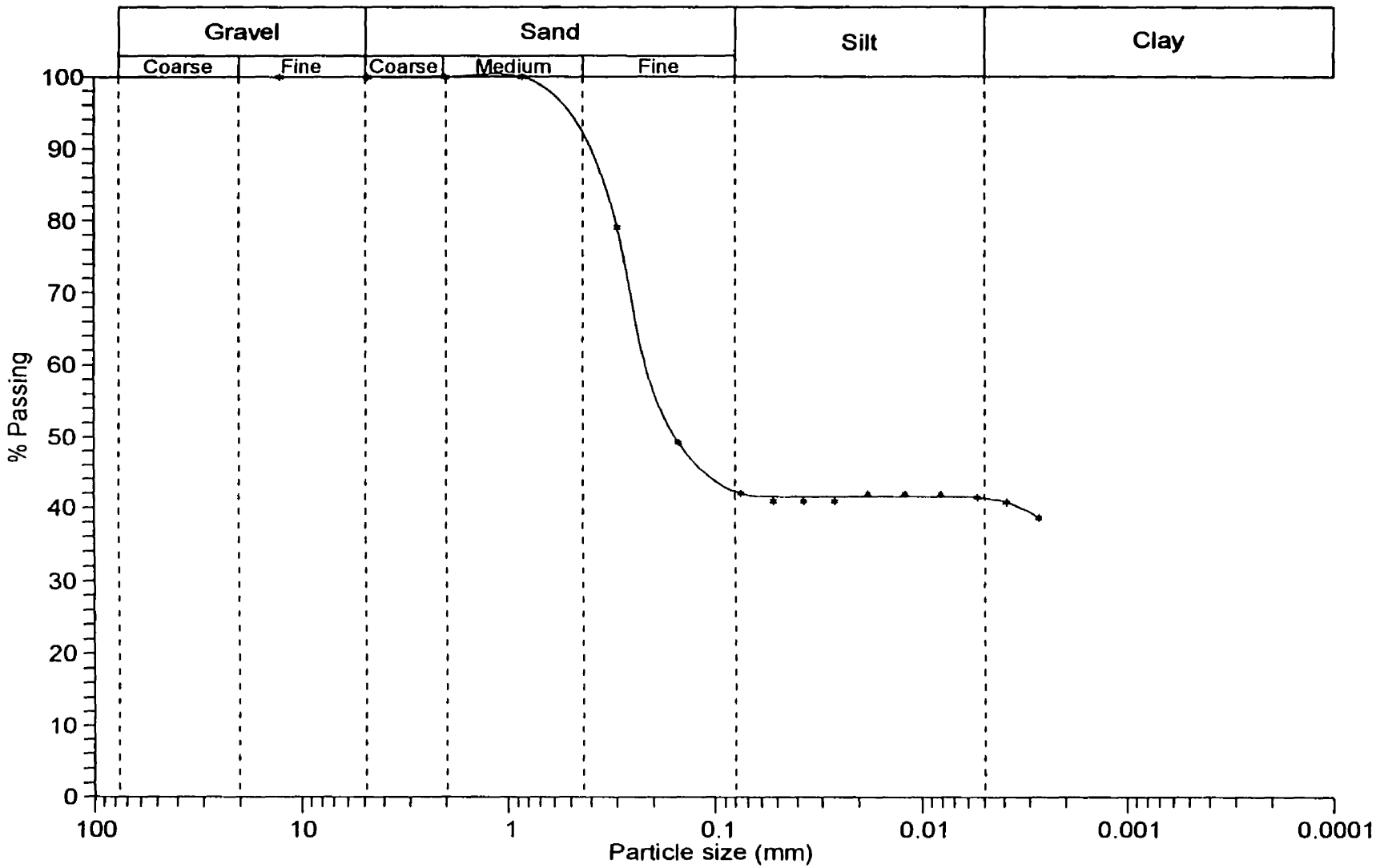

Figure II.2. Particle size distribution for 60% sand and 40% kaolinite.

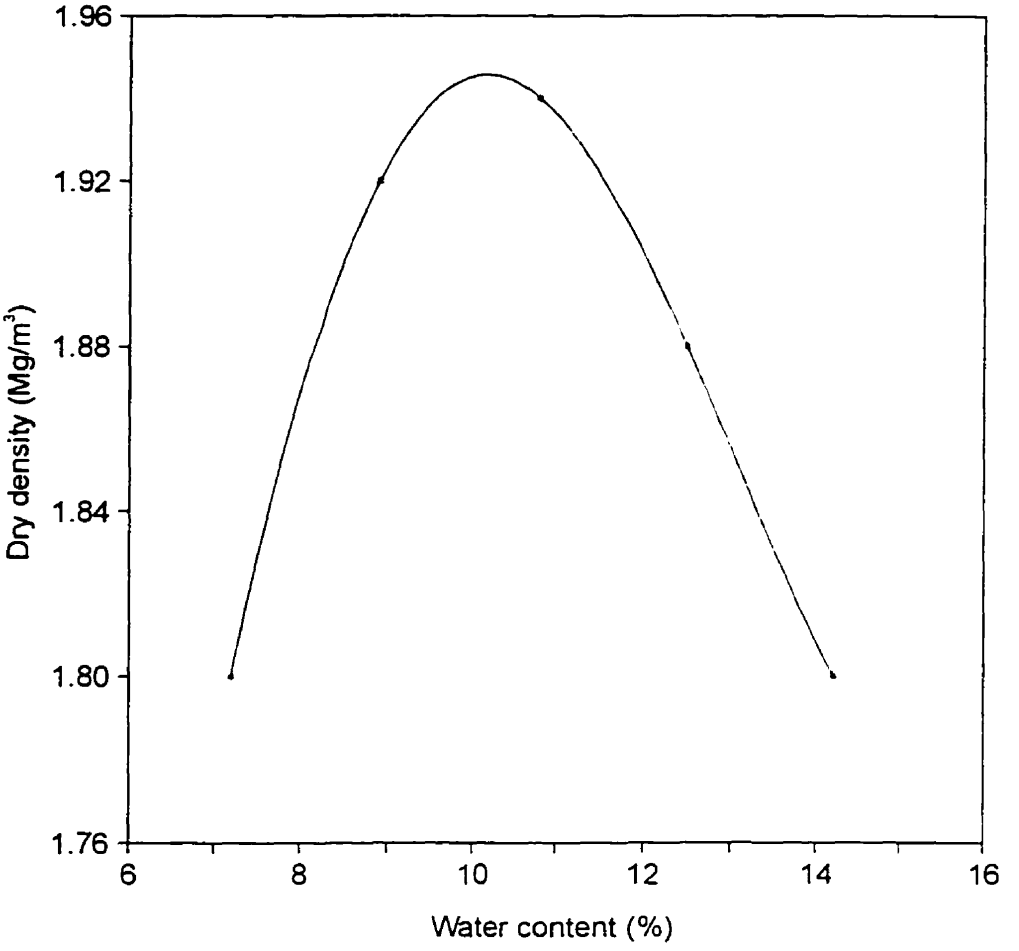

Figure II.3. Dry density-water content relationship for 80 % sand and 20% kaolinite

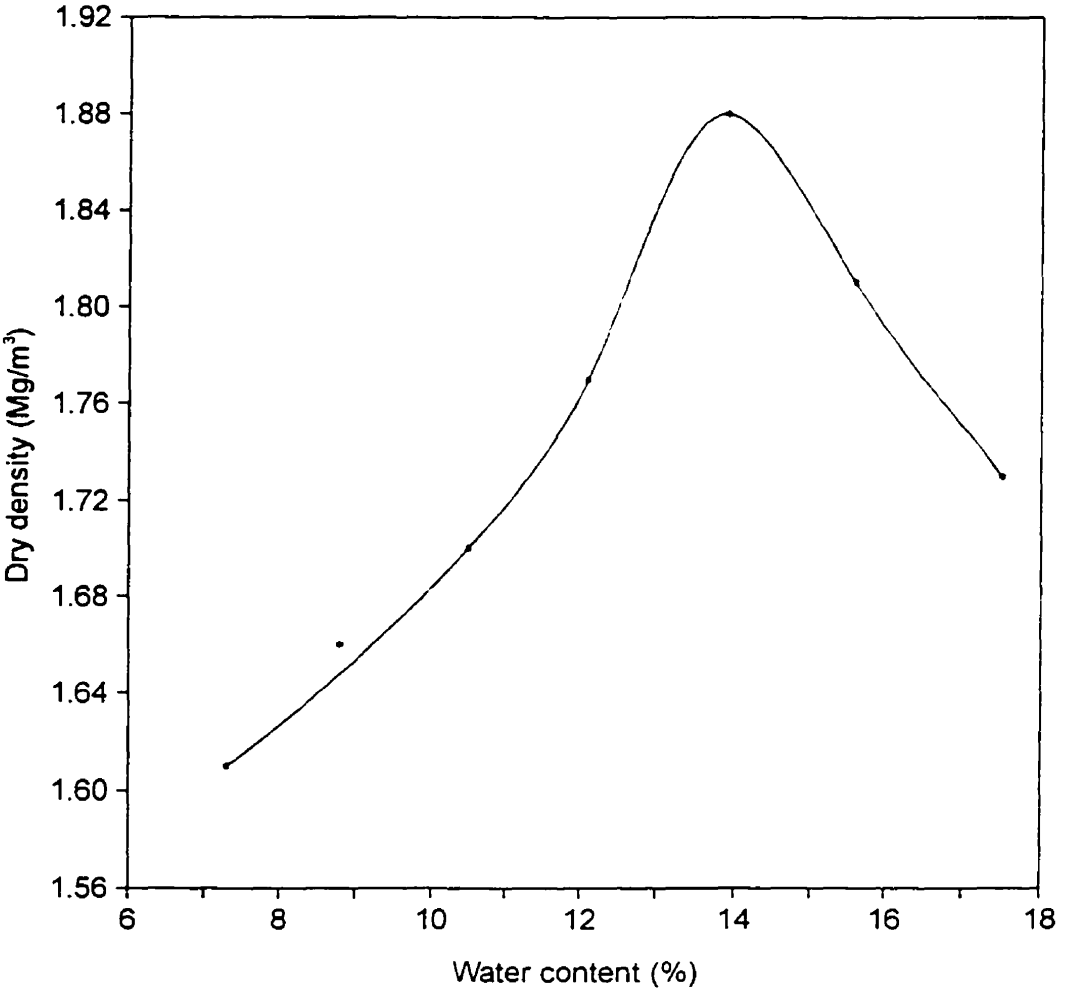

Figure II.4. Dry density-water content relationship for 60% sand and 40% kaolinite.

APPENDIX III

III.1 AVERAGE THICKNESS OF WATER LAYER AROUND SOIL PARTICLES (UNSATURATED CONDITIONS)

For the purpose of this exercise, it is assumed that the moisture is uniformly distributed around the soil particles.

Calculate surface area of sand particles

Assuming the sand particles to be perfect spheres, the surface area, S_{SAND}, is calculated with the following equation:

$$S_{SAND} = \frac{A_{SAND}}{G_{SAND}\, V_{SAND}} \times 10^{-6}$$

where $A_{SAND} = 4\,\pi\, r^2$ (m^2)

G_{SAND} = specific gravity of sand, assumed to be 2.65

$V_{SAND} = 4/3\,\pi\, r^3$ (m^3)

The diameter of the sand grains (mesh #40) is 4.25×10^{-4} m. Therefore the surface area of one sand particle is:

$$S_{SAND} = \frac{4\,\pi \left(\frac{4.25 \times 10^{-4}}{2}\right)^2}{4/3\,\pi \left(\frac{4.25 \times 10^{-4}}{2}\right)^3 \times 2.65} \times 10^{-6}$$

$$= 5.3 \times 10^{-3}\ m^2/g$$

Calculate the average particle surface area for each soil mixture

The average surface area is taken as a weighted average of kaolinite and sand:

$$S_{MIXTURE} = Q_{KAOLINITE} \times S_{KAOLINITE} + Q_{SAND} \times S_{SAND}$$

where $S_{KAOLINITE}$ = 24.0 m^2/g (refer to Table 3.1)

$Q_{KAOLINITE}$ = proportion of kaolinite in mixture

Q_{SAND} = proportion of sand in mixture

1. 80/20 mixture:

$$S_{80/20} = 0.2 \times 24.0 + 0.8 \times 5.3 \times 10^{-3} = 4.8 \ m^2/g$$

2. 60/40 mixture:

$$S_{60/40} = 0.4 \times 24.0 + 0.6 \times 5.3 \times 10^{-3} = 9.6 \ m^2/g$$

Calculate the total area of solid phase of soil mixtures

$$A_{MIXTURE} = S_{MIXTURE} \times M_{SOLID}$$

where $A_{MIXTURE}$ = total area of solid phase (m^2)

$S_{MIXTURE}$ = average surface area of soil mixture (m^2/g)

M_{SOLID} = dry mass of soil in lucite cell (g)

1. 80/20 mixture:

$$A_{80/20} = 4.8 \times 345.6 = 1568.9 \ m^2$$

2. 60/40 mixture:

$$A_{80/20} = 9.6 \times 333.8 = 3204.5 \ m^2$$

Calculate volume of water in soil mixtures

$$V_{WATER} = \frac{\omega \times M_{SOLID}}{\rho_{WATER}} \times 10^{-5}$$

where V_{WATER} = volume of water (m^3)

ω = water content, by mass (%)

ρ_{WATER} = density of water (kg/m^3)

1. 80/20 mixture:

$$V_{WATER} = \frac{6.7 \times 345.6}{1000} \times 10^{-5}$$

$$= 2.3 \times 10^{-5}\ m^3$$

2. 60/40 mixture:

$$V_{WATER} = \frac{10.5 \times 333.8}{1000} \times 10^{-5}$$

$$= 3.5 \times 10^{-5}\ m^3$$

Calculate the average thickness of the water layer

$$t_{WATER} = V_{WATER} / A_{MIXTURE}$$

1. 80/20 mixture:

$t_{WATER} = 2.3 \times 10^{-5} / 1658.9 = 1.4 \times 10^{-8}$ m (14 nm)

2. 60/40 mixture:

$t_{WATER} = 3.5 \times 10^{-5} / 3204.5 = 1.1 \times 10^{-8}$ m (11 nm)

III.2 THICKNESS OF DIFFUSE ION LAYER (SATURATED CONDITIONS)

The thickness of the diffuse ion layer is taken as the inverse of the Debye-Huckle reciprocal length:

$$1/K = \left(\frac{\varepsilon k T}{8 \pi n e^2 \upsilon^2} \right)^{1/2}$$

where K = Debye-Huckle reciprocal length, cm^{-1}

k = Boltzmann constant, 1.36×10^{-16} erg/°K

T = absolute temperature, assumed to be 290°K $\therefore$ kT = 0.4×10^{-13} erg

e = electronic charge, 4.8×10^{-10} esu

n = bulk concentration of counter ions (ions/cm^3)

ε = dielectric constant of soil pore fluid, assumed to be 84

υ = valence of counter ions, assumed to be 1

It is assumed that the only counter ions present in the distilled water are the H^+ cations. Their concentration is computed from the measured pH:

$$n = 10^{-5.8} \text{ mole/L} \times 6.02 \times 10^{23} \text{ ions/mole} \times \frac{1 \text{ L}}{1000 \text{ cm}^3}$$

$$= 9.5 \times 10^{14} \text{ ions/cm}^3$$

The thickness can now be calculated:

$$1/K = \left(\frac{84 \times 0.4 \times 10^{-13}}{8\pi \times 9.5 \times 10^{14} \times (4.8 \times 10^{-10})^2 \times 1^2} \right)^{1/2}$$

$$= 2.5 \times 10^{-5} \text{cm or } 250 \text{ nm}$$

III.3 TOTAL ENERGIES OF INTERACTION

The calculations to determine interaction energies for mixtures moulded with distilled water and 6% surfactant solution are presented in this section. To reflect the soil fabric changes, i.e., becoming more dispersed with surfactant, an edge-to-face configuration is assumed for soils moulded with distilled water, whereas a face-to-face configuration is assumed for surfactant-moulded mixtures.

Calculate particle separation distance

The particle separation distance d is computed with the equation given below:

$$e = G_s \times S_{MIXTURE} \times d \times \rho_w \times 10^3$$

where e = void ratio

G_s = specific gravity of solid, assumed to be 2.65

$S_{MIXTURE}$ = average surface area of solid phase (m^2/g)

ρ_w = density of water (kg/m^3)

The void ratio is calculated from the following relationship:

$$e = \frac{G_s \times \rho_w - \rho_d}{\rho_d}$$

where ρ_d is the soil dry density (kg/m^3).

1. 80/20 mixture:

Computing the void ratio:

$$e = \frac{2.65 \times 1000 - 1760}{1760} = 0.51$$

and computing d:

$$0.51 = 2.65 \times 4.8 \times d \times 1000 \times 10^{3}$$
$$d = 4.0 \times 10^{-8}\ m = 40\ nm$$

2. 60/40 mixture:

Computing the void ratio:

$$e = \frac{2.65 \times 1000 - 1700}{1700} = 0.56$$

and computing d:

$$0.56 = 2.65 \times 9.6 \times d \times 1000 \times 10^{3}$$
$$d = 2.2 \times 10^{-8}\ m = 22\ nm$$

Calculate surface potential (Ψ_o)

To calculate the variable potential of a particle edge, the Nernst equation is used:

$$\Psi_e = \frac{2.303\ kT}{e}\ (pH_o - pH)$$

where Ψ_e = edge potential (erg/esu)

e = electronic charge

pH_o = pH at which the surface potential is zero, around 4.2

To calculate the constant potential of a particle face, the following equations are used:

$$\sinh\left(\frac{z}{2}\right) = \sigma \left(\frac{\pi}{2n\varepsilon kT}\right)^{1/2}$$

and

$$\Psi_f = \frac{kT}{\nu e} z$$

where Ψ_f = face potential (erg/esu)

σ = face charge

z = dimensionless potential

1. Surface potentials in distilled water:

Due to the assumed edge-to-face configuration, both edge and face potentials are calculated. The edge potential is first determined as follows:

$$\Psi_e = \frac{2.303 \times 0.4 \times 10^{-13}}{4.8 \times 10^{-10}} (4.2 - 5.8)$$

$$= -3.1 \times 10^{-4} \text{ erg/esu}$$

It is assumed that the face charge of kaolinite is attributable to atomic substitution in about 0.05% of all Si atoms. One mole of kaolinite $[Al_2Si_2O_5(OH)_4]$ equals approximately 200 g and contains 2 moles of silicon atoms. Consequently, 1 g of kaolinite contains 5×10^{-6} mole of substitution, and the face charge is:

$$\sigma = \frac{5 \times 10^{-6} \text{ eq/g} \times 2.89 \times 10^{14} \text{ esu eq}^{-1}}{24 \times 10^4 \text{ cm}^2 \text{ g}^{-1}}$$

$$= 6.0 \times 10^3 \text{ esu/cm}^2$$

The face potential is then calculated:

$$\sinh\left(\frac{z}{2}\right) = 6.0 \times 10^3 \left(\frac{\pi}{2 \times 9.5 \times 10^{14} \times 84 \times 0.4 \times 10^{-13}}\right)^{1/2}$$

$$= 133.1 \quad \therefore z = -11.2$$

and

$$\Psi_f = \frac{0.4 \times 10^{-13}}{1 \times 4.8 \times 10^{-10}} \times -11.2$$

$$= -9.3 \times 10^{-4} \text{ erg/esu}$$

2. Surface potentials in 6% surfactant solution:

It is assumed that the bulk concentration of counter ions in the surfactant solution is the ratio of distilled water conductivity over 6% surfactant solution conductivity multiplied by the concentration of counter ions in distilled water:

$$n = 9.5 \times 10^{14} \text{ ions/cm}^3 \times \frac{8.65 \times 10^{-3} \text{ S}}{47.5 \times 10^{-6} \text{ S}}$$

$$= 1.7 \times 10^{17} \text{ ions/cm}^3$$

Due to the assumed face-to-face configuration, only the face potential needs to be determined:

$$\sinh\left(\frac{z}{2}\right) = 6.0 \times 10^3 \left(\frac{\pi}{2 \times 1.7 \times 10^{17} \times 84 \times 0.4 \times 10^{-13}}\right)^{1/2}$$

$$= 10.0 \quad \therefore z = -6.0$$

and

$$\Psi_f = \frac{0.4 \times 10^{-13}}{1 \times 4.8 \times 10^{-10}} \times -6.0$$

$$= -5.0 \times 10^{-4} \text{ erg/esu}$$

Calculate energies of interaction

The total energy of interaction, V_T is given as $V_T = V_R + V_A$, where V_R is the repulsion

energy, and V_A is the London - van der Waals attraction energy. For face-to-edge configuration, the repulsion and attractive energies are given as:

$$V_R = \frac{\varepsilon a_f a_e (\Psi_f^2 + \Psi_e^2)}{4 (a_f + a_e)} \left(\frac{2\Psi_f \Psi_e}{\Psi_f^2 + \Psi_e^2} \ln \frac{1 + \exp(-KH_o)}{1 - \exp(-KH_o)} + \ln[1 - \exp(-2KH_o)] \right)$$

$$V_A = -\frac{A}{12} \left(\frac{y}{x^2 + xy + x} + \frac{y}{x^2 + xy + x + y} + 2 \ln \frac{x^2 + xy + x}{x^2 + xy + x + y} \right)$$

For the face-to-face configuration, V_R and V_A are given as:

$$V_R = \frac{4 n k T z^2 \exp\left(\frac{-KH_o}{2}\right)}{K [1 + \exp(-KH_o)]}$$

$$V_A = \frac{-A}{12 \pi H_o^2}$$

where a_f = radius of small sphere (edge), given as 10^{-1} cm

a_e = radius of large sphere (face), given as 8×10^{-6}

K = Debye-Huckle reciprocal length (nm^{-1})

H_o = distance between particles minus distance of closest approach, $d - \delta$ (nm)

δ = distance of closest approach, assumed to be the size of the adsorbed hydrated Na ions (15.8Å)

$x = H_o / (2 a_f)$

$y = a_e / a_f$

A = Hamaker constant for interaction of kaolinite particles in water, given as 4.4×10^{-13} erg

Calculate energies of interaction with distilled water

1. 80/20 mixture:

The energy of repulsion equals:

$$V_R = \frac{84 \times 8 \times 10^{-6} \times 10^{-1} \times [(-3.1 \times 10^{-4})^2 + (-9.3 \times 10^{-4})^2]}{4\,(8 \times 10^{-6} + 10^{-1})} \times$$

$$\left[\frac{2 \times -9.3 \times 10^{-4} \times -3.1 \times 10^{-4}}{(-3.1 \times 10^{-4})^2 + (-9.3 \times 10^{-4})} \times \ln \frac{1 + \exp[-4.05 \times 10^{-3} \times (40 - 1.6)]}{1 - \exp[-4.05 \times 10^{-3} \times (40 - 1.6)]}\right.$$

$$\left. + \ln\{1 - \exp[-2 \times 4.05 \times 10^{-3} \times (40 - 1.6)]\}\right]$$

$$= 3.2 \times 10^{-11} \text{ erg}$$

The attraction energy equals:

$$V_A = \frac{-4.4 \times 10^{-13}}{12}\left(\frac{8 \times 10^{-5}}{(2 \times 10^{-5})^2 + (2 \times 10^{-5} \times 8 \times 10^{-5}) + (2 \times 10^{-5})} + \right.$$

$$\frac{8 \times 10^{-5}}{(2 \times 10^{-5})^2 + (2 \times 10^{-5} \times 8 \times 10^{-5}) + (2 \times 10^{-5}) + (8 \times 10^{-5})} +$$

$$\left. 2 \ln \frac{(2 \times 10^{-5})^2 + (2 \times 10^{-5} \times 8 \times 10^{-5}) + (2 \times 10^{-5})}{(2 \times 10^{-5})^2 + (2 \times 10^{-5} \times 8 \times 10^{-5}) + (2 \times 10^{-5}) + (8 \times 10^{-5})}\right)$$

$$= -5.8 \times 10^{-14} \text{ erg}$$

The total energy equals:

$$V_T = 3.2 \times 10^{-11} - 5.8 \times 10^{-14} = \underline{3.2 \times 10^{-11} \text{ erg}}$$

2. 60/40 mixture:

The energy of repulsion equals:

$$V_R = \frac{84 \times 8 \times 10^{-6} \times 10^{-1} \times [(-3.1 \times 10^{-4})^2 + (-9.3 \times 10^{-4})^2]}{4\,(8 \times 10^{-6} + 10^{-1})} \times$$

$$\left[\frac{2 \times -9.3 \times 10^{-4} \times -3.1 \times 10^{-4}}{(-3.1 \times 10^{-4})^2 + (-9.3 \times 10^{-4})} \times \ln\frac{1 + \exp[\,-4.0 \times 10^{-3} \times (22 - 1.6)\,]}{1 - \exp[\,-4.0 \times 10^{-3} \times (22 - 1.6)\,]}\right.$$

$$\left. + \ln\{\,1 - \exp[\,-2 \times 4.0 \times 10^{-3} \times (22 - 1.6)\,]\,\}\right]$$

$$= 2.4 \times 10^{-12} \text{ erg}$$

The attraction energy equals:

$$V_A = \frac{-4.4 \times 10^{-13}}{12}\left(\frac{8 \times 10^{-5}}{(1.1 \times 10^{-5})^2 + (1.1 \times 10^{-5} \times 8 \times 10^{-5}) + (1.1 \times 10^{-5})} + \right.$$

$$\frac{8 \times 10^{-5}}{(1.1 \times 10^{-5})^2 + (1.1 \times 10^{-5} \times 8 \times 10^{-5}) + (1.1 \times 10^{-5}) + (8 \times 10^{-5})} +$$

$$\left. 2 \ln\frac{(1.1 \times 10^{-5})^2 + (1.1 \times 10^{-5} \times 8 \times 10^{-5}) + (1.1 \times 10^{-5})}{(1.1 \times 10^{-5})^2 + (1.1 \times 10^{-5} \times 8 \times 10^{-5}) + (1.1 \times 10^{-5}) + (8 \times 10^{-5})}\right)$$

$$= -1.4 \times 10^{-13} \text{ erg}$$

The total energy equals:

$$V_T = 2.4 \times 10^{-12} - 1.4 \times 10^{-13} = \underline{2.3 \times 10^{-12} \text{ erg}}$$

Calculate energies of interaction with 6% surfactant solution

Calculate the Debye-Huckle reciprocal length:

$$1/K = \left(\frac{84 \times 0.4 \times 10^{-13}}{8\pi \times 1.7 \times 10^{17} \times (4.8 \times 10^{-10})^2 \times 1^2}\right)^{1/2}$$

$$= 1.8 \times 10^{-6} \text{cm or } 18 \text{ nm}$$

1. 80/20 mixture:

The energy of repulsion equals:

$$V_R = \frac{4 \times 1.7 \times 10^{17} \times 0.4 \times 10^{-13} \times 18 \times 10^{-7} \times 6.0^2}{1 + \exp[\ -5.6 \times 10^{-2} \times (40 - 1.6)\ ]} \times \exp\left(\frac{-5.6 \times 10^{-2} \times (40 - 1.6)}{2}\right)$$

$$= 0.5 \text{ erg/cm}^2$$

The attraction energy equals:

$$V_A = \frac{-4.4 \times 10^{-13}}{12\pi \times (40 - 1.6)^2 \times 10^{-14}}$$

$$= -7.9 \times 10^{-4} \text{ erg/cm}^2$$

The total energy equals:

$$V_T = 0.5 - 7.9 \times 10^{-4} = \underline{0.5 \text{ erg/cm}^2}$$

2. 60/40 mixture:

The energy of repulsion equals:

$$V_R = \frac{4 \times 1.7 \times 10^{17} \times 0.4 \times 10^{-13} \times 18 \times 10^{-7} \times 6.0^2}{1 + \exp[\ -5.6 \times 10^{-2} \times (22 - 1.6)\ ]} \times \exp\left(\frac{-5.6 \times 10^{-2} \times (22 - 1.6)}{2}\right)$$

$$= 0.8 \text{ erg/cm}^2$$

The attraction energy equals:

$$V_A = \frac{-4.4 \times 10^{-13}}{12\pi \times (22 - 1.6)^2 \times 10^{-14}}$$

$$= -2.8 \times 10^{-3} \text{ erg/cm}^2$$

The total energy equals:

$$V_T = 0.8 - 2.8 \times 10\text{-}^3 = \underline{0.8\ erg/cm^2}$$

To compare with distilled water, it is required to convert from erg/cm^2 to erg by multiplying V_T by the face area. Assuming that a typical particle is rectangular with a thickness of 100 nm, it is found that the face area is 1.8×10^{-10} cm^2. For the 80/20 mixture:

$$V_T = 0.5 \times 1.8 \times 10^{-10} = \underline{9.0 \times 10^{-11}\ erg}$$

Similarly, for the 60/40 mixture:

$$V_T = 0.8 \times 1.8 \times 10^{-10} = \underline{1.4 \times 10^{-10}\ erg}$$

These calculations show that the energies of interaction increase when surfactant is the moulding liquid.

APPENDIX IV

```
Program Diffuse;

(*A program that calculates the diffusivity using the method described by Wong (1973).
The input data is provided in an ASCII file. The results are sent to an output file.*)

Uses

WinCrt;

Var
 r, i, count:          Integer;
 tcalc, sumxt,
 deltat, facteur,
 oilcont:              Real;
 x, voc,
 D:                    Array[0..20] of Real;
 fich_inp,
 fich_out:             String[12];
 ftexte:               Text;

(*Description of variables

i:          number of input points on the volumetric oil content versus distance curve,
            i.e., from θ0 to θi.
r:          number of input points excluding point on the x axis, i.e., r = i - 1.
count:      variable used in the loop that performs the calculations. The calculations
            are performed from count = 1 to r.
tcalc:      the time at which the diffusivity is determined.
deltat:     Δθ
voc:        volumetric oil content, θr
x:          distance corresponding to voc, x( θr )
facteur:    [ x( θr+1 ) - x( θr ) ] / ( 2t Δθ )
sumxt:      Σ x(θi) Δθ + x( θi ) ( θn - 1/2 - θi )
D:          diffusivity, D( θr+1/2 )
oilcont:    oil content corresponding to D, θr+1/2
fich_inp:   name of input file
fich_out:   name of output file
ftexte:     variable to which name of file is assigned*)


Begin

ClrScr;

(*Questions to obtain name of input and output files*)
Write('Name of input file (ASCII): ');
ReadLn(fich_inp);
Write('Name of output file: ');
```

```
ReadLn(fich_out);

Assign(ftexte,fich_inp);
Reset(ftexte);
r := 0;

(*On first line of input file, read Δθ*)
ReadLn(ftexte,deltat);

(*On second line of input file, read time of calculation in seconds, tcalc*)
ReadLn(ftexte,tcalc);

(*Up to end of file, read x( θr ) in mm, θr , and count the number of points*)
While Not Eof(ftexte) Do
Begin
ReadLn(ftexte,x[r],voc[r]);
r := r + 1;
End; (*While Not Eof(ftexte) Do*)

Close(ftexte);

i := r - 1;
r := r - 2;

Assign(ftexte,fich_out);
Rewrite(ftexte);

(*Calculate R = x( θi ) ( θn-1/2 - θi )*)
sumxt := x[i] * ( deltat / 2 - voc[i] );

For count := 1 To r Do
Begin

(*Calculate Σ = x( θi ) Δθ + R*)
sumxt := sumxt + x[r - ( count - 1 )] * deltat;

(*Calculate [ x( θr+1 ) - x(θr)] / ( 2t Δθ )*)
facteur := ( x[r - (count - 1)] - x[r - count] ) / ( 2 * tcalc * deltat );

(*Calculate D( θr+1/2 )*)
D[count - 1] := facteur * sumxt / 1000000;

(*Calculate θr+1/2*)
oilcont := deltat / 2 + deltat * count;

(*Send results [ θr+1/2, D( θr+1/2 ) ] to output file. D is given in m²/s*)
WriteLn(ftexte,oilcont:7:5,#9,D[count - 1]);
```

```
End; (*For count := 1 To r Do*)

Close(ftexte);
End.
```

```
0.02018
86400
7.60 0.14128
16.6 0.12110
34.8 0.10092
39.2 0.08073
41.2 0.06055
42.9 0.04037
45.3 0.02018
54.4 0.00000
```

EXAMPLE OF INPUT FILE FOR PROGRAM DIFFUSE (ASCII FORMAT)

0.03027	1.0069444444E-09
0.05045	1.1353009259E-09
0.07063	1.8125000000E-09
0.09081	4.9856481482E-09
0.11099	2.4287731481E-08
0.13117	1.2875000000E-08

EXAMPLE OF OUTPUT FILE FOR PROGRAM DIFFUSE (ASCII FORMAT)

```
Program Oilmig;

(*A program that simulates the migration of oil using the finite difference form of equation
2.10*)

Uses

WinCrt;

Var

a, b, c, d,
efunca, efuncb,
efuncc, tpredday,
Da, Db, Dc,
part1, part2:        Real;
i, dist:             Integer;
tpredsec, timep,
j:                   LongInt;
Selection:           Char;
COxt:                Array [1..2,0..10] of Real;

(*Description of variables

a, b, c, d:   parameters of diffusivity function in m^2/s
efunca:       exponential function at point i - 1
efuncb:       exponential function at point i
efuncc:       exponential function at point i + 1
              when the soil mixture is 80/20, efunc = exp[ ( c - θoil ) / d].
              when the soil mixture is 60/40, efunc = -0.5 [ln( θoil / c) / d]^2
Da, Db, Dc:   diffusivity, D, at point i - 1, i, and i + 1, respectively
tpredday:     time of prediction in days
tpredsec:     time of prediction in seconds
timep:        time at which calculations are made, j x 60. 60 seconds is the time step
i, j:         number of time and space intervals, respectively
part1:        [ D( θ^j_(i+1) ) - D( θ^j_i ) ] [ θ^j_(i+1) - θ^j_i ]
part2:        [ D( θ^j_i ) - D(θ^j_(i-1) ) ] [ θ^j_i - θ^j_(i-1) ) ]
Selection:    character variable used to determine whether the mixture is 80/20 or 60/40.
COxt:         oil concentration or volumetric oil content.

Begin

ClrScr;

Selection := '0';
j := 1;
```

```
timep := j * 60;

(*Questions to obtain input data*)
WriteLn('Provide values for the diffusivity parameters:');
Write('  a: ');
Read(a);
Write('  b: ');
Read(b);
Write('  c: ');
Read(c);
Write('  d: ');
ReadLn(d);
Write('Provide oil concentration at x = 5 mm (mg/100g soil): ');
ReadLn(COxt[1,0]);
Write('Enter time at which profile is desired (days): ');
ReadLn(tpredday);

While Not (Selection In ['1','2']) Do
Begin
WriteLn('Select mixture for which oil content profile is to be computed:');
WriteLn('1. 80% sand and 20% kaolinite.');
WriteLn('2. 60% sand and 40% kaolinite.');
Write('Selection: ');
ReadLn(Selection);
If Not (Selection In ['1','2']) Then
WriteLn('ERROR! WRONG INPUT!');
End; (*While Not (Selection In ['1','2']) Do*)

(*Convert oil concentration in mg/100g soil to volumetric oil content*)
If (Selection In ['1']) Then
Begin
(*Conversion calculation if mixture is 80/20*)
COxt[1,0] := COxt[1,0] * 2.01835E-05;
End (*If mixture is 80/20*)
Else
Begin
(*Conversion calculation if mixture is 60/40*)
COxt[1,0] := COxt[1,0] * 1.94954E-05;
End; (*If (Selection In['1']) Then...Else*)

(*Convert days to seconds*)
tpredsec := Round(tpredday * 86400);

(*Initialization of oil content variable*)
For i := 1 To 10 Do
Begin
COxt[1,i] := 0;
Coxt[2,i] := 0;
```

```
End; (*For i := 1 To 10 Do*)

(*Calculate oil content at various time increments up to specified time*)
While (timep <= tpredsec) Do
Begin

(*Compute volumetric oil content at each node*)
For i := 1 To 9 Do
Begin
If (Selection In ['1']) Then
(*Calculations of D if mixture is 80/20*)
Begin
efunca := exp((c-COxt[1,i - 1]) / d);
efuncb := exp((c-COxt[1,i]) / d);
efuncc := exp((c-COxt[1,i + 1]) / d);

(*The diffusivity is expressed as D = a + b exp[ f(x) ], where f(x) = 1 - exp[ g(x) ] +
( c - x ) / d, where g(x) = ( c - x ) / d, where x is the volumetric oil content. efunc is
exp[ g(x) ]*)

(*To avoid run-time error 205, i.e., floating point overflow, make exponential function ( exp[
f(x) ] ) equal to zero if it becomes too small, i.e., efunc ( exp[ g(x) ] ) more than 80. If
efunc is too big, then the diffusivity, D, becomes equal to a.*)

If (efunca > 80) Then
Begin
Da := a;
End (*If efunca is too big*)
Else
Begin
Da := a + b * exp(1 + (c - COxt[1,i-1]) / d - efunca);
End; (*If (efunca > 80) Then...Else*)

If (efuncb > 80) Then
Begin
Db := a;
End (*If efuncb is too big*)
Else
Begin
Db := a + b * exp(1 + (c - COxt[1,i]) / d - efuncb);
End; (*If (efuncb > 80) Then...Else*)

If (efuncc > 80) Then
Begin
Dc := a;
End (*If efuncc is too big*)
Else
Begin
```

```
Dc := a + b * exp(1 + (c - COxt[1,i+1])/d - efuncc);
End;(*If (efuncc > 80) Then...Else*)

End (*End of calculations of D if mixture is 80/20*)
Else
Begin
(*Calculations of D if mixture is 60/40*)

(*The diffusivity is expressed as D = a + b exp[ -0.5 f(x) ], where f(x) = [ ln(x / c) / d]^2,
where x is the volumetric oil content. efunc is exp[ -0.5 f(x) ]*)

(*To avoid run-time error 205, i.e., floating point overflow, make exponential function( exp[
-0.5 f(x) ] ) equal to zero when f(x) is greater than 160. When f(x) > 160, efunc is too
small*)

(*To avoid ln 0, make diffusivity, D, equal to 'a', if a > 0, or equal to 0 when a < 0, when
x = 0*)

If (COxt[1,i-1] > 0) AND (Sqr((Ln(COxt[1,i-1] / c)) / d) < 160) Then
Begin
efunca := exp(-0.5 * Sqr((Ln(COxt[1,i-1] / c)) / d));
Da := a + b * efunca;
If (Da < 0) Then
(*To avoid a negative diffusivity, when a < 0 and a > b efunc, make D equal to zero under
such conditions*)
Da := 0;
End (*If efunc is not too small and COxt > 0*)
Else
Begin
(*If efunc is too small or COxt = 0*)
If (a > 0) Then
Begin
Da := a;
End (*If (a > 0)*)
Else
Begin
(*If a < 0*)
Da := 0;
End; (*If (a > 0) Then...Else*)

End; (*If (COxt[1,i-1] > 0 AND (Sqr((Ln(COxt[1,i-1] / c)) / d) < 160) Then...Else*)

If (COxt[1,i] > 0) AND (Sqr((Ln(COxt[1,i] / c)) / d) < 160)  Then
Begin
efuncb := exp(-0.5 * Sqr((Ln(COxt[1,i] / c)) / d));
Db := a + b * efuncb;
If (Db < 0) Then
(*To avoid a negative diffusivity, when a < 0 and a > b efunc, make D equal to zero under
```

```
such conditions*)
Db := 0;
End (*If efunc is not too small and COxt > 0*)
Else
Begin
(*If efunc is too small or COxt = 0*)
If (a > 0) Then
Begin
Db := a;
End (*If (a > 0)*)
Else
Begin
(*If a < 0*)
Db := 0;
End; (*If (a > 0) Then...Else*)

End; (*If (COxt[1,i] > 0 AND (Sqr((Ln(COxt[1,i] / c)) / d) < 160) Then...Else*)

If (COxt[1,i+1] > 0) AND (Sqr((Ln(COxt[1,i+1] / c)) / d) < 160)  Then
Begin
efuncc := exp(-0.5 * Sqr((Ln(COxt[1,i+1] / c)) / d));
Dc := a + b * efuncc;
If (Dc < 0) Then
(*To avoid a negative diffusivity, when a < 0 and a > b efunc, make D equal to zero under
such conditions*)
Dc := 0;
End (*If efunc is not too small and COxt > 0*)
Else
Begin
(*If efunc is too small and COxt = 0*)
If (a > 0) Then
Begin
Dc := a;
End (*If (a > 0)*)
Else
Begin
(*If a < 0*)
Dc := 0;
End; (*If (a > 0) Then...Else*)

End; (*If (COxt[1,i+1] > 0 AND (Sqr((Ln(COxt[1,i+1] / c)) / d) < 160) Then...Else*)

End; (*If (Selection In ['1']) Then...Else*)

part1 := (Dc + Db) * (COxt[1,i+1] - COxt[1,i]) * 1000000;
part2 := (Db + Da) * (COxt[1,i] - COxt[1,i-1]) * 1000000;

COxt[2,i] := (part1 - part2) * 60/ 200 + COxt[1,i];
```

```
COxt[2,10] := COxt[2,9];
End; (*For i:= 1 To 9 Do; compute oil concentration at each node*)

For i := 1 To 10 Do
COxt[1,i] := COxt[2,i];

j := j + 1;
timep := j * 60;

End; (*While (timep <= tpredsec) Do*)

(*Show results on screen*)
WriteLn(#13,#10,#13,#10,'OUTPUT RESULTS');
WriteLn(#13,#10,'  Dist. (mm)','     Oil conc. (mg/100g)');

(*Reconvert volumetric oil content to oil concentration in mg/100g soil*)
If (Selection In ['1']) Then
Begin
(*Conversion calculation if mixture is 80/20*)
For i := 0 To 9 Do
Begin
COxt[1,i] := COxt[1,i] / 2.01835E-05;
dist := i * 10 + 5;
WriteLn(dist,'      ',COxt[1,i]:4:0);
End; (*For i := 0 To 10 Do*)
End (*If mixture is 80/20*)
Else
Begin
(*Conversion calculation if mixture is 60/40*)
For i := 0 To 9 Do
Begin
COxt[1,i] := COxt[1,i] / 1.94954E-05;
dist := i * 10 + 5;
WriteLn(dist,'      ',COxt[1,i]:4:0);
End; (*For i := 0 To 9 Do*)
End; (*If (Selection In ['1']) Then...Else*)

End.
```

IMAGE EVALUATION
TEST TARGET (QA-3)

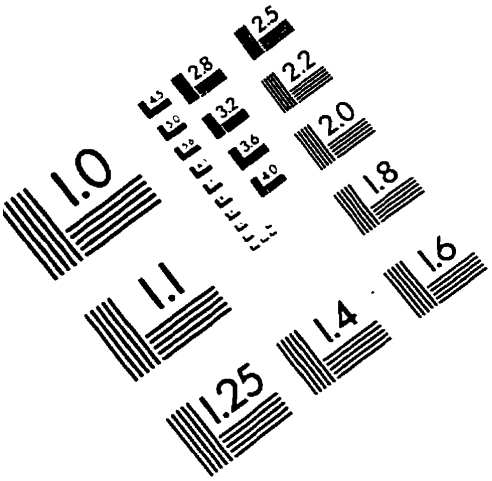

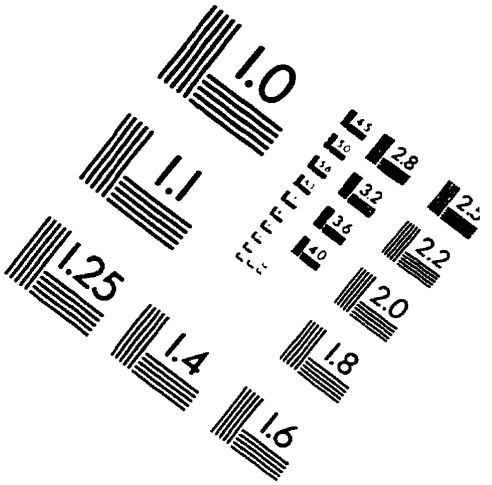

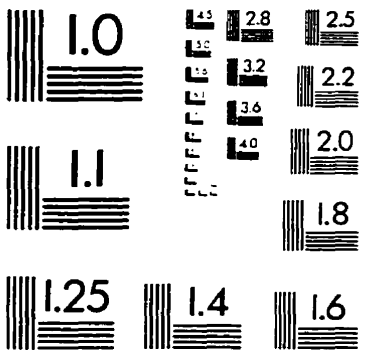

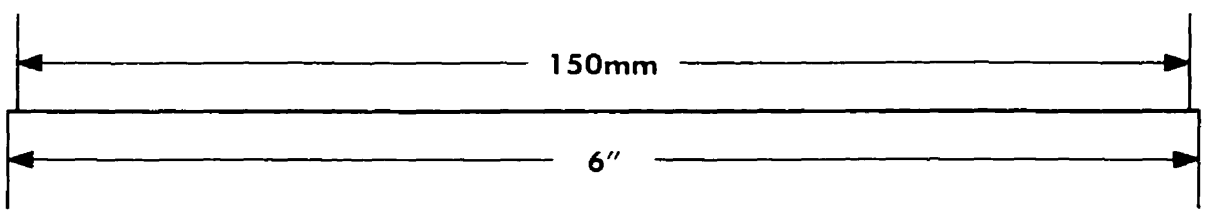

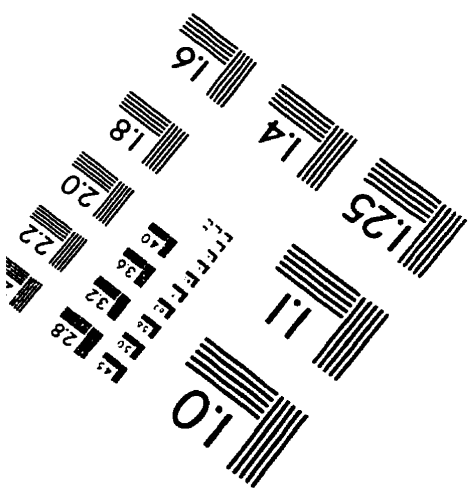

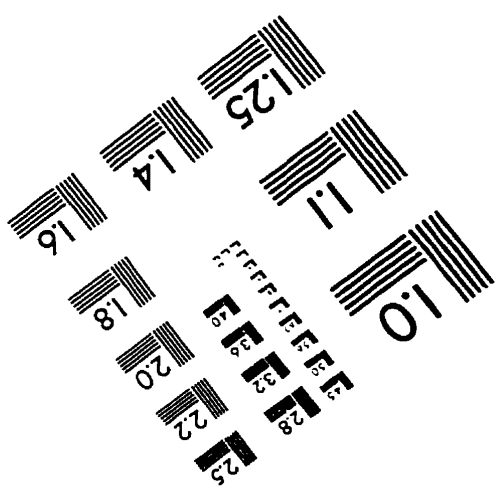

APPLIED IMAGE, Inc
1653 East Main Street
Rochester, NY 14609 USA
Phone: 716/482-0300
Fax: 716/288-5989